Optimum Voltage Droop Control to Support Local Voltage Stability in Transmission Systems with High Share of RES

by

Siam Hasan Khan

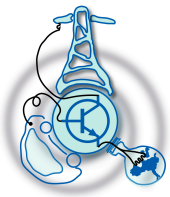

Submitted to the Department of Electrical Engineering, Electronics, Computers and Systems
in partial fulfillment of the requirements for the degree of
Erasmus Mundus Master Course in Sustainable Transportation and Electrical Power Systems
at the
UNIVERSIDAD DE OVIEDO
September 2020

© Universidad de Oviedo 2020. All rights reserved.

Author .....
Siam Hasan Khan

Certified by .....
Rui Pestana
Advisor-Redes Energéticas Nacionais (REN)
Thesis Supervisor

Certified by .....
Cristina Isabel Faustino Agreira
Adjunt Professor-Polytechnic Institute of Coimbra
Thesis Supervisor

Optimum Voltage Droop Control to Support Local Voltage Stability in Transmission Systems with High Share of RES

by

Siam Hasan Khan

Submitted to the Department of Electrical Engineering, Electronics, Computers and Systems
on September 1, 2020, in partial fulfillment of the
requirements for the degree of
Erasmus Mundus Master Course in Sustainable Transportation and Electrical Power Systems

Abstract

In this thesis, I designed a voltage droop control method for the high share of RES connected to the electrical transmission system.The control of voltage profile in transmission system is becoming very complicated with the high amount of RES connected to the VHV substation.Also the reactive power management needs to be ensured in the VHV/HV substation not only in the point of interconnection but also for the individual wind power plant and photo-voltaic plant.Based on the real case study provided by the Portuguese National Transmission system operator named Redes Energéticas Nacionais (REN),this thesis provides a new voltage droop control strategy for avoiding conflicting set-point of each wind power plant and photo-voltaic power plant connected to the transmission system. Before coming up with a final solution which mitigates the voltage fluctuations at the point of interconnection that utilizes the voltage regulation capabilities, different scenarios were analyzed and simulated. The main aim of this thesis was to come up with a control strategy in which the voltage will be in its steady state limits in all the plants which will be examined.

Thesis Supervisor: Rui Pestana
Title: Advisor-Redes Energéticas Nacionais (REN)

Thesis Supervisor: Cristina Isabel Faustino Agreira
Title: Adjunt Professor-Polytechnic Institute of Coimbra

Acknowledgments

First of all I would like to thank the EMJMD STEPS consortium for giving me the opportunity to study in this masters program which has many unique and amazing courses. It has been an amazing journey during these two years of the masters program. Thanks to **Professor Cristina Faustino Agreira** and **Mr. Rui Pestana** for believing me that I am worthy enough to carry out the thesis. The lock down situation of Covid-19 impacted all of our lives and it was very difficult to carry out the thesis work remotely. **Mr. Rui Pestana** has been an immense support for me during this time and the way he supervised me in the whole thesis work, I will be forever grateful for that.

I would like to extend my gratitude to **Ms. Susana Menendez Bustilo**, **Professor Pablo Arboleya**, **Professor Jorge Garcia**, **Professor Fabio Giulii Capponi**, **Professor Giulio De Donato** and all the people associated with the EMJMD STEPS for their assistance during my masters program. I thank all my professors for enhancing my knowledge and skills in different fields. My friends **Irfan**, **Sabbir** and **Asim** thanks for being there for me and supporting me in my hard times.

A big thanks goes to my Family and friends, I would have been nothing without your existence in my life. **Guria**, **Ony**, **Swapnil**, **Rupom**, **Niloy**, **Shovon** you guys are my pillars and no words would ever express my gratitude towards you. I would like to thank my thesis supervisor of BSc program, **Mr. Ahmed Mortuza Saleque** and my cousin **Md. Asifuzzaman Asif** who helped me to grow immense interest in the field of electrical engineering and always supported me with their knowledge and skills. **Maria** and **Giovanni**, thanks for being by my side during the lock down. You guys came in my life as blessings.

Lastly and most importantly I praise God, the almighty Allah for providing all the opportunities and granting me the capabilities to proceed successfully in every aspects.

Contents

1 Introduction **15**

1.1 Company Profile of REN - Redes Energéticas Nacionais 17

1.2 Overview of Electrical Generation and Transmission Systems in Portugal 18

1.3 Government Policy and legislative framework of REN 22

1.4 RES Integration in Portuguese National Grid Systems 22

1.5 Objective of the Thesis 26

1.6 Thesis Structure 27

2 State of Art **29**

2.1 Reactive Energy Tariff: Tangent-ϕ 30

2.2 Voltage Regulation With Reactive Power Limits 31

2.3 Voltage and Reactive Power Control 31

2.3.1 Constant Power Factor Mode (Default, Unity) 32

2.3.2 Voltage Reactive Power Mode (Volt-Var) 32

2.3.3 Active Power-Reactive Power Mode (Watt-Var) 34

2.3.4 Constant Reactive Power Mode 34

2.4 Voltage Active Power Mode (Volt-Watt) 35

2.5 Recommendation for the Voltage Reactive Power Mode 36

2.6 Consideration of Dead-band and Undead-band Zone in the Voltage Reactive Power Mode 37

2.6.1 Undead-band Droop in the Voltage Reactive Power Mode . . . 37

2.6.2 Dead-band Droop in the Voltage Reactive Power Mode 38

2.6.3 Dead-band Droop with Spline in the Voltage Reactive Power Mode . . . 39

3 Design of the Power Systems in PSS®E 43

3.1 Design of Tavira Substation . . . 44

3.1.1 Malhanito and Baixo Alentejo Wind Power plants . . . 45

3.1.2 The Alcoutim PV Power plant . . . 45

3.1.3 São Marcos PV power plant . . . 45

3.2 Scheme of the Overall Power System . . . 46

3.2.1 Machine Data . . . 46

3.2.2 Power Plant Data . . . 48

3.2.3 AC Transmission Line Data . . . 49

3.2.4 Transformers Data . . . 49

3.2.5 Load Data . . . 50

3.2.6 Shunt Device Data . . . 50

3.2.7 Bus Data . . . 51

4 Design of the Optimum Voltage Droop Control with Volt-Var method 53

4.1 Idea of choosing Q_{max} , Q_{min} and Q_{db} . . . 53

4.2 Dead-band Zone . . . 55

4.3 VDC Without Dead-band . . . 56

4.3.1 VDC Without Dead-Band for The Alcoutim PV Power plant (GA) . . . 56

4.3.2 VDC Without Dead-band for The São Marcos PV power plant (GB) . . . 57

4.3.3 VDC Without Dead-band for The Malhanito Wind Power plant (GC) . . . 58

4.3.4 VDC Without Dead-band for The Baixo Alentejo Wind Power plant (GD) . . . 59

4.4 VDC With Dead-band . . . 60

4.4.1 VDC With Dead-Band for The Alcoutim PV Power plant (GA) 61

4.4.2 VDC With Dead-band for The São Marcos PV power plant (GB) 61
4.4.3 VDC With Dead-band for The Malhanito Wind Power plant (GC) . . . 62
4.4.4 VDC With Dead-band for The Baixo Alentejo Wind Power plant (GD) . . . 63
4.5 VDC With Cubic Spline . . . 64
4.5.1 VDC With Cubic Spline for The Alcoutim PV Power plant (GA) 67
4.5.2 VDC With Cubic Spline for The São Marcos PV power plant (GB) . . . 68
4.5.3 VDC With Cubic Spline for The Malhanito Wind Power plant (GC) . . . 70
4.5.4 VDC With Cubic Spline for The Baixo Alentejo Wind Power plant (GD) . . . 70

5 Simulation with Different Case Scenarios 73
5.1 Scenario with Base Case ("B1") . . . 73
5.2 Scenario with Tangent Φ equal to 0 ("C0") . . . 74
5.3 Scenario with tangent Φ equal to -0.2 ("C1") . . . 75
5.4 Scenario with reactive power limits – voltage control scenario ("C2") 75
5.5 Scenario with Voltage Droop Control without Dead-band("C3") . . . 76
5.6 Scenario with Cubic Spline based Voltage Droop Control ("C4") . . . 77

6 Results from the Simulation 79
6.1 Voltage Profile on Tavira Substation . . . 79
6.1.1 Voltage Profile of Tavira substation on The Alcoutim PV plant-GA (400 KV) . . . 79
6.1.2 Voltage Profile of Tavira substation on The São Marcos PV plant-GB (150 KV) . . . 80
6.1.3 Voltage Profile of Tavira substation on The Malhanito and Baixo Alentejo wind power plants- GC & GD (63 KV) . . . 81
6.1.4 Analysis of The Voltage Profiles of Tavira Substation . . . 81

6.2 Reactive Power Profile on Tavira Substation 82
6.2.1 Reactive Power Profile of Tavira substation on The Alcoutim PV plant-GA (400 KV) 82
6.2.2 Reactive Power Profile of Tavira substation on The São Marcos PV plant-GB (150 KV) 82
6.2.3 Reactive Power Profile of Tavira substation on The Baixo Alentejo & Malhanito Wind Power Plant- GC & GD (63 KV) . . . 83
6.2.4 Analysis of The Reactive Power Profiles of Tavira Substation . 84
6.3 Validating the Voltage Droop Control Curves 85
6.3.1 Validation of the VDC curve without Dead-band : Case "C3" 85
6.3.2 Validation of the VDC curve with cubic Spline : Case "C4" . 87
6.4 Absorption of Reactive Power in Tavira Substation 89
6.5 Reactive Power Circulation in Tavira Substation 91

7 Conclusion **93**
7.1 Results from the simulation 93
7.2 Future Works and Areas Left Unexplored 96

List of Figures

1-1 Electricity Supply from diffeerent sources over the last ten years. Source: [1] 18

1-2 Installed capacity and peak evaluation over the last ten years. Source: [1] 19

1-3 Electrical Transmission Line map in Portugal. Source: [1] 21

1-4 Electricity capacity from 1915 to 2015. Source: [2] 23

1-5 Electricity generation from different sources in 2018 and 2019. Source: [1] 24

1-6 Capability factors of Renewable sources of last 10 years and CO_2 emission of last two years. Source: [1] 25

1-7 Generation profile with high share of wind generation (2017-04-30.) . 26

2-1 Reactive Energy Tariff from Tangent-ϕ. Source: [3] 30

2-2 Linear characteristic of the voltage-reactive power mode. Source: [4] . 33

2-3 Linear characteristic of the active power-reactive power mode. Source:[4] 34

2-4 Linear characteristic of the voltage-active power mode. Source: [4] . . 35

2-5 Voltage reactive power mode with undead-band droop. Source: [5] . . 38

2-6 Voltage reactive power mode with dead-band droop. Source: [5] . . . 39

2-7 Derivative of $\frac{\partial Q_v}{\partial V_{reg}}$ in different transition points . Source: [6] 40

2-8 Spline based voltage reactive power mode curve . Source: [6] 40

2-9 Improved derivative of $\frac{\partial Q_v}{\partial V_{reg}}$ in different transition points . Source: [6] 41

3-1 Scheme of the Tavira Substation 44

3-2 Scheme of the Overall Power System 47

3-3 Scheme of the Tavira Substation along with the Bus number 47
3-4 Machine Data of the Power System 48
3-5 Plant Data of the Power System 48
3-6 AC Line Data of the Power System 49
3-7 Transformer Data of the Power System 50
3-8 Load Data of the Power System 50
3-9 Shunt Device Data of the Power System 51
3-10 Bus Data of the Power System 51

4-1 P vs Q/P_{max} curve for type-C and type-D generator (V < 110 KV) . 54
4-2 P vs Q/P_{max} curve for type-D generator (V $\geq$ 110 KV) 55
4-3 VDC Curve Without Dead-band for The Alcoutim PV Power plant (GA) 57
4-4 VDC Curve Without Dead-band for The São Marcos PV power plant (GB) 58
4-5 VDC Curve Without Dead-band for The Malhanito Wind Power plant (GC) 59
4-6 VDC Curve Without Dead-band for The Baixo Alentejo Wind Power plant (GD) 60
4-7 VDC Curve With Dead-band for The Alcoutim PV Power plant (GA) 62
4-8 VDC Curve With Dead-band for The São Marcos PV power plant (GB) 63
4-9 VDC Curve With Dead-band for The Malhanito Wind Power plant (GC) 64
4-10 VDC Curve With Dead-band for The Baixo Alentejo Wind Power plant (GD) 65
4-11 Cubic Spline between two lines. Source: [6] 65
4-12 Cubic Splines in the dead-band zone for The Alcoutim PV Power plant (GA) 68
4-13 VDC Curve with Cubic Spline for The Alcoutim PV Power plant (GA) 68
4-14 Cubic Splines in the dead-band zone for The São Marcos PV power plant (GB) 69
4-15 VDC Curve with Cubic Spline for The São Marcos PV power plant (GB) 69

4-16 Cubic Splines in the dead-band zone for The Malhanito Wind Power plant (GC) 70
4-17 VDC Curve with Cubic Spline for The Malhanito Wind Power plant (GC) 71
4-18 Cubic Splines in the dead-band zone for The Baixo Alentejo Wind Power plant (GD) 71
4-19 VDC Curve with Cubic Spline for The Baixo Alentejo Wind Power plant (GD) 72

6-1 Voltage Profile of Tavira substation on The Alcoutim PV plant-GA (400 KV) 80
6-2 Voltage Profile of Tavira substation on The São Marcos PV plant-GB (150 KV) 80
6-3 Voltage Profile of Tavira substation on The Malhanito and Baixo Alentejo wind power plants- GC & GD (63 KV) 81
6-4 Reactive Power Profile of Tavira substation on The Alcoutim PV plant-GA (400 KV) 82
6-5 Reactive Power Profile of Tavira substation on The São Marcos PV plant-GB (150 KV) 83
6-6 Reactive Power Profile of Tavira substation on The Malhanito Wind Power Plant- GC (63 KV) 83
6-7 Reactive Power Profile of Tavira substation on The Baixo Alentejo Wind Power Plant- GD (63 KV) 84
6-8 Validation of The Case “C3” for The Alcoutim PV plant-GA (400 KV) 85
6-9 Validation of The Case “C3” for The São Marcos PV plant-GB (150 KV) 86
6-10 Validation of The Case “C3” for The Malhanito Wind Power Plant-GC (63 KV 86
6-11 Validation of The Case “C3” for The Baixo Alentejo Wind Power Plant- GD (63 KV) 87

6-12 Validation of The Case “C4” for The Alcoutim PV plant-GA (400 KV) 87
6-13 Validation of The Case “C4” for The São Marcos PV plant-GB (150 KV) 88
6-14 Validation of The Case “C4” for The Malhanito Wind Power Plant-GC (63 KV 88
6-15 Validation of The Case “C4” for The Baixo Alentejo Wind Power Plant- GD (63 KV) 89
6-16 Reactive Power Absorption for The Alcoutim PV plant-GA (400 KV) 90
6-17 Reactive Power Absorption for The Malhanito Wind Power Plant- GC (63 KV) 90
6-18 Reactive Power Absorption for The Baixo Alentejo Wind Power Plant-GD (63 KV) 91
6-19 Reactive Power Circulation Curve for The Tavira Substation 92

7-1 Reactive Power Dependence on Voltage 94

List of Tables

3.1 São Marcos PV power plant Data 46

4.1 VDC Data Without Dead-band for The Alcoutim PV Power plant (GA) 57
4.2 VDC Data Without Dead-band for The São Marcos PV power plant (GB) 58
4.3 VDC Data Without Dead-band for The Malhanito Wind Power plant (GC) 59
4.4 VDC Data Without Dead-band for The Baixo Alentejo Wind Power plant (GD) 60
4.5 VDC Data With Dead-band for The Alcoutim PV Power plant (GA) 61
4.6 VDC Data With Dead-band for The São Marcos PV power plant (GB) 62
4.7 VDC Data With Dead-band for The Malhanito Wind Power plant (GC) 63
4.8 VDC Data With Dead-band for TheBaixo Alentejo Wind Power plant (GD) 64

Chapter 1

Introduction

From the last three decades integration of a large scale renewable energy sources (RES), in the electrical distribution and transmission system has been observed and it is changing the scenario of the power system. The nature of the renewable energy sources specially the non-dispatchable or variable energy sources (solar and wind) are very dynamic. With the change of the weather and the time of the day, the output from the renewable energy changes significantly [7]. For solar energy the most significant factor is the solar irradiance and for wind it is the wind speed. Whatever the energy is produced by the RES the important thing is to meet the load demand. The rate of installation of the renewable energy or the distributed generation is increasing all over the world and day by day it is being integrated to the transmission and distribution system. In the Portugal wind alone is representing more generation of electricity than the load in valley periods as occurred in the recent years. Although the penetration of the RES in the distribution or transmission system sometimes have positive consequences such as improved power quality, smaller power losses, competitive and deregulated electricity markets [8] but it is also creating problems in the electrical power system such as feeder overloads, lack of protection, power quality disturbances, frequency variations and voltage variations [9] among which the voltage and frequency variations are the most challenging one. Advanced control methods regarding the frequency variations has been developed but the variation of voltage is still a big concern.

With the increase amount of integration of RES specially with the non-dispatchable renewable resources the system operator (SO) can not rely only on the synchronous generators for the voltage and frequency control. For controlling the voltage in the power system different equipemts has been introduced such as shunt devices, tap changing transformer, different automatic voltage regulation (AVR) devices etc. and it has been observed the voltage has direct impact on the reactive power. In distributed generation by means of reactive power absorption or generation the voltage can be controlled significantly [10]. Taking this fact into account over the years different voltage droop control characteristics has been developed that interacts with the reactive power. Among them the voltage-reactive power mode is the most efficient one and well popular among the system operators (SO). But injection or absorption of reactive power is not an easy task and it requires proper control in the distributed generation. If the injection of reactive power is controlled in proper way it can significantly increase the active power generation of the distributed generation [11]. However this can also increase the power loss in the system [12]. the reactive power shortage can also create voltage collapse [13]. With high share of RES the coordination of voltage and reactive power is more difficult and that creates problem for the voltage and reactive power management.

To overcome this challenge, in this thesis a new cubic spline based voltage reactive power based droop control has been developed for the optimal management of the voltage and reactive power. This droop control was designed and simulated with the help of the Portuguese national transmission system operator- Redes Energéticas Nacionais (REN). The main motive of this droop control was to come up with an optimal solution of the voltage control with the high share of RES that is existing and to be built in the Portuguese transmission system. The analysis of this thesis was done by taking real data of 24 hours of operation provided by REN. The simulations were performed in the power system simulator named PSS®E by Siemens Power Technologies International (Siemens PTI). To verify the efficiency of the the new droop control method some other operational scenarios were analyzed and simulated for comparison.

1.1 Company Profile of REN - Redes Energéticas Nacionais

Redes Energéticas Nacionais (REN) is a Portuguese Energy sector company which has activities mainly in two business sectors. The first one is the electricity sector in which it is primarily engaged in the transmission of very high voltage (VHV) and high voltage (HV) electricity. It also manages and operates the overall technicalities of the National electricity system of Portugal. The second one is the gas sector in which it offers the technical management of the National Natural Gas System of Portugal. REN undertakes the transmission of natural gas from producers to end distributors and industrial consumers. It also runs regasification of LNG and the underground storage facility of natural gas for Portugal. Beside energy sector and gas sector REN also has a telecommunication segment which operates through the name Rentelecom. Rentelecom includes a range of services such as operation of telecommunication infrastructure, rental of fiber optic cables, services, and consultancy in telecommunication system etc [14].

In 1994 REN started its journey as one of Portugal's sole electricity provider. In November 2000, a legislation and liberalization were performed by the Portuguese Government which made REN as the transmission and distribution system operator of electricity for the Portuguese Republic. In 2006, the gas industry faced similar legislation and liberalization. After this transition REN was structured as the Portugal's transmission operator for both electricity and Natural gas [15]. REN also has activities outside of Portugal and Europe. Back in February 2017, REN obtained 42.5% stake in Electrogas which is a Chilean company that owns 165.6 kms of reversible gas pipelines operating in Chile. On the 1st of October of 2019, REN obtained the entire share capital of Transemel that owns and operates the 92 kms of electricity transmission lines and five substations, located mainly in northern Chile [14].

REN is one of the most efficient European energy transmission system operators for so many years meeting all the required quality and safety criteria. It is creating value for its shareholders within a framework of sustainable development.

1.2 Overview of Electrical Generation and Transmission Systems in Portugal

The energy consumption in Portugal rose by a factor of 15 in 125 years [2]. The consumption of electricity supplied on Portugal from the public grid was totalled 50.3 TWH in 2019 which was 1.1% lower than the previous year. The highest electricity consumption was recorded in the year 2010 which was 3.6% above the consumption recorded in 2019. If we investigate the last 10 years electricity supply of Portugal, we get to see that most of the electricity supply comes from the natural gas and wind [1].

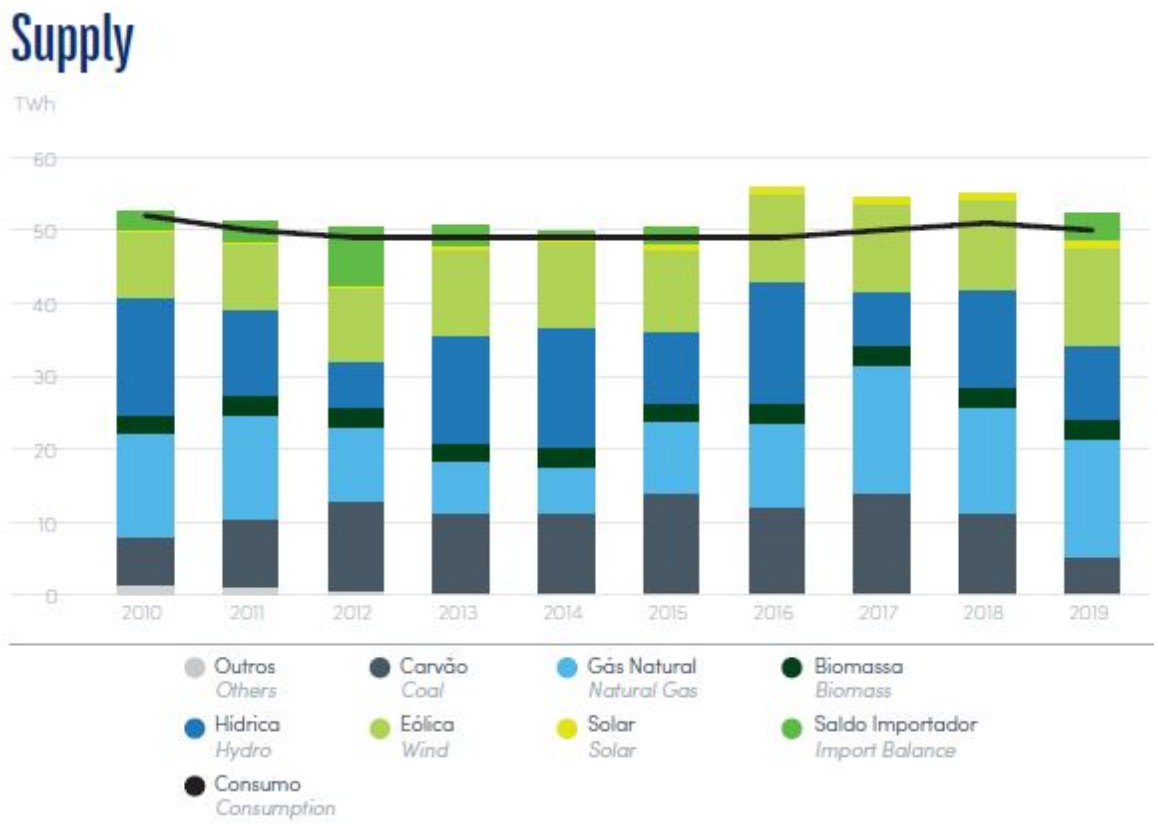

Figure 1-1: Electricity Supply from diffeerent sources over the last ten years. Source: [1]

The total installed capacity at the end of the year 2019 was 20208 MW whereas in 2018 it was 19970 MW. Among the 20208 MW of installed capacity 13847 MW came from the renewable energy sources and 6361 MW came from the non-renewable. The

installed capacity from the hydro and wind power plant at the end of the year 2019 was 7216 MW and 5208 MW, respectively. The peak generation started increasing from the year 2013 also the peak load did not move to much from the last 3 years. From figure 1-2 it can be seen that the generation and load curve from the last 10 years is quite stable and the gap between the generation and load curve is increasing in each year which shows the surplus of the generation in Portugal [1].

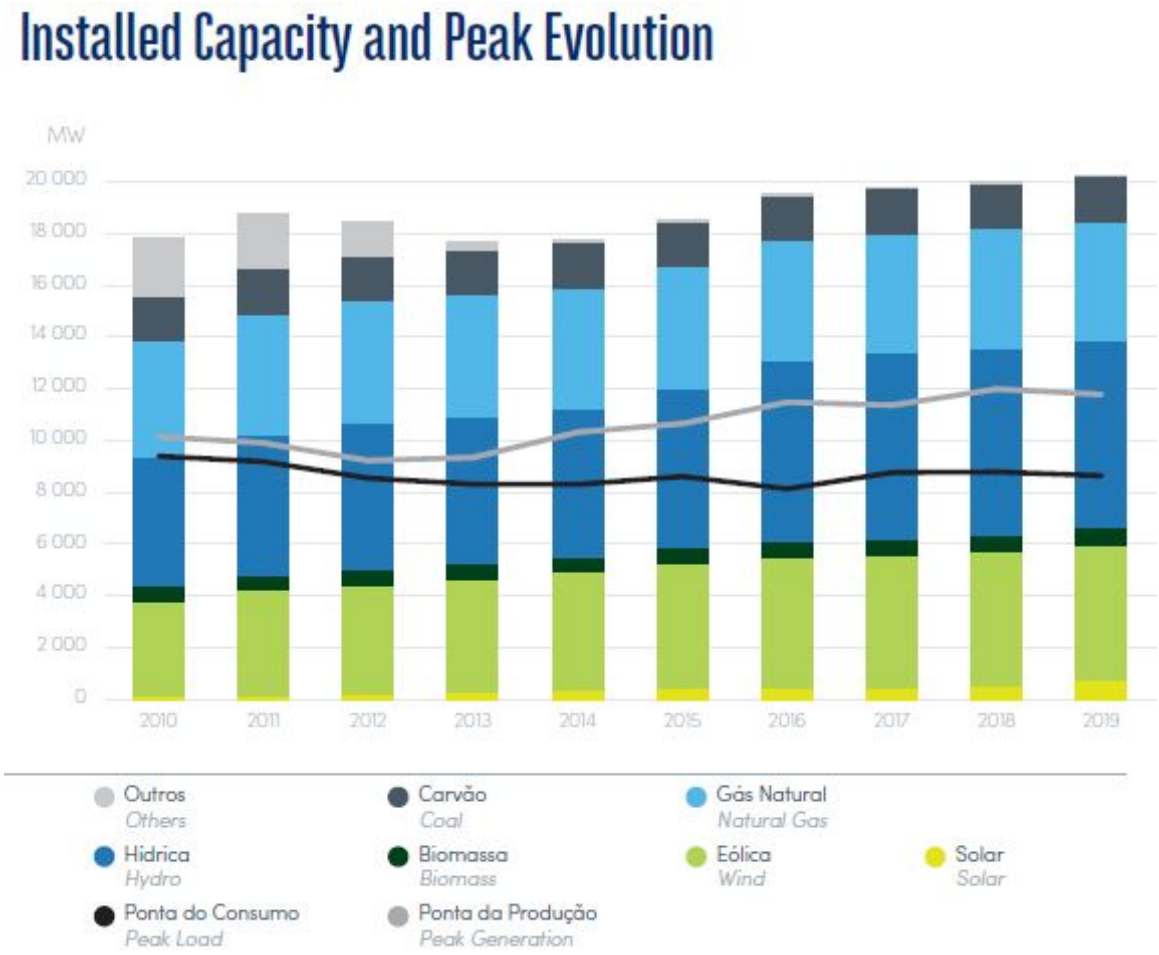

Figure 1-2: Installed capacity and peak evaluation over the last ten years. Source: [1]

According to the data given by REN till the end of the year 2019 the national transmission grid of Portugal has total 9002 kms of lines among which 2711 kms are from 400 KV, 3746 kms are from 220 KV, and 2544 kms are from 150 KV lines. The transformer capacity of the Auto-transformers (VHV/VHV) are of 14470 MVA, Transformers of VHV/HV are of 23673 MVA and VHV/MV Transformers have 320

MVA capacity [1]. The 400 kV transmission lines mainly spreads from north to south near the coast from the Alto Lindoso power station in the north to the Algarve in the south. In west to east it interconnects with the Spanish grid. The 220 kV lines basically run between Lisbon and Oporto, diagonally it spreads between Miranda do Douro and Coimbra, along with the River Douro and in Beira Interior. The 150 KV transmission lines were the first one to be built in 1951 and it is now complimenting the extra high voltage grid [14]. There is a new transmission line of 400 KV in Alcochete – Fanhões. An increase of transformer capacity has been made at the Lavos (400/60 kV), Recarei and Zambujal (220/60 kV) and Sines (150/60 kV) substations. Remodelling has also been made of the Riba d'Ave- Recarei 1 and Rio Maior - Alto Mira lines at 400 kV, and Porto Alto - Palmela 2 at 150 kV. In 2019, the first MAT underwater infrastructure was put into service in Portugal by REN. It is of around 17 kms of underwater cable which connects the renewable energy production off the coast of Viana do Castelo. Although this cable was designed for the operation at 150 kV but at this stage it is operating at 60 kV [1].In figure 1-3 we can see the electrical transmission system map along with the different voltage levels.

Figure 1-3: Electrical Transmission Line map in Portugal. Source: [1]

1.3 Government Policy and legislative framework of REN

REN (Rede Eléctrica Nacional) was certified under the ownership unbundling model in 2014 as a sole transmission system operator in Portugal [16]. It now owns and maintains the overall electrical transmission system of Portugal on an exclusive basis. It has a wide range of legal and regulatory standards and it performs its activities under public service concession contract. REN aims to design an electricity market which will operate to the benefits of all consumers regardless of their size. It is ensuring a better, competitive, more secure, and sustainable energy supply in the European Union [14]. The General Directorate for Energy and Geology (DGEG), Regulatory Entity for Energy Services (ERSE) and Autoridade da Concorrência (AdC) are the responsible entity for regulating the energy sector in Portugal [17]. Under the regularity context of electricity that is imposed to REN on a 50 years concession the main functions of REN as an entity is the planning, operation, construction, and maintenance of the high voltage transmission grid along with the international connections. It also includes the technical operation of the electrical market planning and the compensation of energy imbalances. REN is also responsible to impose transmission grid tariff. These Directives into Portuguese law began in 20^{th} June 2011 under the Decree-Law 78/2011 for the electricity sector [14]. REN also performs it activities maintaining the Directive 2009/72/EC of the European Parliament and of the Council of 13^{th} July 2009 which concerns the common rules for the internal market [18].

1.4 RES Integration in Portuguese National Grid Systems

In Portugal there is a high dependence on the imported fossil fuels for generating electricity which leads to the renewable energy projects. In Portugal the installed electricity capacity since 1915 is provided in figure 1-4 where we can see the most

significant changes that occurred in the 1950s and 1960s, where the installed electricity was increased more than from 247 to 1524 MW. It was a golden year for the hydro-power generation. After the year 1995 electricity production from wind became very popular and it increased drastically in the following years. With the modernization of the country, in between 1980 and 1990 consumption was reached more than doubled and to meet this needs several thermal power plants were built. This increasing thermal power production increased the use of coal. Back in the year 2000 the combustible fuels accounted for the highest share of installed capacity which was 57% of the total installed capacity. The installed capacity from hydro-power was accounted 45% and from other renewable energy sources it was 3%. By the year 2015 the installed capacity of combustible fuels and hydro-power had fallen to 38% and 33%, respectively. The installed capacity from the wind power was recorded 23.7% of the installed capacity whereas around 2% was recorded from solar energy and around 3% from other renewable energy sources such as geothermal, tide and wave. The main driving force of the increased installed capacity in electricity of the 21^{st} century is due to the boom in wind power production [2].

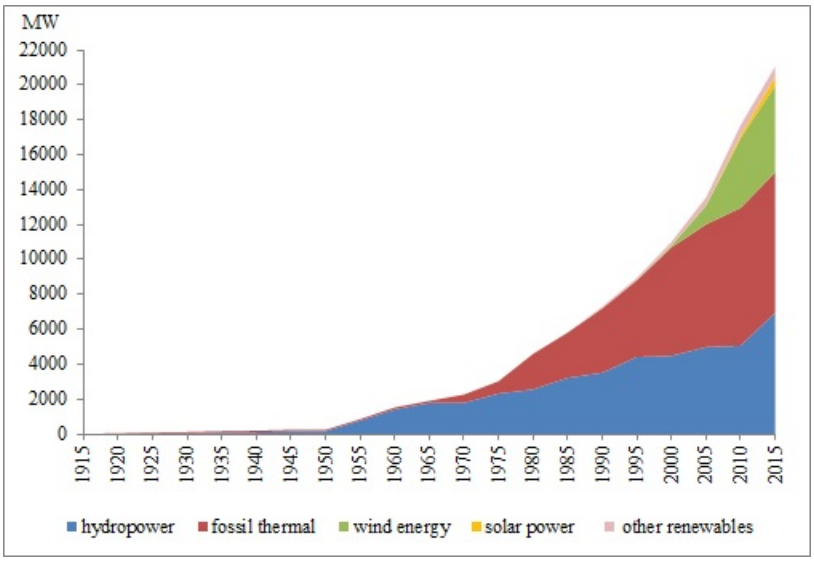

Figure 1-4: Electricity capacity from 1915 to 2015. Source: [2]

If we investigate the last 2 years data, it can be seen that the dependence on the non-renewable sources for electricity is less than the renewable sources. In 2019, from

renewable sources 51% supply came which is slightly below the 52% in the previous year. Wind farms gave the highest ever share of 26% among the 51% consumption with a productivity rate of 1.07. Hydroelectric power stations had a share of 17% with a productivity rate of 0.81. Other renewable sources such as biomass accounted for 5.5% of consumption and solar as 2.1% of consumption. From the non-renewable source, coal fired power stations had a share of 10% whereas while natural gas, including combined cycle and co-generation plants had a share of 32%. 7% of the national consumption was from the foreign import [1]. These statistics is a clear identification that Portugal is giving priority on renewable Energy generation for cleaner and emission free energy supply.

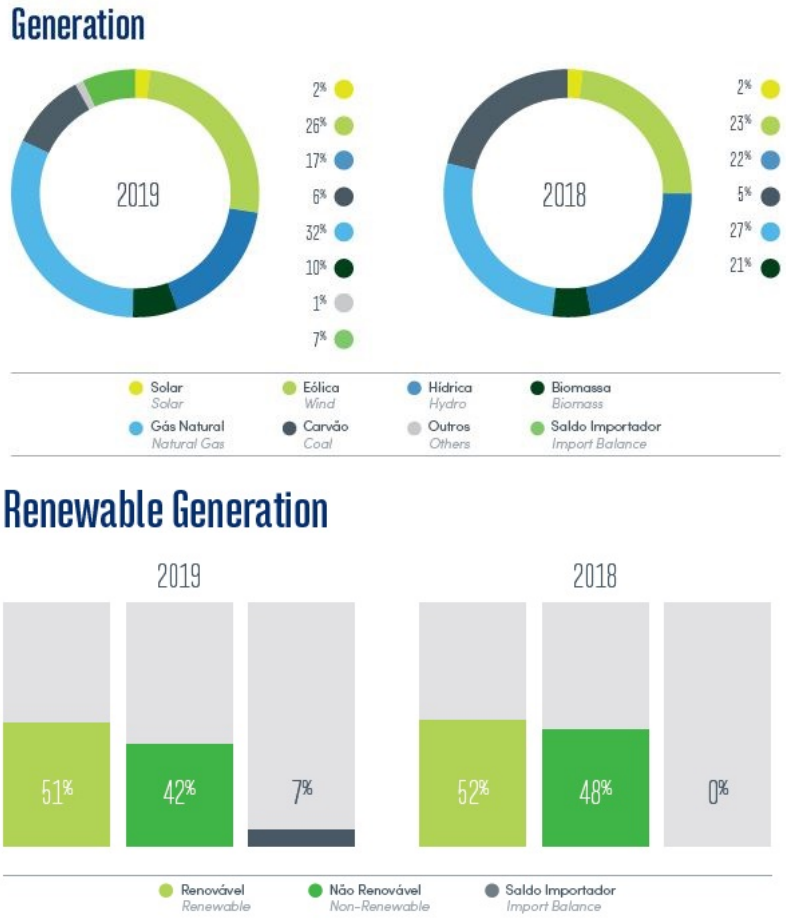

Figure 1-5: Electricity generation from different sources in 2018 and 2019. Source: [1]

The reduction of CO_2 emission in the year 2019 from the coal power generation

is another sign that Portugal is determined to have a dependency on the renewable energy supply in the upcoming years. Also, if we look into the capability factors [1] from the renewable sources over the last 10 years, it can be seen that although it is varying over the years but the dependency on the renewable energy sources is clearly visible.

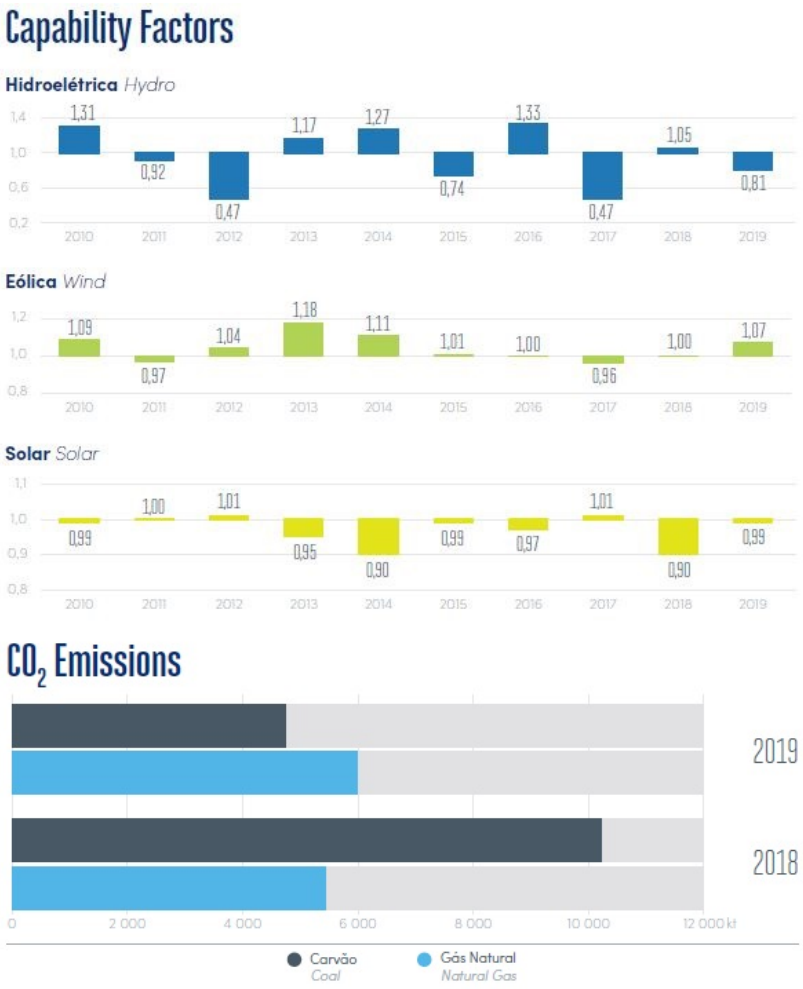

Figure 1-6: Capability factors of Renewable sources of last 10 years and CO_2 emission of last two years. Source: [1]

Generation profile of different energy resources over the last few years shows a huge share of wind power, specially in the valley periods. In 2016 and 2017 wind alone represented more than the load which were 106% in 2016 and 109% in 2017.

[1]The capability factor is the ratio of actual electricity production by a power plant to the theoretically possible electricity production in a year if it is operating continuously at full power during the same period [19]

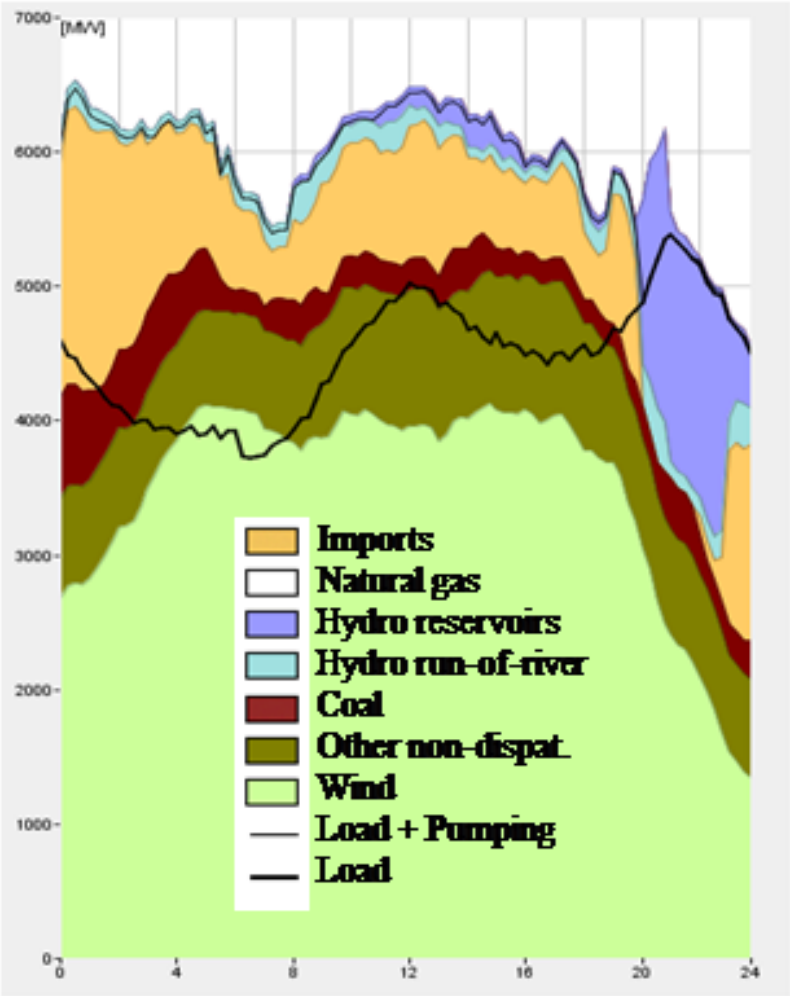

Figure 1-7: Generation profile with high share of wind generation (2017-04-30.)

1.5 Objective of the Thesis

The main objective of this thesis was to design an optimum voltage droop control for the high share of renewable energy systems in the Portuguese transmission system. The whole analysis was done considering the data given by the Portuguese transmission system operator- REN. Here the term optimum is used because with the integration of the multiple RES in a substation, not only the voltage stability should be made but also the reactive power management will be made considering the voltage droop curves (VDC) that should be designed for each RES. These curves represent the dependence of absorbing or generating reactive power in percentage of rated active power of the power plants. This control method will be designed as one

of the operational case scenarios and will be compared to different case scenarios for showing its appropriateness and effectiveness.

1.6 Thesis Structure

Towards the previously mentioned objectives, the thesis work was developed and structured as follows.

Chapter-1: Introduction

This represents the motivation of the works that will be carried out in this thesis.

Chapter-2: State of Art

This chapter reviews the research literature of the different droop control strategy available in electrical power systems. The undeadband and deadband zone of the voltage droop curve (VDC) curve will also be discussed along with the necessity of the cubic spline in the VDC curve.

Chapter-3: Design of the Power System in PSS®E

In this chapter the process of designing the base case of the power system is discussed. For the simulation purpose of this thesis the software PSS®E was used which is a high-performance transmission planning and analysis software by Siemens.

Chapter-4: Design of the Optimum Voltage Droop Control with Voltage Reactive Power (volt-var) method

In this chapter the design process of the VDC curves are discussed. Both the undeadbad and deadband based VDC curves are deigned in Excel. Based on the formulation of the cubic spline a new VDC curve is the main focus of this chapter.

Chapter-5: Simulation with different Scenarios

The whole simulation process of PSS®E and the interaction with the VDC curves

which are designed in Excel is discussed in this chapter. The simulations are performed for all the operational case scenarios and the process of simulation varies for most cases. The whole simulation process of PSS®E and the interaction with the VDC curves which are designed in Excel is discussed in this chapter.

Chapter-6: Result from the simulations

This chapter compares the different case scenarios along with the effectiveness of the voltage droop control method. Here different charts will be provided to show the effectiveness of the voltage droop control method for the new integrated RES in the examined substation.

Chapter-7: Conclusion

This chapter indicates the conclusion reached at the end of the thesis work and the future works that can be performed in the relevant research area.

Chapter 2

State of Art

This chapter incorporates the whole theory behind this thesis. As we progress to the different operational case scenarios we need to know the theory behind those.To manage the voltage regulations different methods have been used over the years. Normally from the distributed grid operator and also from transmission side for the tariff purpose the reactive energy tariff management is used which utilizes the tangent phi system. This system is good enough for tariff management system but it requires a reactive optimal power flow (ROPF) tool for efficient voltage management which is very complex to implement.

The other way of controlling the voltage is the use of automatic voltage regulator. With this the variation of the voltage can be controlled by means of voltage control equipments placed in several places of the power systems such as transformers, feeders and generators. This voltage control equipments are necessary in power systems but without the efficient reactive power management it is not that much useful and sometimes it might create system mismatch on other parts of the power systems.

With the advancement of the electrical power systems more robust and advanced voltage management systems has been developed which takes into account the droop control method. This chapter introduces all this control methods along with reason behind choosing a specif one.

2.1 Reactive Energy Tariff: Tangent-ϕ

The reactive energy tariff is a process in which a price is applied to the distribution network and the transmission network for maintaining the reactive energy production capacity. A scale is set based on the tangent(ϕ) rule where specific penalties are applied when this scale is exceeded [20]. According to the tangent(ϕ) rule reactive power is proportional to the active power.In the distributed generation, reactive power is proportional to the wind speed or solar radiation and not according to the grid condition. In Portugal the tangent(ϕ) is set as $+0.3$ in the distribution level while in the transmission level it is -0.2. Using this reactive energy tariff control method more suitable behaviour is expected in terms of voltage regulation but it requires reactive optimal power flow (ROPF) tool for calculating the set point for each hour and sending it to the wind farms and photo-voltaic generators which is really difficult to implement.Also using the distributed generation the voltage set points in real time is required from the ROPF to implement the secondary voltage control scheme which at present is not feasible.

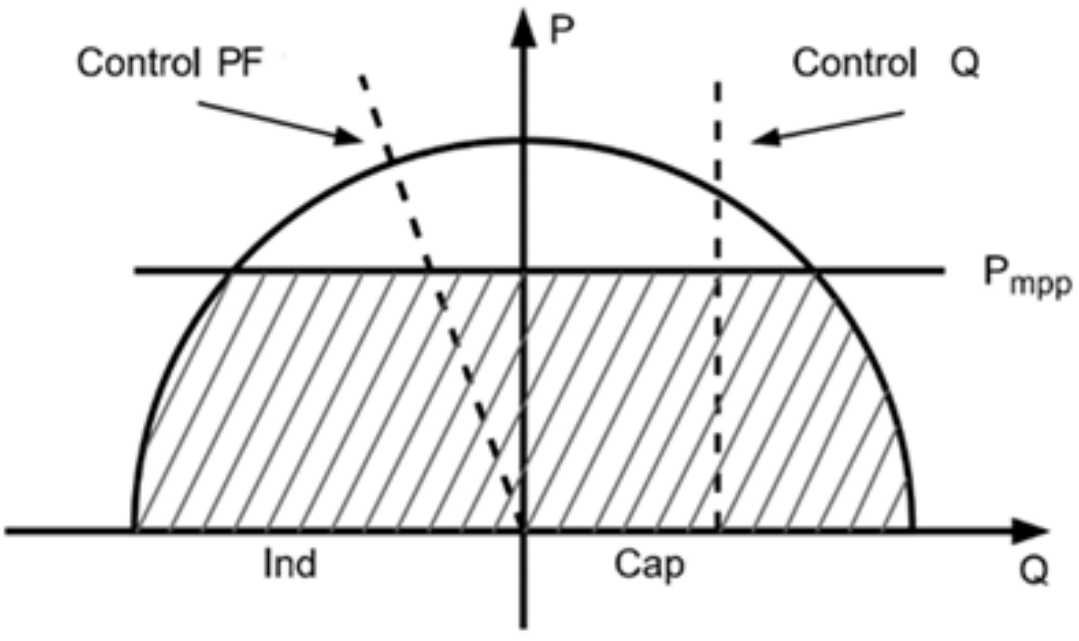

Figure 2-1: Reactive Energy Tariff from Tangent-ϕ. Source: [3]

2.2 Voltage Regulation With Reactive Power Limits

The voltage regulation With reactive power limits is used mainly in synchronous generator application. The renewable energy plants such as wind power plants and photo-voltaic plants work as synchronous generators in electrical power systems [21]. With the fluctuation of wind speed and solar radiation the problem with the distributed generation is the variable speed and in-stable output voltages. To overcome the voltage fluctuation the voltage regulation With reactive power limits technique is used to control and monitor the voltage by switching the multi-tapped transformer to ensure the set point voltage [22]. Generally there is a limit for absorbing and generating reactive power. Usually the limit is set on a specific percentage of the power plant‘s rated power.To maintain the set point voltage of the plant where the voltage regulation is required, the reactive loads are divided between the synchronous generators on the point of interconnection based on the reactive power limits. The problem with this sort of control scheme is that although the voltage can be maintained exactly same as the set point but the reactive power management is inefficient and not well planned.

2.3 Voltage and Reactive Power Control

With the high share of RES in the electrical transmission system there is always an effect of voltage fluctuation and reverse power flows. These things are creating new challenges for the reactive power control [23]. The voltage fluctuation equation in the transmission line due to the addition of RES can be given by,

$$\Delta V = \frac{R(P_L + P_{DG}) + X(Q_L + Q_{DG)}}{V_N} \tag{2.1}$$

Here Δ V is the voltage fluctuation, R and X are the resistance and reactance of the transmission line, P_L and Q_L are the active and reactive power consumption in the

load, P_{DG} and Q_{DG} are the active and reactive powers of the distributed generation plants and V_N is the nominal voltage.

From the equation it can be seen that the reactive power of the distributed generation Q_{DG} does have impact on the voltage fluctuation. Thus controlling Q_{DG} can eventually control the voltage level. However in power system the voltage regulation is decided by the line resistance and reactance (R/X) ratio. In Medium and High voltage levels the R/X ratio is smaller than the low voltage level. So in the MV and HV level the reactive power support is more relative than LV level. According to the IEEE $1547-2018$ standard, there has been new rules of interconnection of the distributed energy resources in the existing electrical power systems [24]. According to these rules the voltage management in the grid tied distributed generation plants can be done in various ways. Such as, Constant Power Factor method [25], Voltage-Reactive Power method Q(V) [26], Active Power-Reactive Power method Q(P) [27], Constant Reactive Power method and the new addition which is Voltage-Active Power method P(V) [4].

2.3.1 Constant Power Factor Mode (Default, Unity)

According to this method the distributed energy resources should maintain a constant or unity power factor regardless of their output. The target power factor setting is adjusted by the EPS operator. The adjustment can be done locally or remotely. The response time to maintain the constant power factor should be 10s or less [4]. This reactive power management is simple and it can easily mitigate the voltage but the problem with this management is that it absorbs reactive power at all time even when it is not needed [28].

2.3.2 Voltage Reactive Power Mode (Volt-Var)

In this mode the distributed energy resource should control its reactive power output as the function of the voltage by means of a piece-wise linear characteristic of a voltage-reactive power. The piece-wise linear characteristic is defined by the EPS

operator locally or remotely in a way that it operates in a adjustable range [4]. In figure 2-2 we can see the linear characteristic linear characteristic of the voltage-reactive power where different zone of the curve is shown. Here V_1 is the lower voltage limit in per unit below which the reactive power is maximum. Also V_4 is the upper voltage limit in per unit above which the reactive power is minimum. V_L and V_H are the lower and upper voltage limit for the continuous operation of the Distributed generation plant. Also there is a dead-band zone defined with specific voltage limit for which the reactive power is zero [29].

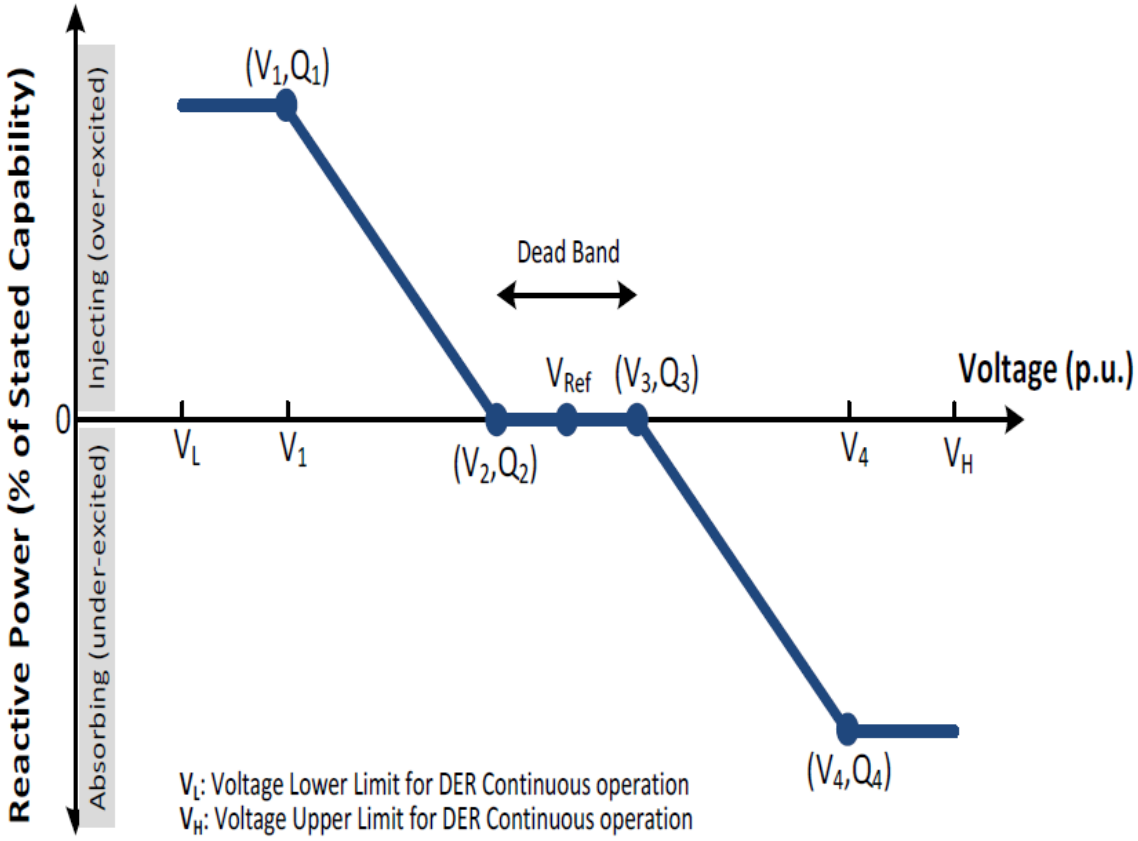

Figure 2-2: Linear characteristic of the voltage-reactive power mode. Source: [4]

The best thing about this method is that it can control both the high and low voltage profile while not creating any additional reactive power. The challenging thing about this control method is the curtailment w/o headroom [28], and also in the transition of the linear curves specially in the corner points the reactive power management is not efficient.

2.3.3 Active Power-Reactive Power Mode (Watt-Var)

In this mode the distributed energy plants control the reactive power as a function of its active power power based on a piece-wise linear characteristic of the active and reactive power. In no case shall the response time be greater than 10s [4]. Again the characteristic curve is adjusted by the EPS operator and the values are defined in a optional adjustable range.

In figure 2-3 we can see the linear characteristic linear characteristic of the active-reactive power where different zone of the curve is shown. Here $P_3^{'}$ is the active power limit below which the reactive power is maximum. Below $P_2^{'}$ the generation plant is over excited and injecting reactive power. Also P_3 is the active power limit above which the reactive power is minimum.Above P_2 the generation plant is under excited and absorbing reactive power. Also there is a dead-band zone defined with specific active power limit for which the reactive power is zero. The power setting curve is adjusted by the EPS operator within an adjustable range locally or remotely.

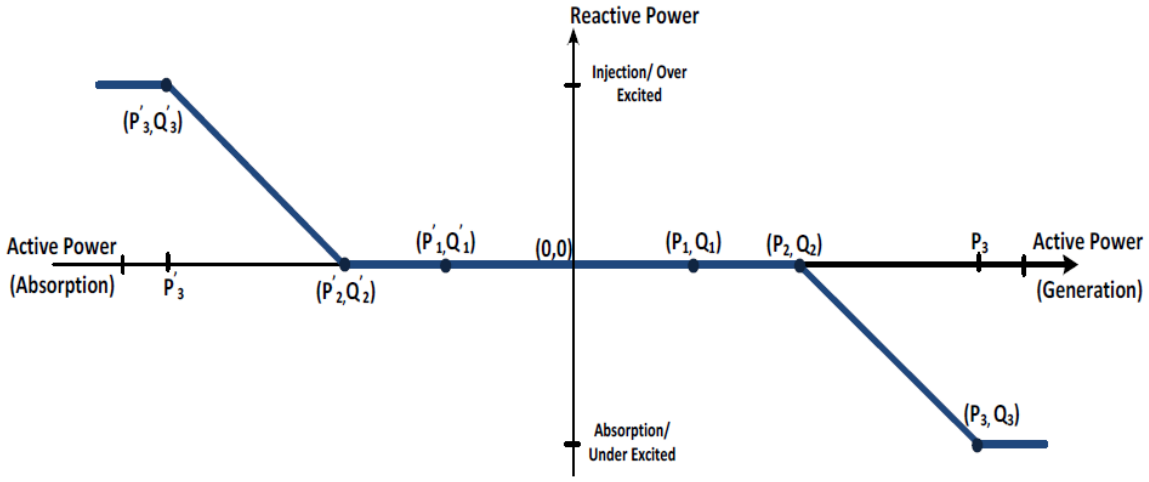

Figure 2-3: Linear characteristic of the active power-reactive power mode. Source:[4]

2.3.4 Constant Reactive Power Mode

In this mode the distributed generation plant should maintain a constant reactive power within a specific range adjusted by the EPS operator. While defining the

range the injection and absorption of the reactive power should be considered. The response time to adjust the reactive power should be 10s or less [4].

2.4 Voltage Active Power Mode (Volt-Watt)

In this method the distributed generation plants limit the active power output as a function of the voltage based on a voltage-active power piece-wise linear characteristic. There are basically two linear characteristics. The characteristic curves operate only when the previously explained voltage reactive power modes are enabled.

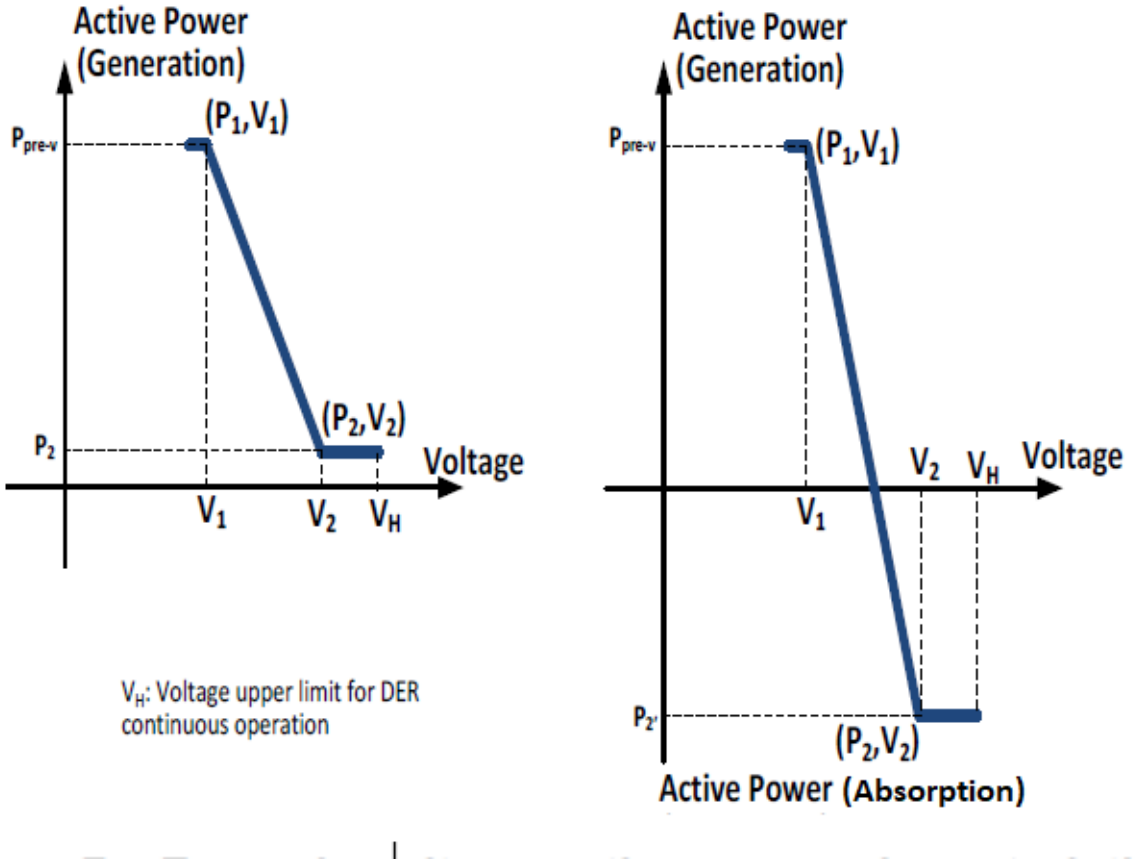

Figure 2-4: Linear characteristic of the voltage-active power mode. Source: [4]

For the distributed generation which is not absorbing active power, P_2 is the minimum set point for active power generation due to over-voltage. If P_2 is outside the continuous operation region of the distributed generation plant, the active power

generation is allowed to be reduced to the minimum capability of the distributed generation plant.

For the distributed generation which is either absorbing or injecting active power, $P_2^{'}$ is the maximum set point for active power generation due to system over-voltage. If $P_2^{'}$ is outside the continuous operation region of the distributed generation plant, the active power absorption is allowed to be reduced to the maximum absorption capability of the distributed generation plant [4].

The best thing about this management is that it can increase the hosting capacity for the active power while mitigating the impacts from the reconfiguration circuits. Although it can also results some curtailment [28].

2.5 Recommendation for the Voltage Reactive Power Mode

The most recommended voltage management setting according to IEEE standard $1547-2018$ is the voltage reactive power mode (volt-var) [28]. The reasons are many and they are listed below.

- The voltage reactive power mode control the voltage by using the lowest reactive power.
- There is no conflict with other voltage management system existing in the system.
- This is the management system that can be utilized in the future.
- It considers the inverter headroom to reduce real power losses.
- The voltage and reactive power settings are really efficient which makes it a standard system.

Although the voltage reactive power (volt-var) mode is considered as the standard mode for reactive power management but to avoid the numerical problems with the

reactive power in the corner points of the voltage reactive linear characteristic, the splines are used [5]. The splines make the corner points smooth and the reactive power management becomes more effective and efficient.

2.6 Consideration of Dead-band and Undead-band Zone in the Voltage Reactive Power Mode

In the voltage droop control strategy by means of reactive power control with the voltage reactive power mode the linear characteristics of the voltage and reactive power is an important phenomenon. While defining the linear curve usually a dead-band is considered. If it is not considered then with the undead-band curve we are not considering the disturbed operation. Dead-band and undead-band droop controls are usually the combinations of the voltage margin along with the voltage droop control strategies [30]. The most efficient voltage reactive power mode is with the deadband along with the splines in the corner points.

2.6.1 Undead-band Droop in the Voltage Reactive Power Mode

In the undead-band droop control, relation between the voltage and the reactive power is always linear. For this case there is not voltage range in which the reactive power is constant or zero.So in case of the disturbed operation the reactive power management is different from the voltage reactive power mode with dead-band [30]. If we look into the figure 2-5 we can see in between V_1 and V_4 there is a linear characteristic from reactive power Q_1 to Q_3. In between V_1 and V_4 there is no range for which the reactive power is constant and thus we are considering an undead-band zone.

The main disadvantage in the undead-band droop control is that it is a rigorous process and it has vulnerability while determining the operating points in the transient events [31].

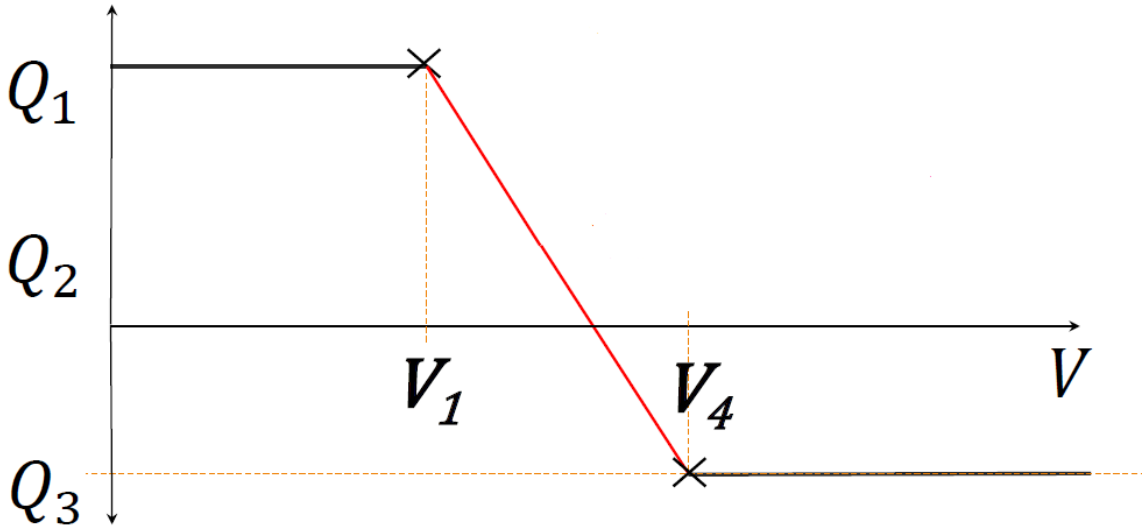

Figure 2-5: Voltage reactive power mode with undead-band droop. Source: [5]

2.6.2 Dead-band Droop in the Voltage Reactive Power Mode

In the dead-band droop control the relation between the voltage and reactive power is piece-wise linear. In the dead-band it has a constant or zero reactive power for a given voltage range. Outside this voltage range a negative slope characteristic is followed for the absorption of reactive power and a positive slope characteristic is followed for the injection of the reactive power. If we look into the figure 2-6 we can see that there is a dead-band zone within the voltage range V_{dblow} and V_{dbhigh} where the reactive power Q_{db} is constant. V_{dblow} is the voltage in per unit above which the reactive power is Q_{db} whereas V_{dbhigh} is the voltage in per unit below which the reactive power is Q_{db}. The voltage range in the dead-band is usually taken as 0.98 to 1.02 per unit voltage [5].

The dead-band based droop control works efficiently under both normal and unusual condition. The advantage of using dead-band is that it improves the stability and damping of the synchronous generators [32].

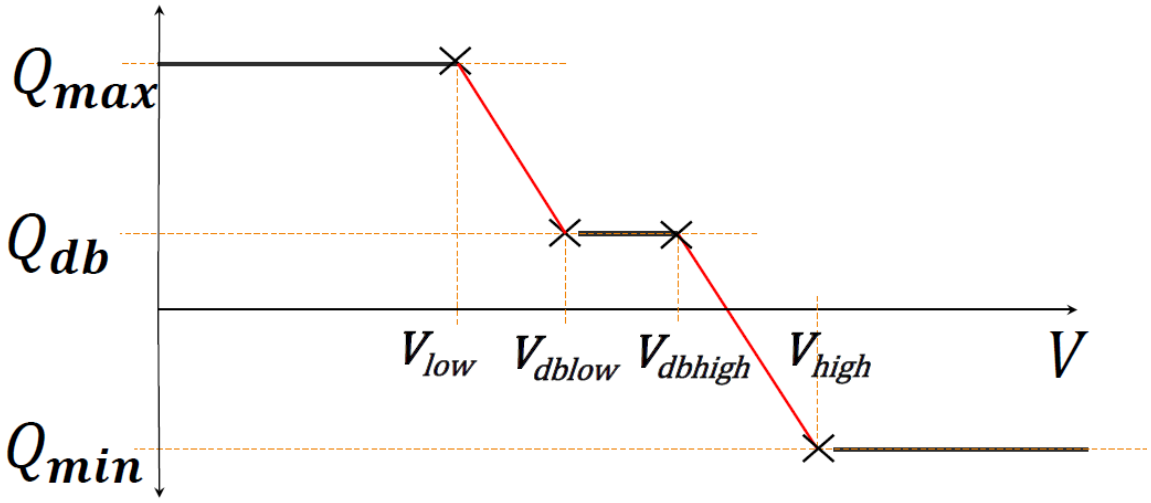

Figure 2-6: Voltage reactive power mode with dead-band droop. Source: [5]

2.6.3 Dead-band Droop with Spline in the Voltage Reactive Power Mode

The reactive power in the voltage droop control of the voltage reactive power mode is static and it is a function of the voltage. This creates numerical complexities. For the efficient operation of the voltage droop curve these complexities needs to be resolved [29].

If we consider the derivative $\frac{\partial Q_v}{\partial V_{reg}}$ in different transition points between the sections of the curve the derivative becomes non continuous which creates problem in the iterative solutions of the power flow equation [6]. The derivative $\frac{\partial Q_v}{\partial V_{reg}}$ in different transition points is shown in figure 2-7

For the transient stability problem these edge points don't create that much of a problem however for the iterative power flow solution the equations are used simultaneously and this discontinuous derivatives create numerical problem for the iterative solution algorithm [6].

To overcome this issue the discontinuous derivatives are needed to be solved. The solution is achieved by providing spline functions in the corner points of the voltage reactive mode curve. Specially it is needed near the dead-band for getting the correct reactive power in the iterative solution. Usually cubic spline function or a

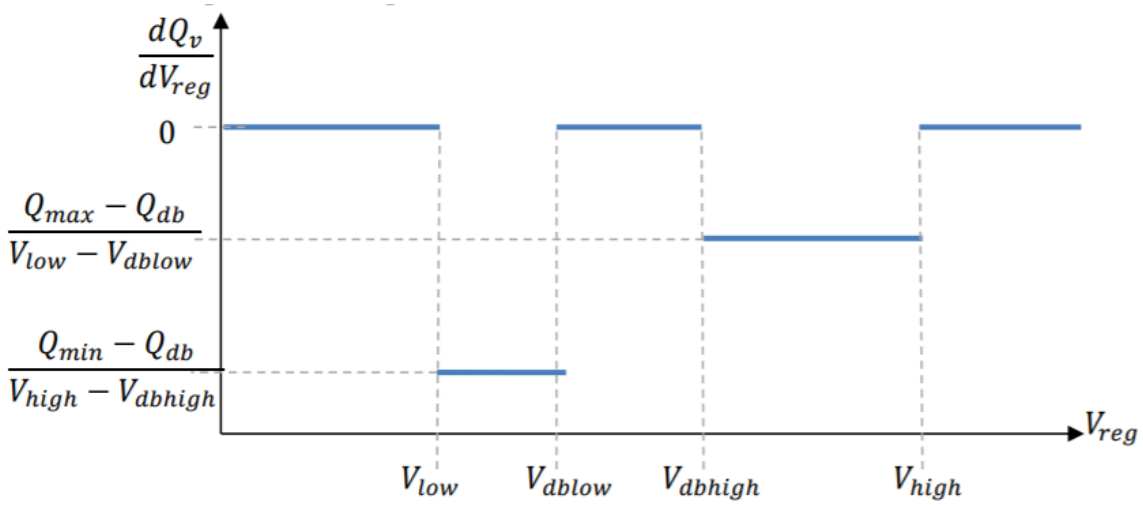

Figure 2-7: Derivative of $\frac{\partial Q_v}{\partial V_{reg}}$ in different transition points . Source: [6]

circular spline function is provided in the corner points. The new spline based voltage reactive power mode curve is sufficiently close enough to the previous one for limiting the variance in the result [29]. In figure 2-8 the spline based curve can be seen.

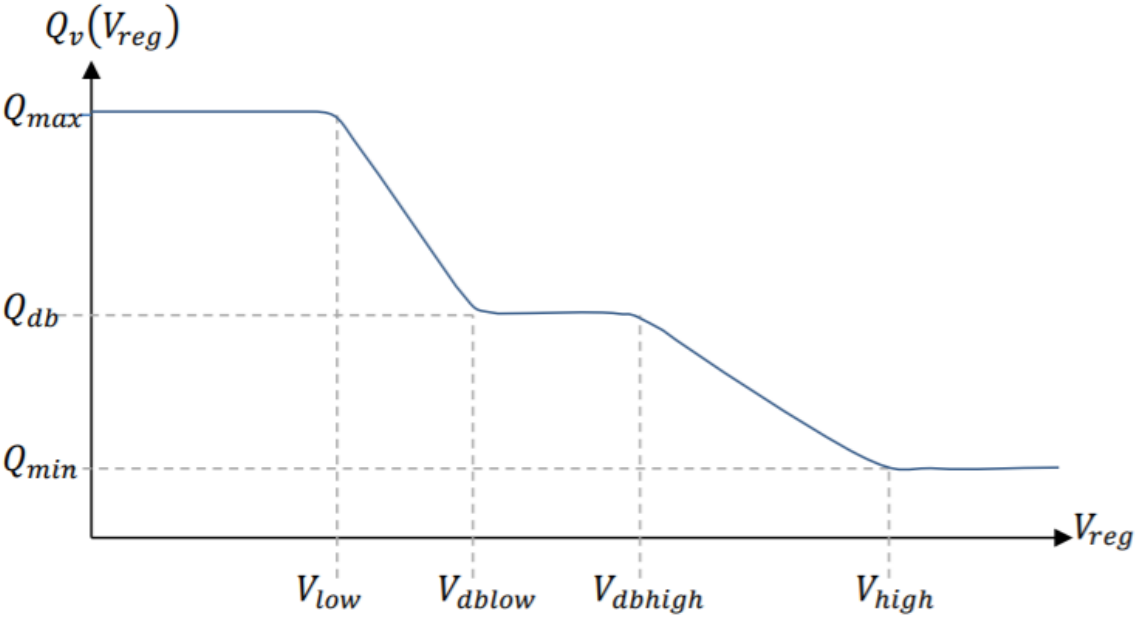

Figure 2-8: Spline based voltage reactive power mode curve . Source: [6]

After imposing the spline function the derivative $\frac{\partial Q_v}{\partial V_{reg}}$ is not continuous anymore and there is a transition in the corner points of the voltage reactive power mode curve. In figure 2-9 we can see the improved derivative of $\frac{\partial Q_v}{\partial V_{reg}}$ in different transition points.

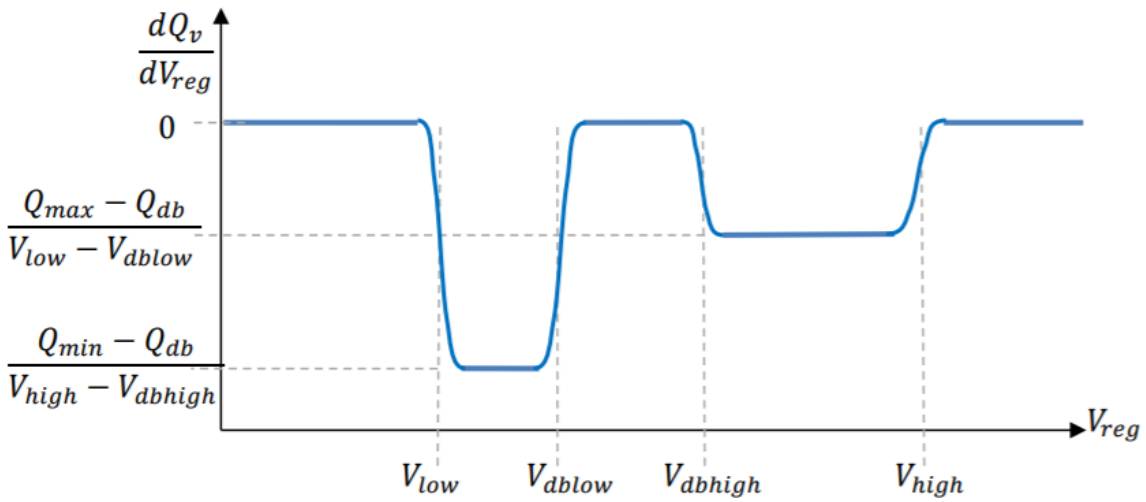

Figure 2-9: Improved derivative of $\frac{\partial Q_v}{\partial V_{reg}}$ in different transition points . Source: [6]

Although both circular and cubic splines can be used but in this case the cubic spline has advantage because if the angle difference between two line segments is less than 12 degrees or $\frac{\pi}{15}$ radians the circular function results in a circle with a huge radius in the curve and it is not desirable as with the huge radius the spline will be very big and with this very big spline the reactive power management will be invalid [6].

Chapter 3

Design of the Power Systems in PSS®E

Before running the operational case scenarios a base case was designed in PSS®E which includes all the loads, lines, transformers, shunt devices, plants, machines and mainly the Tavira substation which includes the distributed generation plants. These RES were the main concern of the simulation and here in this chapter we are going to see how these plants have been made.

As we have done our work on the PSS®E Xplore 34 version which is a 50 bus power system simulator we could not analyze the whole power system of the Portugal in our simulation. Based on the suggestion and given data of REN the whole power system was limited to 40 bus. For designing the power system the IEEE-39 bus system was used as base which has total 10 generators and 46 lines [33]. For our own design purpose this was modified according to the data given by REN.

The IEEE-39 bus system comes in the form of sav (saved case file) file. To make sure that the file is not altered, compressed, or manipulated, while designing and after each simulation the files were save as raw data file.

3.1 Design of Tavira Substation

The main focus point of the simulation was the Tavira Substation of the Portuguese national transmission grid which consist 400, 150 and 60 kV bus bars. The Tavira Substaion has 4 renewable energy based generation plants. The Alcoutim PV plant is connected to the 400 KV bus bar and São Marcos PV plant is connected to the 150 KV bus bar. The other two plants, the Malhanito and Baixo Alentejo wind power plants are connected at the 63 KV bus bar. Among this 4 generators the São Marcos PV plant is going to be operated in the near future (2021). In figure 3-1 we can see the scheme of the Tavira Substation.

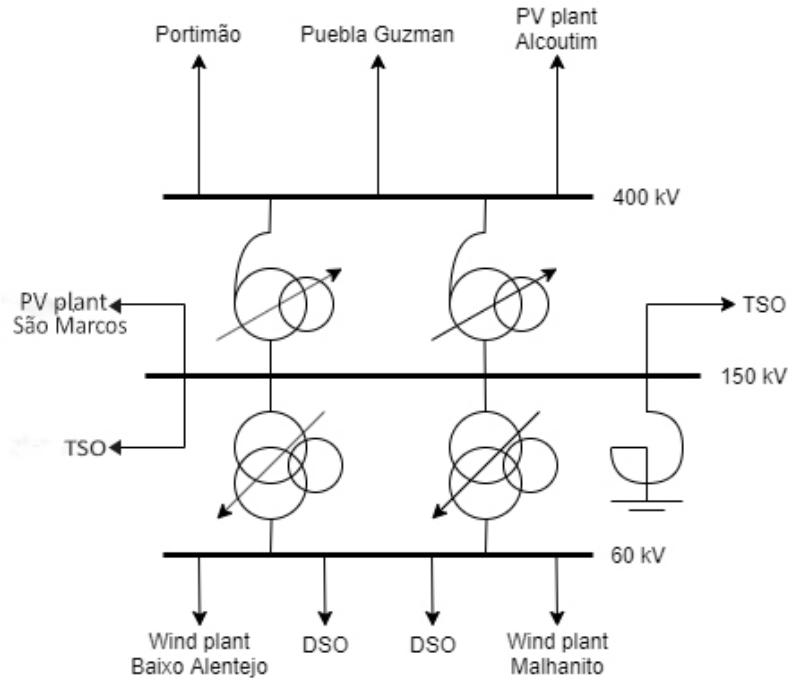

Figure 3-1: Scheme of the Tavira Substation

For the research purpose to have an idea about more future and realistic scenarios, the whole system was considered without the coal power plant as the coal power plant will be decommissioning in Portugal soon. The day 2019-07-26 was chosen with the high share of wind generation and as future PV plants were considered so it is more of a scenario than a date.

3.1.1 Malhanito and Baixo Alentejo Wind Power plants

The two wind power plants connected to the Tavira substaion are the Malhanito and Baixo Alentejo Wind Power plants. Both of them are connected at the 63 KV bus system. According to REN data Baixo Alentejo has rated active power of 43.7 MW and Malhanito has 66.7 MW. So in any hour of a day the plants should not exceed this active power limit. There are two two-winding transformers which step up the voltage to 150 KV and it is connected to the São Marcos PV power plant. For the simplification in the simulation the Malhanito Wind Power plant was tagged as GC and the Baixo Alentejo Wind Power plant was tagged as GD.

3.1.2 The Alcoutim PV Power plant

The Alcoutim PV Power plant is connected to the 400 KV bus bar of the Tavira substation. It has total 820128 number of panels with a nominal power of 270 W in each panel. Considering around efficiency and other factors in mind the rated active power was set as 200 MW of the Alcoutim PV Power plant. In the simulation it was tagged as the power plant GA. Two two-winding transformers are there in this bus system to step down the voltage at 150 KV which will be connected to the 150 KV bus of the São Marcos PV power plant.

3.1.3 São Marcos PV power plant

The São Marcos PV power plant is yet to be built in the year 2021 but in our simulation we have considered it and it is connected in the 150 KV bus of the Tavira substation. This plant is basically an aggregation of 4 different PV power plants of Albercas, Pereiro, São Marcos and Viçoso which are connected together at São Marcos before connecting to the grid. In the simulation this plant was tagged as GB. In total it has 513332 number of panels with each panel having 300 W nominal power. Considering the efficiency and other factors in mind the rated active power was set as 140 MW for this plant. This plant also has a fixed shunt device connected to maintain the required voltage level in the system. The configuration of the São

Marcos PV power plant is shown in table.

Table 3.1: São Marcos PV power plant Data

Name	**No. of Panels**	**Nominal Power**	**Active Power)**
Albercas	94662	300	25.5
Pereiro	95670	300	25.9
São Marcos	163001	300	44.9
Viçoso	159999	300	43.7
Total No. of Panels →	513332	**Rated Active Power →**	140

3.2 Scheme of the Overall Power System

Before making the design in PSS®E some modifications were performed in the IEEE-39 bus system. One extra bus was added in the overall scheme which was attached in the Tavira Substaion for making the system simple. The scheme in figure 3-2 was designed in PSS®E which includes the Tavira substation based on the data given from REN. The area under the red line consist the Tavira substaion with the other elements connected to it.

In figure 3-3 we can see the scheme of the Tavira substation along with the bus number and the name that we will be analyzing.

3.2.1 Machine Data

In our analysis total 14 generators have been used among which 4 of them are the generators of Tavira substation. In PSS®E these 4 generators are named as PVGU4 (Alcoutim PV Power plant), PVGU5 (São Marcos PV power plant), $WT3\_40$ with ID 1 (Malhanito WF) and $WT3\_40$ with ID 2 (Baixo Alentejo WF). The IEEE-39 bus originally have 10 generators. Here the 4 generators are connected in different bus system with addition of one new bus which is the bus number 40. The area and zone of the previous 10 generators of the IEEE-39 bus system were not changed. Also the

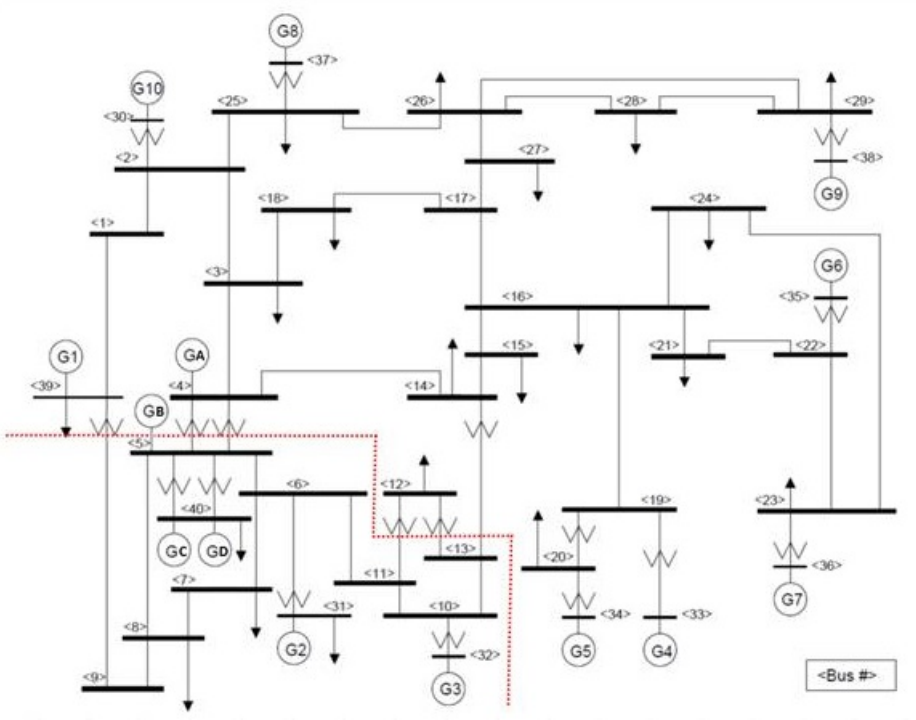

Figure 3-2: Scheme of the Overall Power System

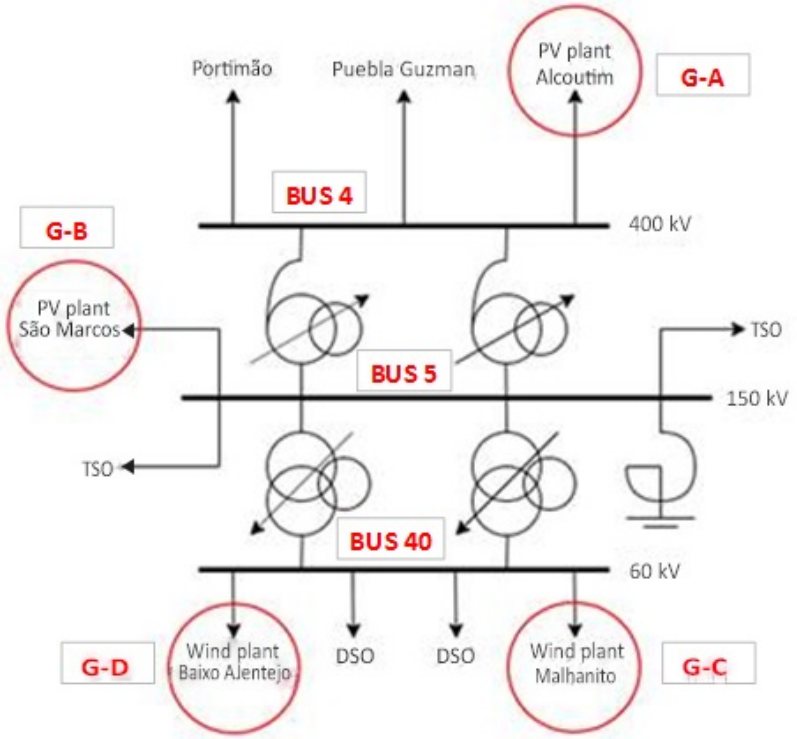

Figure 3-3: Scheme of the Tavira Substation along with the Bus number

area for bus 3,4 after converting it to generator bus were also not changed. The two wind power plants were added just to avoid complexity and as they are connected near the swing bus 39 there zone and area were also not changed. Here except bus number 39 which is the swing bus of the system, all the buses are the generator buses. In PSS®E the swing bus is defined with code 3 and the generator bus is defined with code 2. Here with each bus name the base bus voltage is written. As we can see we have total 8 different bus voltages in the system. All the machine data for configuring the generator buses were provided by REN including the resistance and reactances. In figure 3-4 the machine data from PSS®E is provided.

Bus Number	Bus Name	Id	Area Num	Area Name	Zone Num	Zone Name	Code	VSched (pu)	Remote Bus Number	In Service	PGen (MW)	PMax (MW)	PMin (MW)	QGen (Mvar)	QMax (Mvar)	QMin (Mvar)	Mbase (MVA)
4	PVGU4 400.	1	1	WEST	2	SWEST	2	1.0125	0	☑	108.1000	200.0000	0.0000	-1.8270	145.0000	-145.0000	220.00
5	PVGU5 150.	1	1	WEST	2	SWEST	2	1.0200	0	☑	75.6000	140.0000	0.0000	-9.2330	100.0000	-100.0000	150.00
30	GEN30 34.5	1	1	WEST	1	NWEST	2	1.0400	0	☑	250.0000	250.0000	0.0000	110.2610	153.1800	-58.0840	275.00
31	GEN31 34.5	1	1	WEST	2	SWEST	2	1.0500	0	☑	200.0000	760.0000	0.0000	160.0180	429.8040	-122.6650	836.00
32	GEN32 21.0	1	1	WEST	2	SWEST	2	1.0400	0	☑	650.0000	767.0000	0.0000	123.2180	446.7220	-180.2180	843.70
33	GEN33 21.0	1	2	EAST	4	SEAST	2	1.0400	0	☑	632.0000	1068.0000	0.0000	55.7560	548.2080	-213.7800	1174.80
34	GEN34 15.5	1	2	EAST	4	SEAST	2	1.0400	0	☑	508.0000	982.0000	0.0000	124.1350	611.4950	-188.0280	1080.20
35	GEN35 15.5	1	2	EAST	3	NEAST	2	1.0493	0	☑	650.0000	987.0000	0.0000	207.1850	593.7880	-234.9720	1085.70
36	GEN36 12.5	1	2	EAST	4	SEAST	2	1.0635	0	☑	560.0000	932.0000	0.0000	100.3540	568.3720	-249.1320	1025.20
37	GEN37 12.5	1	1	WEST	1	NWEST	2	1.0500	0	☑	540.0000	882.0000	0.0000	90.8940	443.4680	-216.1220	970.20
38	GEN38 34.5	1	2	EAST	3	NEAST	2	1.0265	0	☑	830.0000	1531.0000	0.0000	62.8430	834.7751	-356.8890	1684.10
39	GEN39 400.	1	1	WEST	2	SWEST	3	1.0300	0	☑	864.1681	1090.0000	0.0000	-0.0080	574.8500	-173.2610	1199.00
40	WT3_40 63.0	1	1	WEST	1	NWEST	2	1.0000	0	☑	25.6000	66.7000	0.0000	-6.1780	30.0000	-30.0000	72.50
40	WT3_40 63.0	2	1	WEST	1	NWEST	2	1.0000	0	☑	22.2000	43.7000	0.0000	-5.3580	30.0000	-30.0000	47.50

Figure 3-4: Machine Data of the Power System

3.2.2 Power Plant Data

The two wind farms Malhanito and Baixo Alentejo are connected in the bus number 40. So bus number 40 is basically a plant consisting two generators. The other generators in the system are not connected together in a single bus. So we have total 13 plants in our system. In figure 3-5 the plant data from PSS®E is provided.

Bus Number	Bus Name	Area Num	Area Name	Code	PGen (MW)	QGen (Mvar)	QMax (Mvar)	QMin (Mvar)	VSched (pu)	Remote Bus Number	Remote Bus Name	Voltage (pu)	RMPCT
4	PVGU4 400.	1	WEST	2	108.1	-1.8	145.0	-145.0	1.0125	0		1.0125	100.00
5	PVGU5 150.	1	WEST	2	75.6	-9.2	100.0	-100.0	1.0200	0		1.0200	100.00
30	GEN30 34.5	1	WEST	2	250.0	110.3	153.2	-58.1	1.0400	0		1.0400	100.00
31	GEN31 34.5	1	WEST	2	200.0	160.0	429.8	-122.7	1.0500	0		1.0500	100.00
32	GEN32 21.0	1	WEST	2	650.0	123.2	446.7	-180.2	1.0400	0		1.0400	100.00
33	GEN33 21.0	2	EAST	2	632.0	55.8	548.2	-213.8	1.0400	0		1.0400	100.00
34	GEN34 15.5	2	EAST	2	508.0	124.1	611.5	-188.0	1.0400	0		1.0400	100.00
35	GEN35 15.5	2	EAST	2	650.0	207.2	593.8	-235.0	1.0493	0		1.0493	100.00
36	GEN36 12.5	2	EAST	2	560.0	100.4	568.4	-249.1	1.0635	0		1.0635	100.00
37	GEN37 12.5	1	WEST	2	540.0	90.9	443.5	-216.1	1.0500	0		1.0500	100.00
38	GEN38 34.5	2	EAST	2	830.0	62.8	834.8	-356.9	1.0265	0		1.0265	100.00
39	GEN39 400.	1	WEST	3	864.2	-0.0	574.9	-173.3	1.0300	0		1.0300	100.00
40	WT3_40 63.0	1	WEST	2	47.8	-11.5	60.0	-60.0	1.0000	0		1.0000	100.00

Figure 3-5: Plant Data of the Power System

All the data along with scheduled voltage (the voltage the bus will try to maintain) of the power plants are given by the system operator (SO). After running each simulation the voltage in PU will be checked of each plant which is the output voltage provided by the plant.

3.2.3 AC Transmission Line Data

Here in our base system in PSS®E total 31 AC line can be observed among which 4 lines are directly connected with the Tavira substation. These line are from bus 3 to 4, 4 to 14, 5 to 6 and 5 to 8. In figure 3-6 the AC line from PSS®E can be seen.

From Bus Number	From Bus Name	To Bus Number	To Bus Name	Id	Line R (pu)	Line X (pu)	Charging B (pu)	RATE1 (I as MVA)	RATE2 (I as MVA)	RATE3 (I as MVA)
1	BUS1 400.0	2	BUS2 400.0	1	0.003500	0.041100	0.698700	175.0	192.0	192.0
1	BUS1 400.0	39	GEN39 400.	1	0.001000	0.025000	0.750000	125.0	137.0	137.0
2	BUS2 400.0	3	LOAD3 400.	1	0.001300	0.015100	0.257200	650.0	715.0	715.0
2	BUS2 400.0	25	LOAD25 400.	1	0.007000	0.008600	0.146000	260.0	286.0	286.0
3	LOAD3 400.	4	PVGU4 400.	1	0.001300	0.021300	0.221400	125.0	137.0	137.0
3	LOAD3 400.	18	LOAD18 400.	1	0.001100	0.013300	0.213800	125.0	137.0	137.0
4	PVGU4 400.	14	LOAD14 400.	1	0.000800	0.012900	0.138200	300.0	330.0	330.0
5	PVGU5 150.	6	BUS6 150.0	1	0.000200	0.002600	0.043400	462.0	508.0	508.0
5	PVGU5 150.	8	LOAD8 150.	1	0.000800	0.011200	0.147600	462.0	508.0	508.0
6	BUS6 150.0	7	LOAD7 150.	1	0.000600	0.009200	0.113000	700.0	770.0	770.0
6	BUS6 150.0	11	BUS11 150.	1	0.000700	0.008200	0.138900	466.0	512.0	512.0
7	LOAD7 150.	8	LOAD8 150.	1	0.000400	0.004600	0.078000	462.0	508.0	508.0
8	LOAD8 150.	9	BUS9 150.0	1	0.002300	0.036300	0.380400	466.0	512.0	512.0
10	BUS10 150.	11	BUS11 150.	1	0.000400	0.004300	0.072900	462.0	508.0	508.0
10	BUS10 150.	13	BUS13 150.	1	0.000400	0.004300	0.072900	429.0	471.0	471.0
14	LOAD14 400.	15	LOAD15 400.	1	0.001800	0.021700	0.366000	125.0	137.0	137.0
15	LOAD15 400.	16	LOAD16 400.	1	0.000900	0.009400	0.171000	429.0	471.0	471.0
16	LOAD16 400.	17	BUS17 400.	1	0.000700	0.008900	0.134200	260.0	286.0	286.0
16	LOAD16 400.	19	BUS19 400.	1	0.001600	0.019500	0.304000	552.0	607.0	607.0
16	LOAD16 400.	21	LOAD21 400.	1	0.000800	0.013500	0.254800	429.0	471.0	471.0
16	LOAD16 400.	24	LOAD24 400.	1	0.000300	0.005900	0.068000	230.0	253.0	253.0
17	BUS17 400.	18	LOAD18 400.	1	0.000700	0.008200	0.131900	300.0	330.0	330.0
17	BUS17 400.	27	LOAD27 400.	1	0.001300	0.017300	0.321600	125.0	137.0	137.0
21	LOAD21 400.	22	BUS22 400.	1	0.000800	0.014000	0.256500	650.0	715.0	715.0
22	BUS22 400.	23	LOAD23 400.	1	0.000600	0.009600	0.184600	125.0	137.0	137.0
23	LOAD23 400.	24	LOAD24 400.	1	0.002200	0.035000	0.361000	466.0	512.0	512.0
25	LOAD25 400.	26	LOAD26 400.	1	0.003200	0.032300	0.513000	125.0	137.0	137.0
26	LOAD26 400.	27	LOAD27 400.	1	0.001400	0.014700	0.239600	380.0	418.0	418.0
26	LOAD26 400.	28	LOAD28 400.	1	0.004300	0.047400	0.780200	175.0	192.0	192.0
26	LOAD26 400.	29	LOAD29 400.	1	0.005700	0.062500	1.029000	230.0	253.0	253.0
28	LOAD28 400.	29	LOAD29 400.	1	0.001400	0.015100	0.249000	400.0	440.0	440.0

Figure 3-6: AC Line Data of the Power System

3.2.4 Transformers Data

The base system has total 18 transformers from which 4 of them are in the Tavira substation. The voltage control mode has been provided in these 4 transformers. All of these transformers are 2-winding and no 3-winding transformers has been used in this system. Figure 3-7 is showing the transformer data used in the system.

From Bus Number	From Bus Name	To Bus Number	To Bus Name	Id	Tap Positions	Control Mode	Specified R (pu or	Specified X (pu)	RATE1 (MVA)	RATE2 (MVA)	RATE3 (MVA)	Magnetizing G (pu or	Magnetizing B (pu)
2	BUS2 400.0	30	GEN30 34.5	1	999	None	0.000000	0.018100	380.0	418.0	418.0	0.00000	0.00000
4	PVGU4 400.	5	PVGU5 150.	2	25	Voltage	0.000440	0.034780	450.0	450.0	450.0	0.00189	-0.00112
4	PVGU4 400.	5	PVGU5 150.	3	25	Voltage	0.000760	0.034680	450.0	450.0	450.0	0.00070	-0.00178
5	PVGU5 150.	40	WT3_40 63.0	2	25	Voltage	0.002500	0.097300	126.0	126.0	126.0	0.00050	-0.00220
5	PVGU5 150.	40	WT3_40 63.0	3	25	Voltage	0.002540	0.098000	126.0	126.0	126.0	0.00051	-0.00244
6	BUS6 150.0	31	GEN31 34.5	1	999	None	0.000000	0.025000	700.0	770.0	770.0	0.00000	0.00000
9	BUS9 150.0	39	GEN39 400.	2	999	None	0.000500	0.001500	450.0	510.0	510.0	0.00000	0.00000
10	BUS10 150.	32	GEN32 21.0	1	999	None	0.000000	0.020000	816.0	897.0	897.0	0.00000	0.00000
11	BUS11 150.	12	LOAD12 63.0	1	999	None	0.001600	0.043500	125.0	137.0	137.0	0.00000	0.00000
12	LOAD12 63.0	13	BUS13 150.	1	999	None	0.001600	0.043500	125.0	137.0	137.0	0.00000	0.00000
13	BUS13 150.	14	LOAD14 400.	2	999	None	0.000500	0.035000	450.0	450.0	450.0	0.00000	0.00000
19	BUS19 400.	20	LOAD20 63.0	1	999	None	0.000700	0.013800	230.0	253.0	253.0	0.00000	0.00000
19	BUS19 400.	33	GEN33 21.0	1	999	None	0.000700	0.014200	700.0	770.0	770.0	0.00000	0.00000
20	LOAD20 63.0	34	GEN34 15.5	1	999	None	0.000900	0.018000	560.0	616.0	616.0	0.00000	0.00000
22	BUS22 400.	35	GEN35 15.5	1	999	None	0.000000	0.014300	715.0	786.0	786.0	0.00000	0.00000
23	LOAD23 400.	36	GEN36 12.5	1	999	None	0.000500	0.027200	560.0	616.0	616.0	0.00000	0.00000
25	LOAD25 400.	37	GEN37 12.5	1	999	None	0.000600	0.023200	552.0	607.0	607.0	0.00000	0.00000
29	LOAD29 400.	38	GEN38 34.5	1	999	None	0.000800	0.015600	837.0	920.0	920.0	0.00000	0.00000

Figure 3-7: Transformer Data of the Power System

3.2.5 Load Data

Here in our base system in PSS®E total 20 loads can be observed. The Tavira substation has only one load which is connected in the bus no. 40 along with the Malhanito and Baixo Alentejo Wind Power plants. In figure 3-8 the load data of the whole power system can be observed.

Bus Number	Bus Name	Id	Code	Area Num	Area Name	Zone Num	Zone Name	Owner Num	Owner Name	In Service	Scalable	Pload (MW)	Qload (Mvar)
3	LOAD3 400.	1	1	1	WEST	1	NWEST	1	GENS	☑	☑ Yes	600.000	100.000
7	LOAD7 150.	1	1	1	WEST	1	NWEST	1	GENS	☑	☑ Yes	233.800	50.0000
8	LOAD8 150.	1	1	1	WEST	1	NWEST	1	GENS	☑	☑ Yes	522.000	75.0000
12	LOAD12 63.0	1	1	1	WEST	1	NWEST	1	GENS	☑	☑ Yes	120.000	30.0000
14	LOAD14 400.	1	1	1	WEST	1	NWEST	1	GENS	☑	☑ Yes	450.000	50.0000
15	LOAD15 400.	1	1	1	WEST	1	NWEST	1	GENS	☑	☑ Yes	320.000	50.0000
16	LOAD16 400.	1	1	1	WEST	1	NWEST	1	GENS	☑	☑ Yes	329.400	50.0000
18	LOAD18 400.	1	1	1	WEST	1	NWEST	1	GENS	☑	☑ Yes	158.000	30.0000
20	LOAD20 63.0	1	1	1	WEST	1	NWEST	1	GENS	☑	☑ Yes	680.000	103.000
21	LOAD21 400.	1	1	1	WEST	1	NWEST	1	GENS	☑	☑ Yes	274.000	75.0000
23	LOAD23 400.	1	1	1	WEST	1	NWEST	1	GENS	☑	☑ Yes	247.500	84.6000
24	LOAD24 400.	1	1	1	WEST	1	NWEST	1	GENS	☑	☑ Yes	308.600	-92.2000
25	LOAD25 400.	1	1	1	WEST	1	NWEST	1	GENS	☑	☑ Yes	224.000	47.2000
26	LOAD26 400.	1	1	1	WEST	1	NWEST	1	GENS	☑	☑ Yes	139.000	17.0000
27	LOAD27 400.	1	1	1	WEST	1	NWEST	1	GENS	☑	☑ Yes	281.000	75.5000
28	LOAD28 400.	1	1	1	WEST	1	NWEST	1	GENS	☑	☑ Yes	206.000	27.6000
29	LOAD29 400.	1	1	1	WEST	1	NWEST	1	GENS	☑	☑ Yes	283.500	75.0000
31	GEN31 34.5	1	2	1	WEST	1	NWEST	1	GENS	☑	☑ Yes	80.0000	40.0000
39	GEN39 400.	1	3	1	WEST	1	NWEST	1	GENS	☑	☑ Yes	400.000	100.000
40	WT3_40 63.0	1	2	1	WEST	1	NWEST	1	GENS	☑	☑ Yes	15.2000	8.5000

Figure 3-8: Load Data of the Power System

3.2.6 Shunt Device Data

Shunt devices control the reactive power flow in the power system and by doing that it controls the voltage fluctuations and transient stability [34]. Mainly two types of

shunt devices are used, capacitive and inductive. The shunt capacitive compensation is used to improve the power factor while the shunt inductive compensation is used to maintain the required voltage level. Here in our system a fixed shunt device is used in the São Marcos PV plant (150 KV bus) of the Tavira substation which is capacitive. In figure 3-9 the shunt device data of the power system is shown.

Bus Number	Bus Name	Id	Area Num	Area Name	Zone Num	Zone Name	Code	In Service	G-Shunt (MW)	B-Shunt (Mvar)
5	PVGU5 150.	1	1	WEST	2	SWEST	2	☑	0.00	-75.00
								☑		

Figure 3-9: Shunt Device Data of the Power System

3.2.7 Bus Data

After configuring the machine, plant, AC line, transformer and Shunt data we can look into the buses in our power system. The bus data sums up all the load, generators and line in the power system. Figure 3-10 shows the bus data of our power system from PSS®E.

Bus Number	Bus Name	Base kV	Area Num	Area Name	Zone Num	Zone Name	Owner Num	Owner Name	Code	Voltage (pu)	Angle (deg)	Normal Vmax (pu)	Normal Vmin (pu)	Emergency Vmax (pu)	Emergency Vmin (pu)
1	BUS1	400.0	1	WEST	1	NWEST	2	TRANSMIS	1	1.0485	-1.48	1.1000	0.9000	1.1000	0.9000
2	BUS2	400.0	1	WEST	1	NWEST	2	TRANSMIS	1	1.0473	-3.80	1.1000	0.9000	1.1000	0.9000
3	LOAD3	400.0	1	WEST	1	NWEST	2	TRANSMIS	1	1.0233	-8.16	1.1000	0.9000	1.1000	0.9000
4	PVGU4	400.0	1	WEST	2	SWEST	2	TRANSMIS	2	1.0125	-7.58	1.1000	0.9000	1.1000	0.9000
5	PVGU5	150.0	1	WEST	2	SWEST	2	TRANSMIS	2	1.0200	-6.36	1.1000	0.9000	1.1000	0.9000
6	BUS6	150.0	1	WEST	2	SWEST	2	TRANSMIS	1	1.0218	-6.11	1.1000	0.9000	1.1000	0.9000
7	LOAD7	150.0	1	WEST	2	SWEST	2	TRANSMIS	1	1.0153	-7.32	1.1000	0.9000	1.1000	0.9000
8	LOAD8	150.0	1	WEST	2	SWEST	2	TRANSMIS	1	1.0146	-7.34	1.1000	0.9000	1.1000	0.9000
9	BUS9	150.0	1	WEST	2	SWEST	2	TRANSMIS	1	1.0280	-0.28	1.1000	0.9000	1.1000	0.9000
10	BUS10	150.0	1	WEST	2	SWEST	2	TRANSMIS	1	1.0240	-3.90	1.1000	0.9000	1.1000	0.9000
11	BUS11	150.0	1	WEST	2	SWEST	2	TRANSMIS	1	1.0233	-4.75	1.1000	0.9000	1.1000	0.9000
12	LOAD12	63.0	1	WEST	2	SWEST	2	TRANSMIS	1	1.0313	-6.09	1.1000	0.9000	1.1000	0.9000
13	BUS13	150.0	1	WEST	2	SWEST	2	TRANSMIS	1	1.0202	-4.57	1.1000	0.9000	1.1000	0.9000
14	LOAD14	400.0	2	EAST	3	NEAST	2	TRANSMIS	1	1.0131	-8.94	1.1000	0.9000	1.1000	0.9000
15	LOAD15	400.0	2	EAST	3	NEAST	2	TRANSMIS	1	1.0212	-8.54	1.1000	0.9000	1.1000	0.9000
16	LOAD16	400.0	2	EAST	3	NEAST	2	TRANSMIS	1	1.0300	-6.74	1.1000	0.9000	1.1000	0.9000
17	BUS17	400.0	1	WEST	1	NWEST	2	TRANSMIS	1	1.0304	-7.41	1.1000	0.9000	1.1000	0.9000
18	LOAD18	400.0	1	WEST	1	NWEST	2	TRANSMIS	1	1.0264	-8.13	1.1000	0.9000	1.1000	0.9000
19	BUS19	400.0	2	EAST	4	SEAST	2	TRANSMIS	1	1.0317	-1.95	1.1000	0.9000	1.1000	0.9000
20	LOAD20	63.0	2	EAST	4	SEAST	2	TRANSMIS	1	1.0270	-3.24	1.1000	0.9000	1.1000	0.9000
21	LOAD21	400.0	2	EAST	3	NEAST	2	TRANSMIS	1	1.0339	-4.35	1.1000	0.9000	1.1000	0.9000
22	BUS22	400.0	2	EAST	3	NEAST	2	TRANSMIS	1	1.0505	0.10	1.1000	0.9000	1.1000	0.9000
23	LOAD23	400.0	2	EAST	4	SEAST	2	TRANSMIS	1	1.0450	-0.10	1.1000	0.9000	1.1000	0.9000
24	LOAD24	400.0	2	EAST	3	NEAST	2	TRANSMIS	1	1.0359	-6.63	1.1000	0.9000	1.1000	0.9000
25	LOAD25	400.0	1	WEST	1	NWEST	2	TRANSMIS	1	1.0595	-2.90	1.1000	0.9000	1.1000	0.9000
26	LOAD26	400.0	1	WEST	1	NWEST	2	TRANSMIS	1	1.0490	-4.83	1.1000	0.9000	1.1000	0.9000
27	LOAD27	400.0	1	WEST	1	NWEST	2	TRANSMIS	1	1.0343	-7.17	1.1000	0.9000	1.1000	0.9000
28	LOAD28	400.0	2	EAST	3	NEAST	2	TRANSMIS	1	1.0446	-1.28	1.1000	0.9000	1.1000	0.9000
29	LOAD29	400.0	2	EAST	3	NEAST	2	TRANSMIS	1	1.0437	1.52	1.1000	0.9000	1.1000	0.9000
30	GEN30	34.5	1	WEST	1	NWEST	1	GENS	2	1.0400	-1.36	1.1000	0.9000	1.1000	0.9000
31	GEN31	34.5	1	WEST	2	SWEST	1	GENS	2	1.0500	-4.51	1.1000	0.9000	1.1000	0.9000
32	GEN32	21.0	1	WEST	2	SWEST	1	GENS	2	1.0400	3.12	1.1000	0.9000	1.1000	0.9000
33	GEN33	21.0	2	EAST	4	SEAST	1	GENS	2	1.0400	2.83	1.1000	0.9000	1.1000	0.9000
34	GEN34	15.5	2	EAST	4	SEAST	1	GENS	2	1.0400	1.66	1.1000	0.9000	1.1000	0.9000
35	GEN35	15.5	2	EAST	3	NEAST	1	GENS	2	1.0493	5.06	1.1000	0.9000	1.1000	0.9000
36	GEN36	12.5	2	EAST	4	SEAST	1	GENS	2	1.0635	7.76	1.1000	0.9000	1.1000	0.9000
37	GEN37	12.5	1	WEST	1	NWEST	1	GENS	2	1.0500	3.70	1.1000	0.9000	1.1000	0.9000
38	GEN38	34.5	2	EAST	3	NEAST	1	GENS	2	1.0265	8.61	1.1000	0.9000	1.1000	0.9000
39	GEN39	400.0	1	WEST	2	SWEST	1	GENS	3	1.0300	0.00	1.1000	0.9000	1.1000	0.9000
40	WT3_40	63.0	1	WEST	1	NWEST	1	GENS	2	1.0000	-5.44	1.1000	0.9000	1.1000	0.9000

Figure 3-10: Bus Data of the Power System

Chapter 4

Design of the Optimum Voltage Droop Control with Volt-Var method

As we have seen the voltage droop control with the volt-var methods mainly has three main aspects. The Q_{max}, Q_{min} and the dead-band zone. In this chapter we will be discussing the implementation of the voltage droop control considering with dead-band, without dead-band and dead-band with the cubic spline for the 400 KV, 150 KV and the 63 KV buses. All these designs has been done in Microsoft Excel.

4.1 Idea of choosing Q_{max} , Q_{min} and Q_{db}

Connecting a micro-grid in the existing power system is not an easy task. There are a lots of rules and regulations for a power generation unit to be able to connect in the power system. According to European standard any generator connecting at 110 kV or higher is classified as type-D regardless of its capacity. So in our system the 400 and 150 KV generators are the type D generators. The 63 KV generators that we have in our system are operating in the voltage of less than 110 KV. The generators which operates under 110 KV and above 45 MW capacity are of type D. Here in our system in the 63 KV bus system of Tavira substation we have two generators which

are operating at 66.7 MW and 43.7 MW. Although 43.7 MW doesnt define the type-D criteria but as it is connected with the generator of high MW rating we define both of them together as the type-D generators. [35].

The generators connecting to the existing transmission and distribution system should also have the ability to provide reactive power at any point of operation within the limits set in the P vs Q/P_{max} curve. The P vs Q/P_{max} curve set by the Rede Elétrica de Serviço Público (RESP) for the type-C and type-D generators varies according to the voltage limit [36]. From figure 4-1 we can see the P vs Q/P_{max} curve which acts under 110 KV.

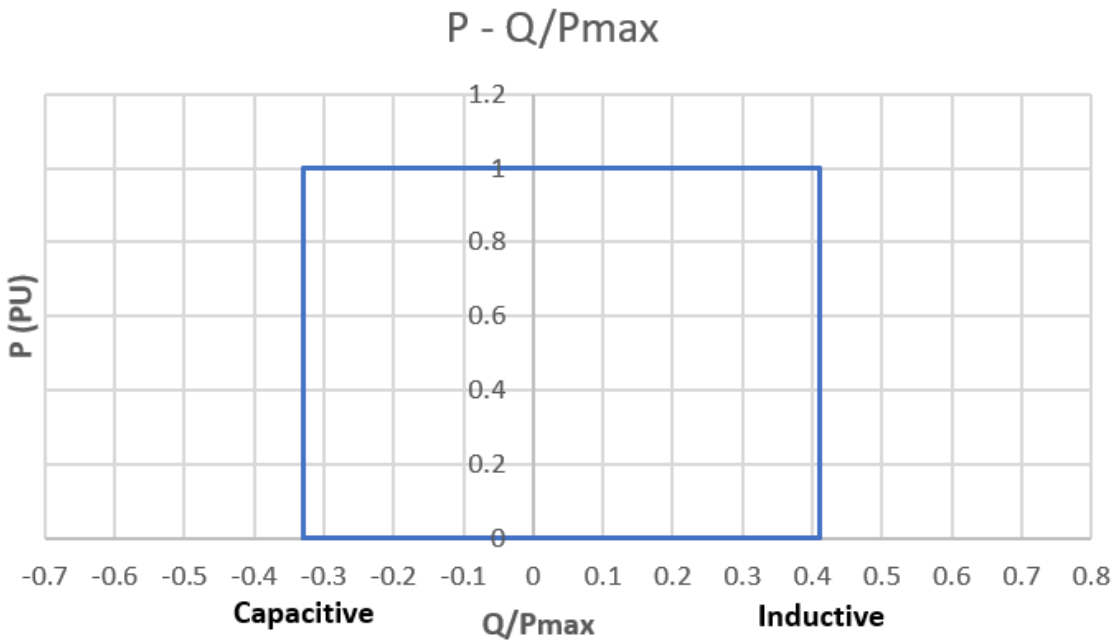

Figure 4-1: P vs Q/P_{max} curve for type-C and type-D generator (V < 110 KV)

For type-D generators which operates in the voltage equal or higher than 110 KV this curve is different. It can be seen from the figure 4-2.

These two curves basically define the reactive power capacity of the generators that are being used in our simulation. According to the definition and the voltage limits, all the four generators in the Tavira substation are of type-D. The reactive power capacity of the GC and GD at 63 kV (<110 kV) ranges from −33% to +41%. The GA and GB are operating at the voltage more than 110 KV and the reactive

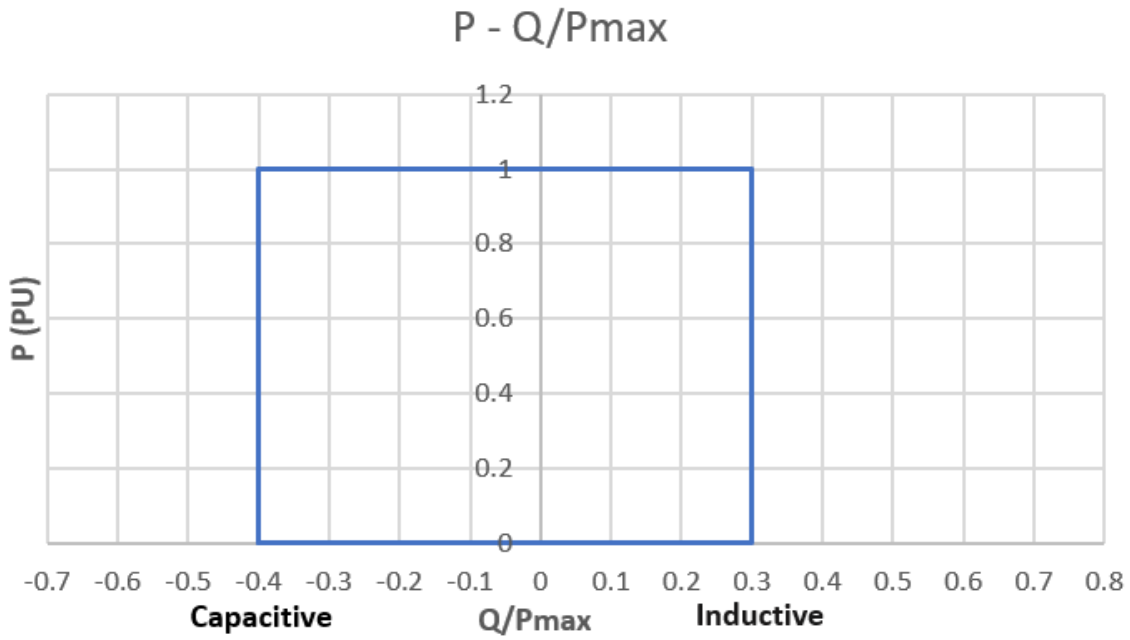

Figure 4-2: P vs Q/P_{max} curve for type-D generator (V $\geq$ 110 KV)

power capacity ranges -40% to $+30\%$.

Based on these curves the Q_{max} , Q_{min} and Q_{db} has been chosen on the percentage of Q/P_{max}. For GA and GB the Q_{max} , Q_{min} and Q_{db} have been chosen as $+30\%$, -40% and 0% of their rated active power. Although the reactive power capacity of the GC and GD ranges -33% to $+41\%$ for simplicity the Q_{max} , Q_{min} and Q_{db} of these generators have been chosen as $+40\%$, -30% and 0% of their rated active power.

4.2 Dead-band Zone

The reactive power in the dead-band zone for all the generators have been considered as zero. Normally the dead-band voltage is given 0.98 to 1.02 of its per unit voltage. Here the dead-band voltages for the generators of Tavira substation have been chosen on the percentage of their set point voltages. The set point voltage for the droop controls in which the four generators of Tavira substation will be working are different. These set point voltages are choosen based on the voltage distribution profile of an year. These set point voltages are necessary to define the dead-band voltages. The

Alcoutim PV Power plant (GA) which is operating at 400 KV, the set point voltage for this plant was set as 405 KV. For the São Marcos PV power plant (GB) the set point voltage was chosen as 153 KV although it is operating as 150 KV. The operating voltage and the set point voltage of the Malhanito Wind Power plant (GC) and the Baixo Alentejo Wind Power plant (GD) was same which is 63 KV for both.

For the Alcoutim PV Power plant (GA), Malhanito Wind Power plant (GC) and the Baixo Alentejo Wind Power plant (GD) the dead-band voltage was given 99.5% to 100.5% of their set point voltage. For the São Marcos PV power plant (GB) the dead-band zone was considered slightly higher than other plants and here dead-band voltage was given 99% to 101% of its set point voltage.

4.3 VDC Without Dead-band

There is one case scenario in which a voltage droop curve without the dead-band is considered. The implementation process of the voltage droop curve without dead-band was same as the voltage droop curve with dead-band only exception was here on the dead-band zone 100% of the set point voltage was considered.

4.3.1 VDC Without Dead-Band for The Alcoutim PV Power plant (GA)

Considering no dead-band zone in the VDC curve a table was formed with the specified Q_{max}, Q_{min} and Q_{db}. The table 4.1 shows the value which were considered for implementaing the VDC Without Dead-Band for The Alcoutim PV Power plant (GA). Considering the values from table 4.1 a curve was designed and it is shown in the figure 4-3.

Table 4.1: VDC Data Without Dead-band for The Alcoutim PV Power plant (GA)

Node	**Voltage(%)**	**Voltage (KV)**	**Q (MVAR)**	**% of Q/P_{max}**
1	0%	0	60	+30%
2	98.0%	396.9	60	+30%
3	98.0%	396.9	60	+30%
4	100.0%	405	0	0%
5	100.0%	405	0	0%
6	102.0%	413.1	-80	−40%
7	102.0%	413.1	-80	−40%
8	200.0%	810	-80	−40%

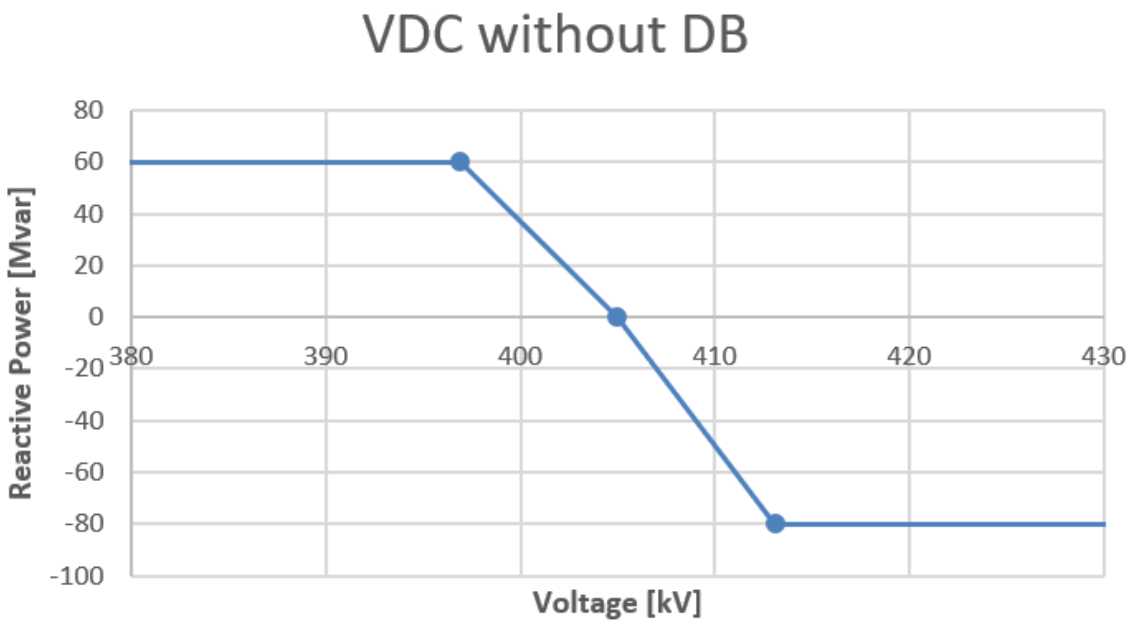

Figure 4-3: VDC Curve Without Dead-band for The Alcoutim PV Power plant (GA)

4.3.2 VDC Without Dead-band for The São Marcos PV power plant (GB)

The data table for the VDC Without Dead-band for the São Marcos PV power plant (GB) is shown in the table 4.2. Considering thesese values a VDC curve was implemented and it is shown in the figure 4-4

Table 4.2: VDC Data Without Dead-band for The São Marcos PV power plant (GB)

Node	**Voltage(%)**	**Voltage (KV)**	**Q (MVAR)**	**% of Q/P_{max}**
1	0%	0	42	+30%
2	97.5%	149.175	42	+30%
3	97.5%	149.175	42	+30%
4	100.0%	153	0	0%
5	100.0%	153	0	0%
6	102.5%	156.825	-56	−40%
7	102.5%	156.825	-56	−40%
8	200.0%	306	-56	−40%

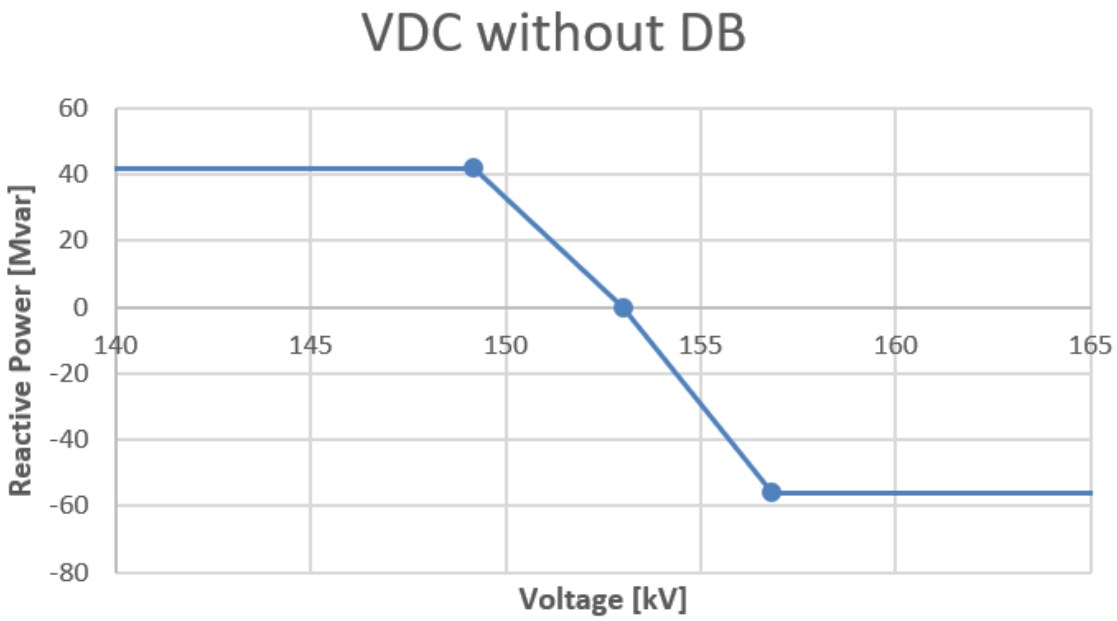

Figure 4-4: VDC Curve Without Dead-band for The São Marcos PV power plant (GB)

4.3.3 VDC Without Dead-band for The Malhanito Wind Power plant (GC)

The values for implementing the VDC curve without dead-band of the Malhanito Wind Power plant (GC) is shown in table 4.3. Based on these values the VDC curve is shown in figure 4-5.

Table 4.3: VDC Data Without Dead-band for The Malhanito Wind Power plant (GC)

Node	**Voltage(%)**	**Voltage (KV)**	**Q (MVAR)**	**% of Q/P_{max}**
1	0%	0	26.68	+40%
2	98.0%	61.74	26.68	+40%
3	98.0%	61.74	26.68	+40%
4	100.0%	63	0	0%
5	100.0%	63	0	0%
6	102.0%	64.26	-20.01	−30%
7	102.0%	64.26	-20.01	−30%
8	200.0%	126	-20.01	−30%

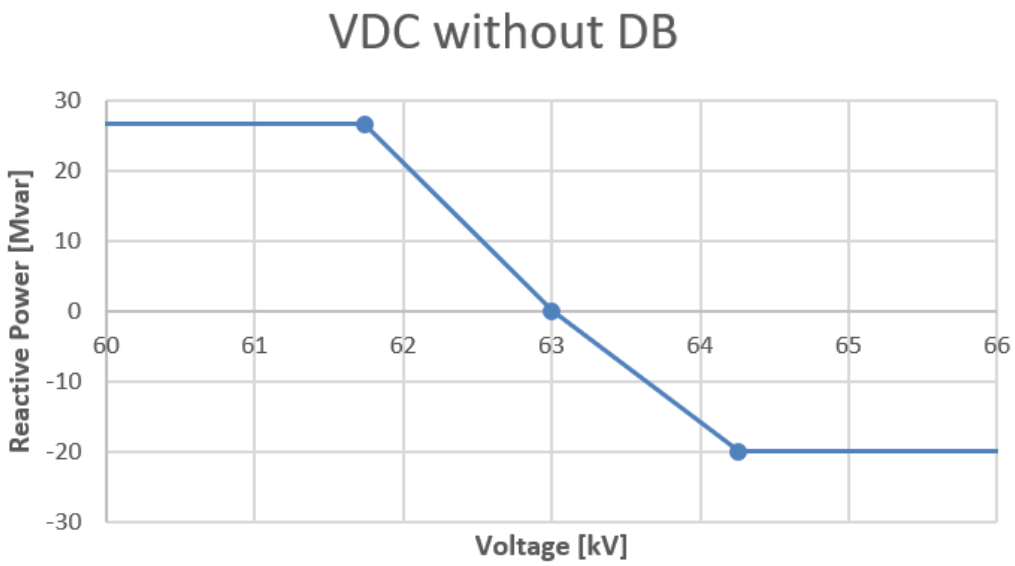

Figure 4-5: VDC Curve Without Dead-band for The Malhanito Wind Power plant (GC)

4.3.4 VDC Without Dead-band for The Baixo Alentejo Wind Power plant (GD)

The data table for the Baixo Alentejo Wind Power plant (GD) for implementing the VDC curve without dead-band will be the same except only the reactive power values in this case will be different. The data table for implementing the VDC curve for the Baixo Alentejo Wind Power plant (GD) is shown in the table 4.4. Based on these values the VDC curve is drawn and it is shown in the figure 4-6.

Table 4.4: VDC Data Without Dead-band for The Baixo Alentejo Wind Power plant (GD)

Node	**Voltage(%)**	**Voltage (KV)**	**Q (MVAR)**	**% of Q/P_{max}**
1	0%	0	17.48	+40%
2	98.0%	61.74	17.48	+40%
3	98.0%	61.74	17.48	+40%
4	100.0%	63	0	0%
5	100.0%	63	0	0%
6	102.0%	64.26	-13.11	−30%
7	102.0%	64.26	-13.11	−30%
8	200.0%	126	-13.11	−30%

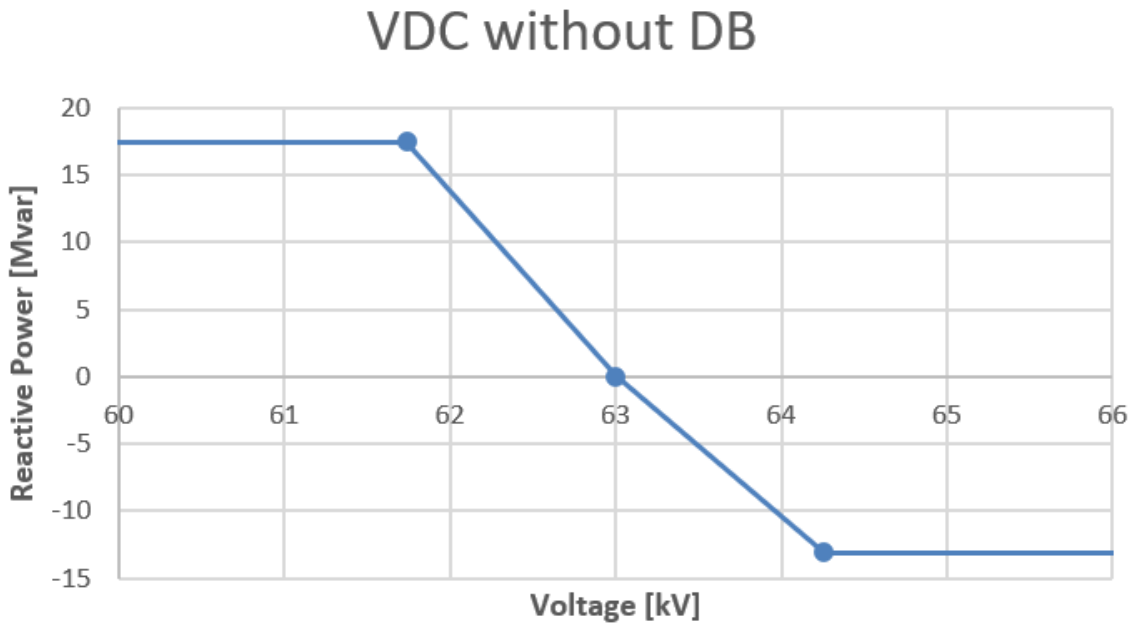

Figure 4-6: VDC Curve Without Dead-band for The Baixo Alentejo Wind Power plant (GD)

4.4 VDC With Dead-band

Although we will be simulating for the voltage droop control curve with cubic spline but to impose the cubic spline, it is necessary to design the VDC curve with the dead-band first. For the four generators in the Tavira substation the VDC curve with dead-band was designed considering a range of voltage values in the dead-band zone. The consideration for the Q_{max} , Q_{min} and Q_{db} were same as before along with the

other voltage values. The only exception was the voltage range in the dead-band zone.

4.4.1 VDC With Dead-Band for The Alcoutim PV Power plant (GA)

Considering the dead-band zone in the VDC curve a table was formed with the specified Q_{max}, Q_{min} and Q_{db}. The table 4.5 shows the value which were considered for implementing the VDC With Dead-Band for The Alcoutim PV Power plant (GA). Considering the values from table 4.5 a curve was designed and it is shown in the figure 4-7.

Table 4.5: VDC Data With Dead-band for The Alcoutim PV Power plant (GA)

Node	**Voltage(%)**	**Voltage (KV)**	**Q (MVAR)**	**% of Q/P_{max}**
1	0%	0	60	+30%
2	98.0%	396.9	60	+30%
3	98.0%	396.9	60	+30%
4	99.5%	402.975	0	0%
5	100.5%	407.025	0	0%
6	102.0%	413.1	-80	−40%
7	102.0%	413.1	-80	−40%
8	200.0%	810	-80	−40%

4.4.2 VDC With Dead-band for The São Marcos PV power plant (GB)

The data table for the VDC With Dead-band for the São Marcos PV power plant (GB) is shown in the table 4.6. Considering theses values a VDC curve was implemented and it is shown in the figure 4-8

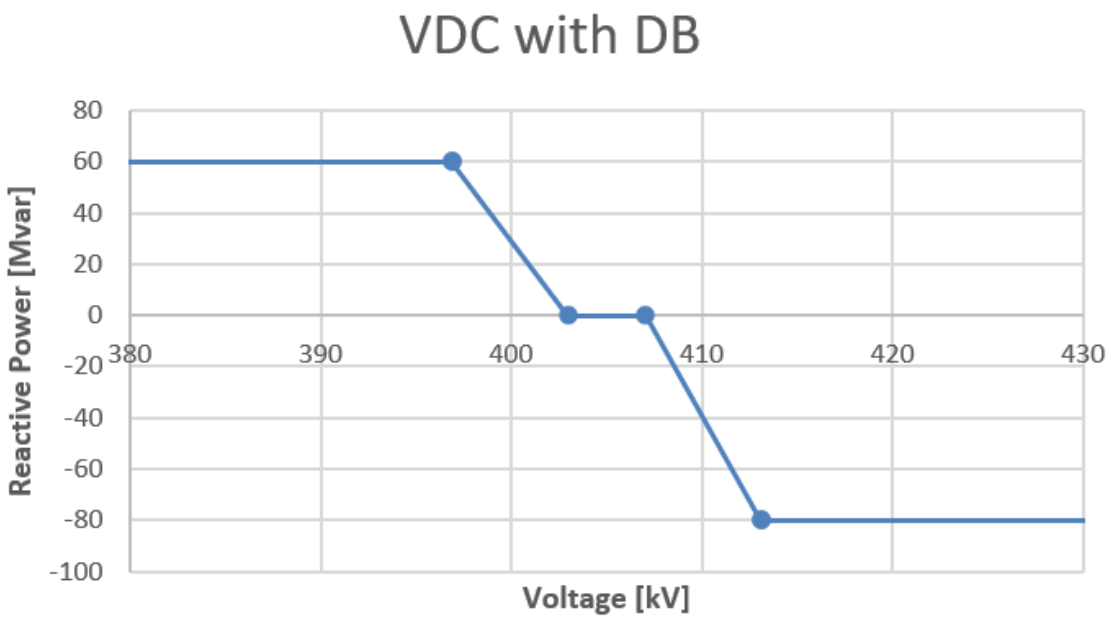

Figure 4-7: VDC Curve With Dead-band for The Alcoutim PV Power plant (GA)

Table 4.6: VDC Data With Dead-band for The São Marcos PV power plant (GB)

Node	**Voltage(%)**	**Voltage (KV)**	**Q (MVAR)**	**% of Q/P_{max}**
1	0%	0	42	+30%
2	97.5%	149.175	42	+30%
3	97.5%	149.175	42	+30%
4	99.0%	151.47	0	0%
5	101.0%	154.53	0	0%
6	102.5%	156.825	-56	−40%
7	102.5%	156.825	-56	−40%
8	200.0%	306	-56	−40%

4.4.3 VDC With Dead-band for The Malhanito Wind Power plant (GC)

The values for implementing the VDC curve with dead-band of the Malhanito Wind Power plant (GC) is shown in table 4.7. Based on these values the VDC curve is shown in figure 4-9.

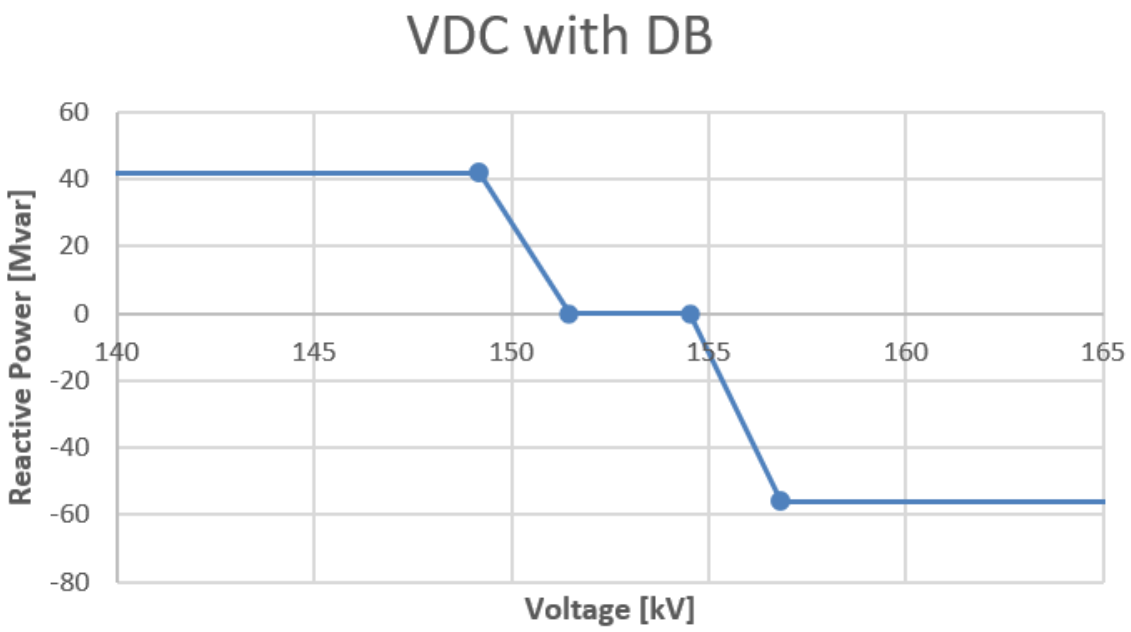

Figure 4-8: VDC Curve With Dead-band for The São Marcos PV power plant (GB)

Table 4.7: VDC Data With Dead-band for The Malhanito Wind Power plant (GC)

Node	**Voltage(%)**	**Voltage (KV)**	**Q (MVAR)**	**% of Q/P_{max}**
1	0%	0	26.68	+40%
2	98.0%	61.74	26.68	+40%
3	98.0%	61.74	26.68	+40%
4	99.5%	62.685	0	0%
5	100.5%	63.315	0	0%
6	102.0%	64.26	-20.01	−30%
7	102.0%	64.26	-20.01	−30%
8	200.0%	126	-20.01	−30%

4.4.4 VDC With Dead-band for The Baixo Alentejo Wind Power plant (GD)

The data table for the Baixo Alentejo Wind Power plant (GD) for implementing the VDC curve with the dead-band will be the same except only the reactive power values in this case will be different. The data table for implementing the VDC curve for the Baixo Alentejo Wind Power plant (GD) is shown in the table 4.8. Based on these values the VDC curve is drawn and it is shown in the figure 4-10.

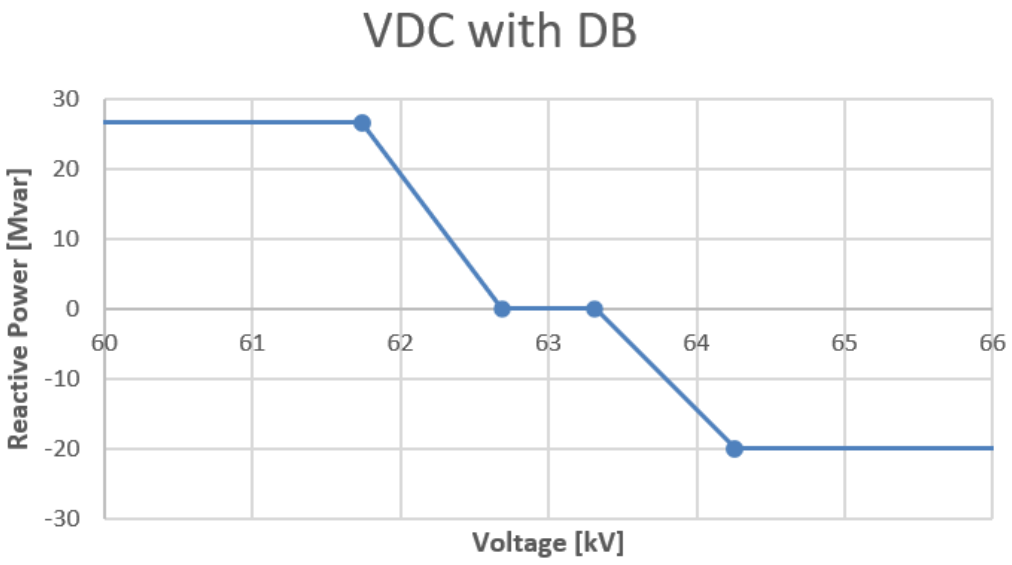

Figure 4-9: VDC Curve With Dead-band for The Malhanito Wind Power plant (GC)

Table 4.8: VDC Data With Dead-band for TheBaixo Alentejo Wind Power plant (GD)

Node	**Voltage(%)**	**Voltage (KV)**	**Q (MVAR)**	**% of Q/P_{max}**
1	0%	0	17.48	+40%
2	98.0%	61.74	17.48	+40%
3	98.0%	61.74	17.48	+40%
4	99.5%	62.685	0	0%
5	100.5%	63.315	0	0%
6	102.0%	64.26	-13.11	−30%
7	102.0%	64.26	-13.11	−30%
8	200.0%	126	-13.11	−30%

4.5 VDC With Cubic Spline

After the design of the VDC curve with Dead-band is done, the VDC curve with the cubic spline can be proceeded. The importance of spline in the VDC curve has already been discussed. Although the spline can be done in all corner points of the curve but as all of the voltages and reactive power values will be converging near the dead-band zone, here in this design we will be considering the cubic spline in the two corner points of the dead-band zone for all the four generators of the Tavira

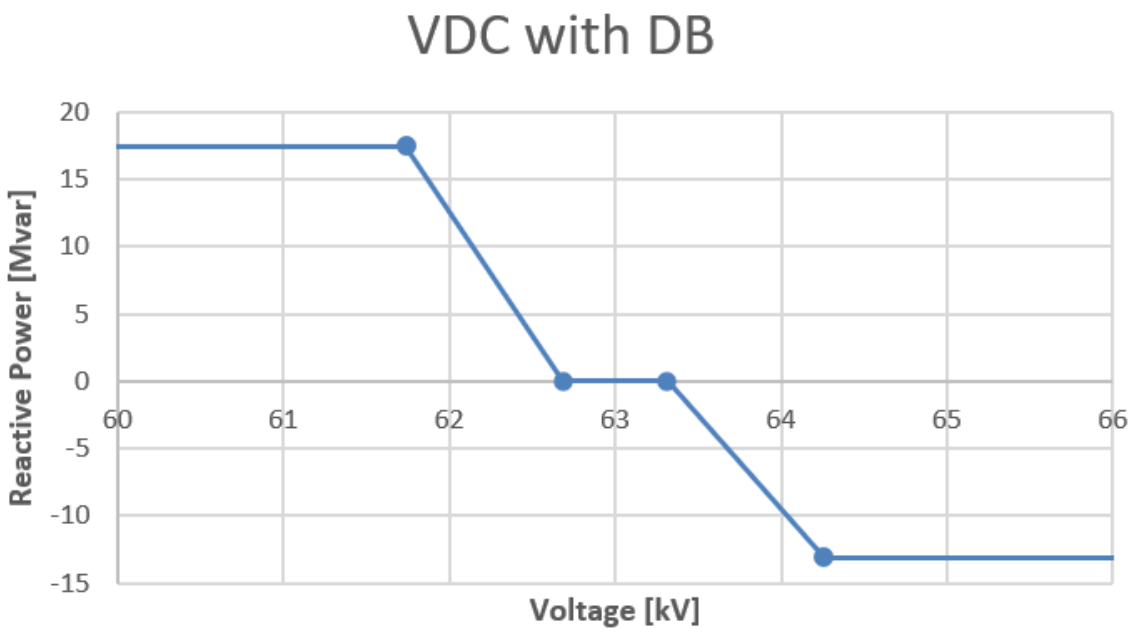

Figure 4-10: VDC Curve With Dead-band for The Baixo Alentejo Wind Power plant (GD)

substation.

To design the cubic spline 3 points were considered. The points were (x_1, y_1), (x_0, y_0), and (x_2, y_2). These basically define two lines which connects the point 1 to 0 and point 0 to point 2. The cubic function was designed in such a way that in point 1 and 2, both the value and derivative of the intersecting lines of cubic function matches. To design the cubic function the first thing was to calculate the coefficients which are a,b,c, and d. Figure 4-11 shows the idea of taking the cubic spline between two lines [6].

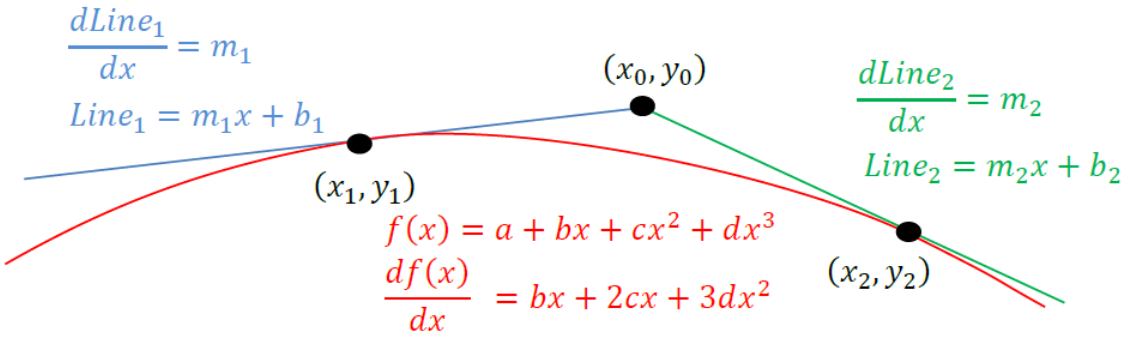

Figure 4-11: Cubic Spline between two lines. Source: [6]

For the design consideration mainly two cubic spline were designed. One for the first point of the dead-band zone and the other for the last point of the dead-band zone. For both cases these points were considered as (x_0, y_0). The distances between point (x_1, y_1), (x_0, y_0), and (x_2, y_2) were considered equal and the difference between the voltages from one point to the next one was chosen as 0.20% of the set point voltage. For those specific voltages, the reactive powers were taken by extracting the values from the VDC curve with the dead-band. To design the cubic splines the values of the coefficients were taken based on some equations. The equations are provided below.

$$m_1 = \frac{(y_0 - y_1)}{(x_0 - x_1)} \tag{4.1}$$

$$m_2 = \frac{(y_0 - y_2)}{(x_0 - x_2)} \tag{4.2}$$

$$a^{'} = \frac{(y_1 + y_2)}{2} - \frac{(x_1 - x_2)(m_1 - m_2)}{8} \tag{4.3}$$

$$b^{'} = \frac{3}{2}\frac{(y_1 - y_2)}{(x_1 - x_2)} - \frac{(m_1 + m_2)}{4} \tag{4.4}$$

$$c^{'} = \frac{(m_1 - m_2)}{2(x_1 - x_2)} \tag{4.5}$$

$$d^{'} = \frac{(m_1 + m_2)}{(x_1 - x_2)^2} - \frac{2(y_1 - y_2)}{(x_1 - x_2)^3} \tag{4.6}$$

$$a = a^{'} - b^{'}(\frac{x_1 + x_2}{2}) + c^{'}(\frac{x_1 + x_2}{2})^2 - d^{'}(\frac{x_1 + x_2}{2})^3 \tag{4.7}$$

$$b = b^{'} - 2c^{'}(\frac{x_1 + x_2}{2}) + 3d^{'}(\frac{x_1 + x_2}{2})^2 \tag{4.8}$$

$$c = c^{'} - 3d^{'}(\frac{x_1 + x_2}{2}) \tag{4.9}$$

$$d = d^{'} \tag{4.10}$$

After finding all the coefficient values finally the cubic spline can be found using the below equation.

$$f(x) = a + bx + cx^2 + dx^3 \tag{4.11}$$

For both the cubic spline functions in each VDC curve, these equations were used. The cubic splines were first made separately and then they were aligned with the VDC curve that has the dead-band zone in it.

4.5.1 VDC With Cubic Spline for The Alcoutim PV Power plant (GA)

For The Alcoutim PV Power plant (GA), considering the starting and ending dead band voltages of 402.975 and 407.025 the cubic spline equations were used. For both the cubic splines the x_0 values were 402.975 and 407.025 so the values of x_1 and x_2 were considered by taking a difference of 0.20% of the set point voltage (405 KV). The y_0, y_1, and y_3 values were the reactive power values and they were extracted from the VDC curve with dead-band zone by simply using the line equation formula y=mx+b. After finding all the coefficients (a,b,c, and d) the cubic spline function equation was used for some different voltage values starting from x_1 and finishing at x_2. From figure 4-12 the two cubic splines in the corner points of the dead-band zone of the Alcoutim PV Power plant (GA) can be seen.

As we can see from the figure, the cubic spline curves are different from each other. For Cubic Splin-1 curve all the reactive powers are positive and for Cubic Splin-2 the reactive powers are negative. for After these cubic splines were designed they were attached in the VDC curve with dead-band. Figure 4-13 shows the final design of the VDC curve with cubic spline.

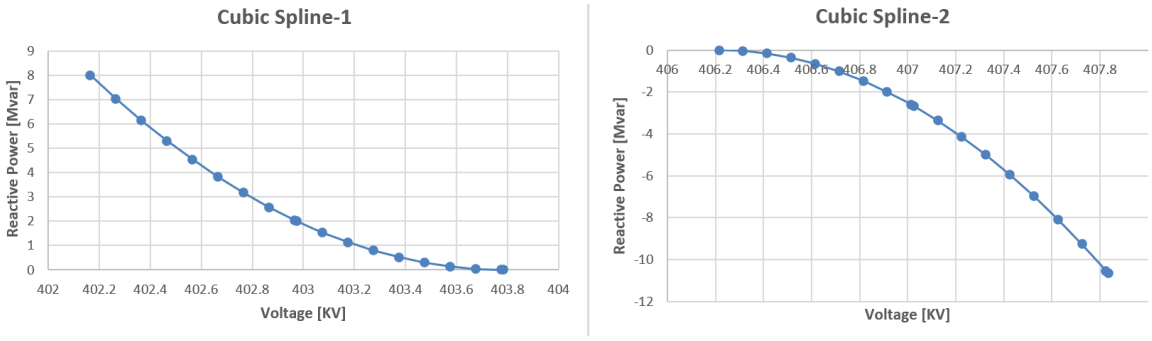

Figure 4-12: Cubic Splines in the dead-band zone for The Alcoutim PV Power plant (GA)

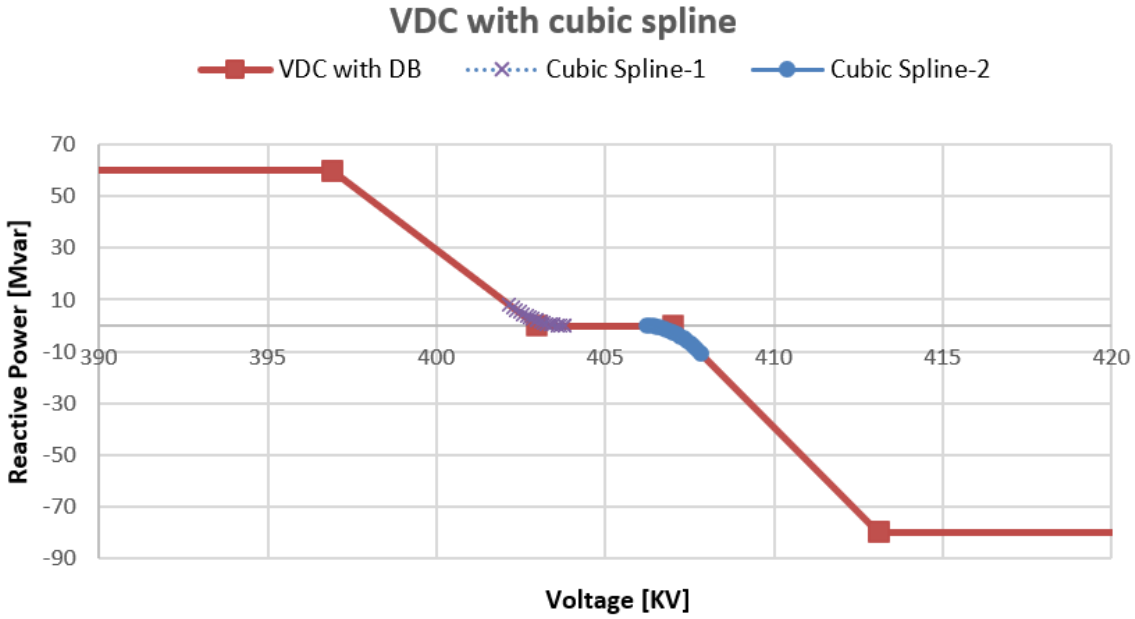

Figure 4-13: VDC Curve with Cubic Spline for The Alcoutim PV Power plant (GA)

4.5.2 VDC With Cubic Spline for The São Marcos PV power plant (GB)

For The São Marcos PV power plant (GB) the two corner point voltages in the dead-band zone were 151.470 and 154.53. To design the cubic splines the same procedure was followed as before. After using the cubic spline functions for different voltage values the two cubic splines were designed for the two corner points of the dead-band zone. Figure 4-14 shows the two cubic spline curves for the São Marcos PV power plant (GB).

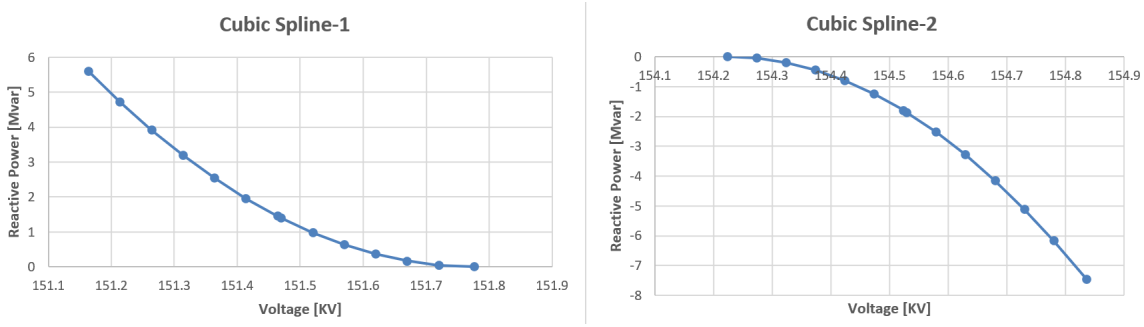

Figure 4-14: Cubic Splines in the dead-band zone for The São Marcos PV power plant (GB)

These two curves look same as before where for Cubic Splin-1 curve all the reactive powers are positive and for Cubic Splin-2 the reactive powers are negative. Now after aligning these two curves in the VDC curve with dead-band zone the final curve of VDC with cubic spline for The São Marcos PV power plant (GB) was found and it is shown in figure.

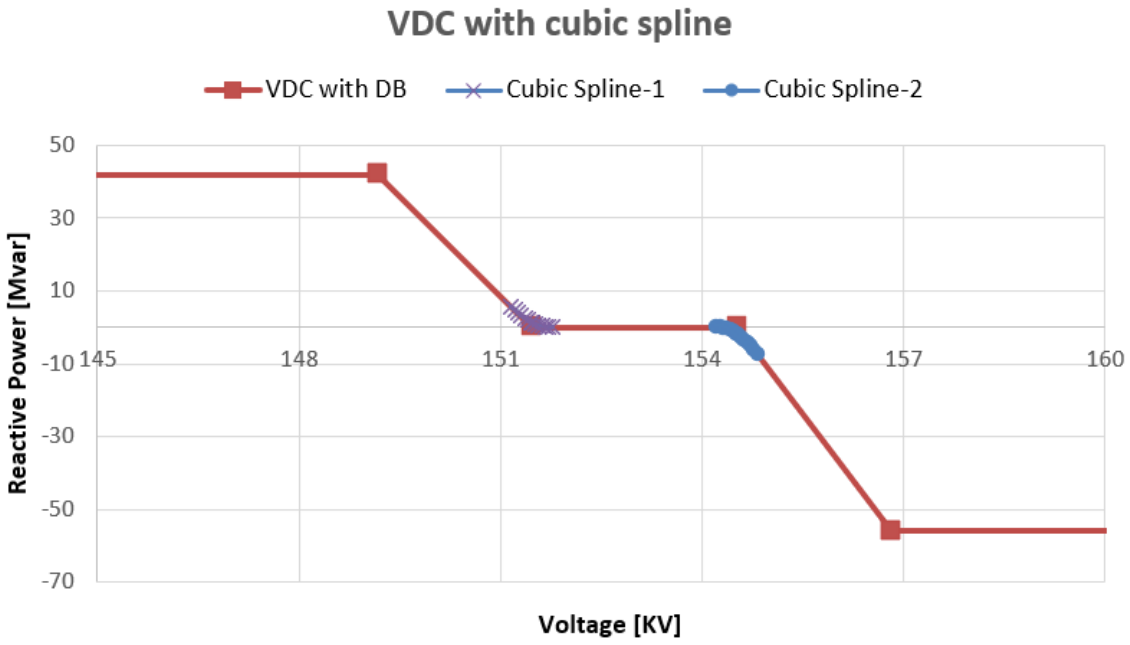

Figure 4-15: VDC Curve with Cubic Spline for The São Marcos PV power plant (GB)

4.5.3 VDC With Cubic Spline for The Malhanito Wind Power plant (GC)

For the Malhanito Wind Power plant (GC) two corner point voltages in the dead-band zone were 62.685 and 63.315. Same procedures were followed as before for designing the two cubic spline curves. The two curves of the cubic spline in the dead-band zone are provided in the figure 4-16.

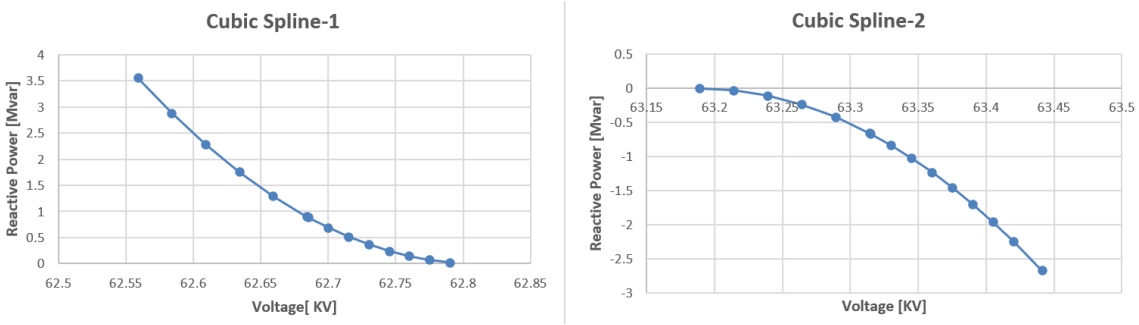

Figure 4-16: Cubic Splines in the dead-band zone for The Malhanito Wind Power plant (GC)

After the alignment of these two curves in the VDC curve with dead-band the final design looks like as figure 4-17 below.

4.5.4 VDC With Cubic Spline for The Baixo Alentejo Wind Power plant (GD)

For The Baixo Alentejo Wind Power plant (GD) the two corner point voltages in the dead-band zone were same as the Malhanito Wind Power plant (GC) which were 62.685 and 63.315. This is because this two plants are operating in the same voltage level (63 KV). The two cubic spline are provided in the figure 4-18 below.

The final design of the VDC curve with cubic spline for the Baixo Alentejo Wind Power plant (GD) looks like as figure 4-19 below.

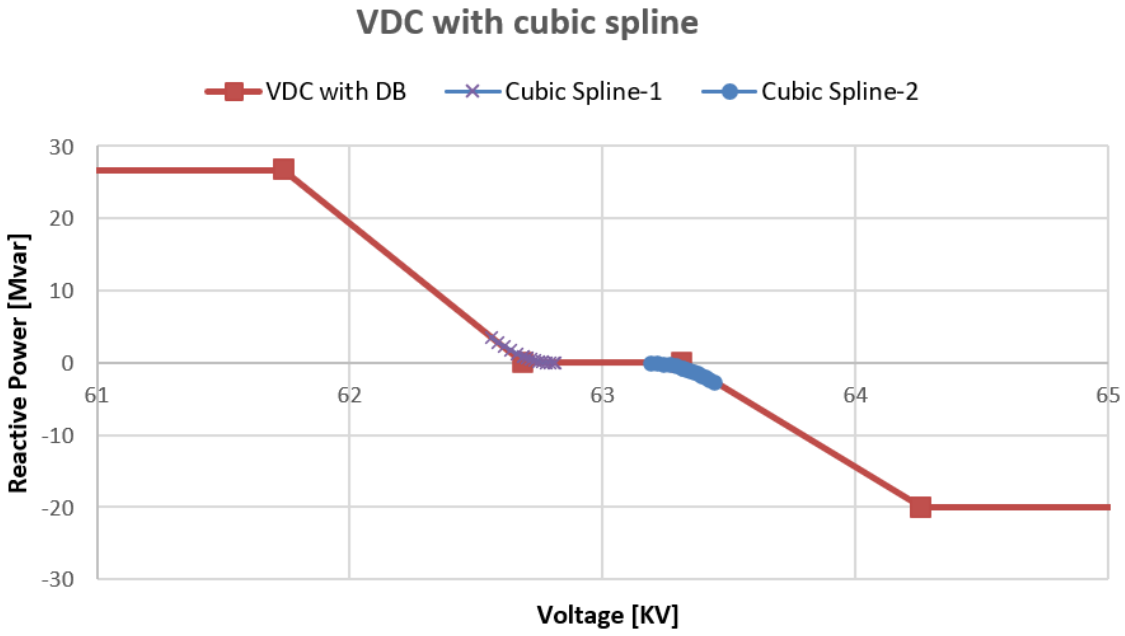

Figure 4-17: VDC Curve with Cubic Spline for The Malhanito Wind Power plant (GC)

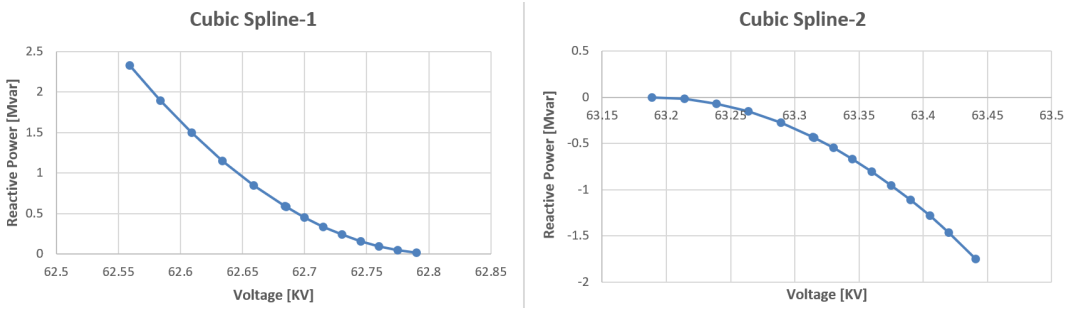

Figure 4-18: Cubic Splines in the dead-band zone for The Baixo Alentejo Wind Power plant (GD)

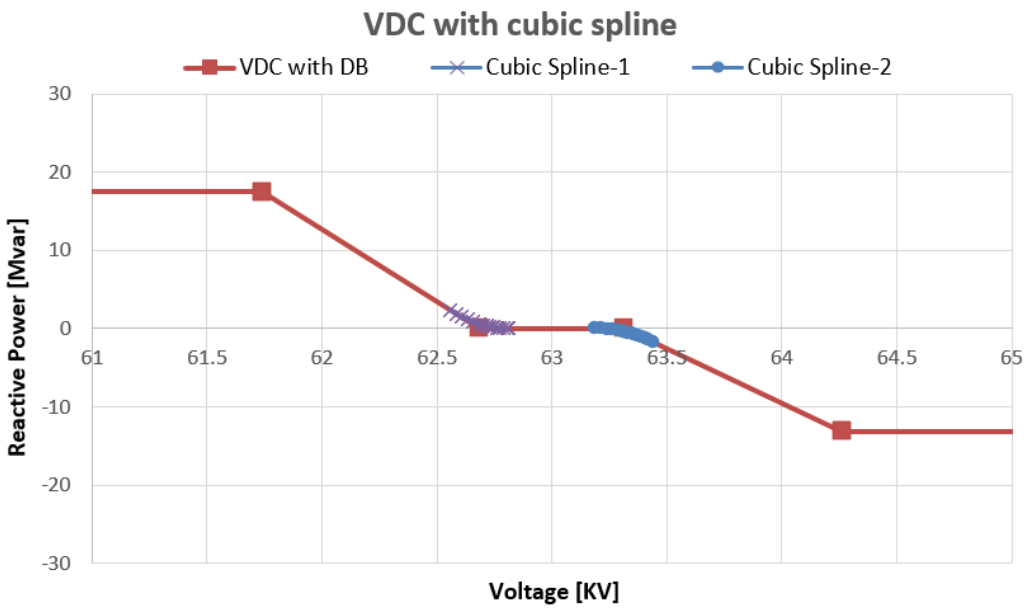

Figure 4-19: VDC Curve with Cubic Spline for The Baixo Alentejo Wind Power plant (GD)

Chapter 5

Simulation with Different Case Scenarios

In this thesis total six case scenarios were performed. The main consideration about the simulations were the four generators of the Tavira Substation. These four generators are connected in the bus 4,5, and 40 of our design. While doing the simulations, the different parameters of all the buses of our system were not changed except bus no. 4,5, and 40. But after running each simulation the whole system was checked to see if there were any mismatch in the voltage level, reactive and active power in each bus. To simulate the whole system all the 24 hours of a day was considered and the day was chosen as. The description of all the case scenarios along with the simulation procedure is discussed in this chapter.

5.1 Scenario with Base Case ("B1")

The base case of our system contains the actual information of the active and reactive power of the four generators and its bus-bar voltage levels connected to the Tavira substation. Here the real data were simulated which were given by the Portuguese National transmission system operator (TSO)- REN.

The 24 hours active and reactive power profiles of each of the four generators were given by REN. For doing the simulation of each hour every time, the P_{Gen} values of

the four generators GA, GB, GC, and GD were set as the rated active power provided by REN. The P_{Max} and P_{Min} values were not changed. The P_{Max} and P_{Min} sets the range of the active power of each generator. These ranges were set while doing the design of the system in such a way that the P_{Gen} values are in between the ranges. These ranges were also set by REN. The reactive powers provided by REN of each generators were set as the Q_{Gen}, Q_{Max} and Q_{Min}. So as we can see here the range of the reactive powers of the four generators are not maintained. It is because if we maintain the range of the reactive powers, each time we run the simulation the exact reactive power that was set by the TSO is changed. So, to fix the reactive powers even after running the simulation, the exact reactive power was set in Q_{Gen}, Q_{Max} and Q_{Min} in all the four generators of the Tavira substation. For all the other buses the range of the reactive and active power and all the other parameters were unchanged. In this way the simulations were performed for all the 24 hours data and the voltage values were extracted from the bus bars 4,5, and 40 where these four generators are connected.

5.2 Scenario with Tangent Φ equal to 0 ("C0")

This represents the case where the four generators of the Tavira substation does not absorb or generate any reactive power (tangent $\phi = 0$).

So over here the active powers for the four generators were same provided by REN and they were provided in the simulation just like the previous case. The only difference was in the simulation, instead of providing fix reactive power values, we considered the value zero in Q_{Gen}, Q_{Max} and Q_{Min} for all the four generators of the Tavira substation. Again the simulations were performed for all the 24 hours data and the voltage values were extracted from the bus bars 4,5, and 40.

5.3 Scenario with tangent Φ equal to -0.2 ("C1")

This represents the case where the power plants connected in the Tavira substation absorb reactive power 20% of its active generating power (tangent Φ = -0.2). This is actually the setup of the reactive power for the distributed generation in the Portuguese transmission grid.

As before, here the active powers for the generators of Tavira substation were same. they were provided exactly same as before in P_{Gen} values. The reactive power absorption of 20% of its active generating power for each generators were calculated and these values were provided in Q_{Gen}, Q_{Max} and Q_{Min}. The simulations were performed in the same way and again the voltage values were extracted from the bus bars 4,5, and 40.

5.4 Scenario with reactive power limits – voltage control scenario ("C2")

This represenets the case where the generators in Tavira substation have limits for absorbing and generating reactive power. The limits are set at 20% of the power plants' rated power. The voltage control method is approached where in Tavira substation for the 400 KV generator (GA) the set point voltage is set as 405 KV, for the 150 KV generator (GB) the set point voltage is set as 153 KV and for the other two generators of 63 KV (GC & GD) the set point voltage remained same. These set point voltages are chosen due to there voltage distribution profile. Here the power plants which are connected to the same bus-bar will maintaining the voltage level on the point of interconnection bus-bar of Tavira substation for avoiding the reactive power flow between them.

The process of simulation for this case is different from the previous three cases. Here the set point voltage doesn't change. It remains same for all the 24 hours. The P_{Gen} value is set by the data provided by REN. The output that will be extracted from this case will be the reactive power values. Like previous cases, over here the

same reactive powers were not chosen in the simulation for Q_{Gen}, Q_{Max} and Q_{Min}. Based on the range of Q_{Max} and Q_{Min} for the four generators of Tavira substation that were set from the base case, the P_{Gen} values which are provided and the set point voltages, The Q_{Gen} values were changed after running the solution in each hour.These Q_{Gen} values of the four generators were extracted from the simulation and stored in Excel.

5.5 Scenario with Voltage Droop Control without Dead-band("C3")

This is the case where the generators connected to Tavira substation not only have limits for absorbing and generating reactive power, but they also behave in accordance with the voltage droop control (VDC) curves without the dead-band. As we stated in the previous chapter, there is a dependency of absorbing and generating reactive power in percentage of rated active power of the generator. Based on that the voltage droop control curves are created for each generators of Tavira Substation. In this case the VDC curve without the dead-band is considered.

The simulation process of this case scenario is kind of tricky as it involves the newton raphson iteration process. Firstly, for the first run any of the previous scenario was chosen along with the data. Here in this process the C2 case was chosen for the first run. After running the simulation the voltage outputs were taken from the bus number 4.5, and 40. These voltages then were put in the corresponding VDC curves of each generators in Excel. From that the reactive power in each generators were extracted. After that these reactive powers were put as Q_{Gen}, Q_{Max} and Q_{Min} for the corresponding generators of Tavira substation. Then the simulation was run again. Again the voltage values were extracted and the corresponding reactive power values were taken by the VDC curves from Excel. The average of this reactive power and the previous reactive power of each generator was then provided in the simulation. From here the iteration process started, taking the average of the previous two

reactive powers from excel and again providing it to the simulation. The moment the reactive powers from excel and the reactive power outputs from PSS®E matches closely or exactly for all the four generators we then stop the simulation. These reactive powers from the PSS®E along with their voltages from corresponding buses are our desired voltage and reactive power. This same process along with the iterations were performed for the other time data.

5.6 Scenario with Cubic Spline based Voltage Droop Control ("C4")

This is the same case as before where the generators connected to Tavira substation have limits for absorbing and generating reactive power and also behave in accordance with the voltage droop control (VDC) curves. But here the dead-band zone along with the cubic spline were considered in each VDC curve of the generators. As we considered the cubic spline here, the reactive powers in the dead-band zone will not be zero entirely rather it will provide some specific values.

The simulation process over here was same as before which starts with the case C2. Any other case can also be considered in the starting but not the previous case C3. The extraction process of voltages and reactive powers of each generators were same as before but in the zone of cubic splines the reactive powers were taken from the cubic spline curves. The iteration process was also same and again the simulation process was stopped at the moment when the reactive powers from excel and the reactive power outputs from PSS®E matches closely or exactly for all the four generators. Considering the cubic splines along with the dead-band in the VDC curves these reactive powers from the PSS®E along with their voltages from corresponding buses are the optimum desired voltage and reactive power that we wanted to achieve. The same simulation process again was followed for the later times and all the simulation for the 24 hours data were achieved. One thing over here is to be mention is that the number of iterations in this case were less than the previous case and the optimum

voltages and reactive powers were achieved quite early.

Chapter 6

Results from the Simulation

The results of this thesis is presented in figure. Here the voltage and reactive power profiles are presented of generators of the Tavira substation. Also the validation of the implemented voltage droop control is presented. Based on the validation it will be shown how the implemented VDC curve with cubic spline is the optimum solution of the power flow.

6.1 Voltage Profile on Tavira Substation

Here the voltage profile of the generators of Tavira substation which are the Alcoutim PV plant (400 KV), São Marcos PV plant (150 KV), the Malhanito and Baixo Alentejo wind power plants (63 KV) are shown. As we worked based on a 24 hours of data, the variation of the voltages are shown in the whole day.

6.1.1 Voltage Profile of Tavira substation on The Alcoutim PV plant-GA (400 KV)

The Alcoutim PV plant is connected in the system at the bus no. 4. The voltage profile of different case scenarios of The Alcoutim PV plant is shown in figure 6-1.

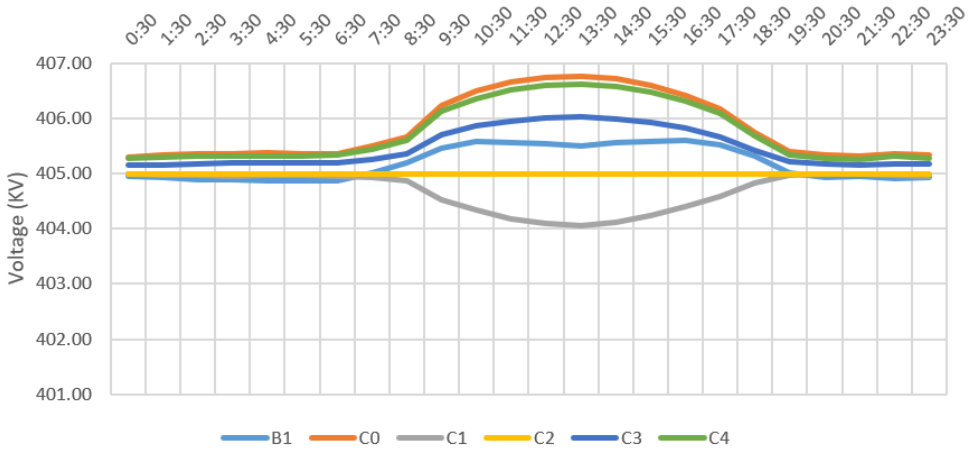

Figure 6-1: Voltage Profile of Tavira substation on The Alcoutim PV plant-GA (400 KV)

6.1.2 Voltage Profile of Tavira substation on The São Marcos PV plant-GB (150 KV)

The São Marcos PV plant is connected at the bus no. 5. The voltage profile of different case scenarios of the São Marcos PV plant is shown in figure 6-2.

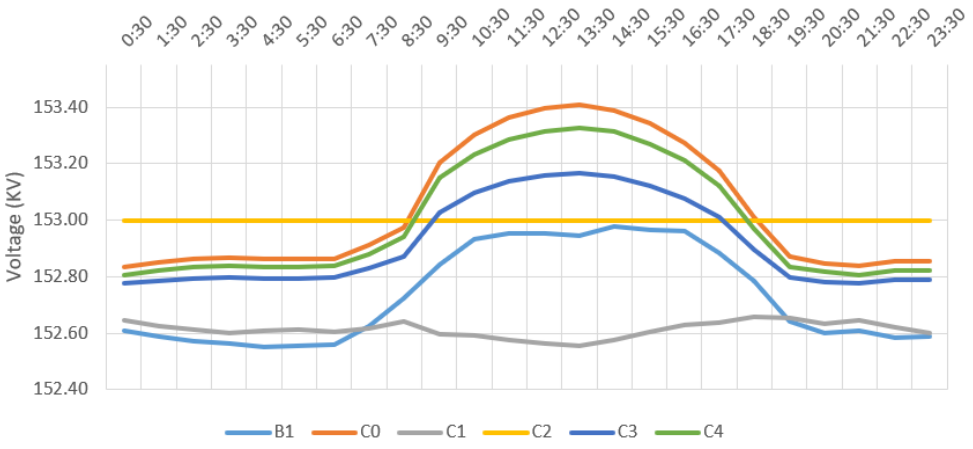

Figure 6-2: Voltage Profile of Tavira substation on The São Marcos PV plant-GB (150 KV)

6.1.3 Voltage Profile of Tavira substation on The Malhanito and Baixo Alentejo wind power plants- GC & GD (63 KV)

The Malhanito and Baixo Alentejo wind power plants are both operating at 63 KV voltage level. They are both connected in the same bus which is bus no. 40. The voltage profile of different case scenarios of the Malhanito and Baixo Alentejo wind power plants is shown in figure 6-3.

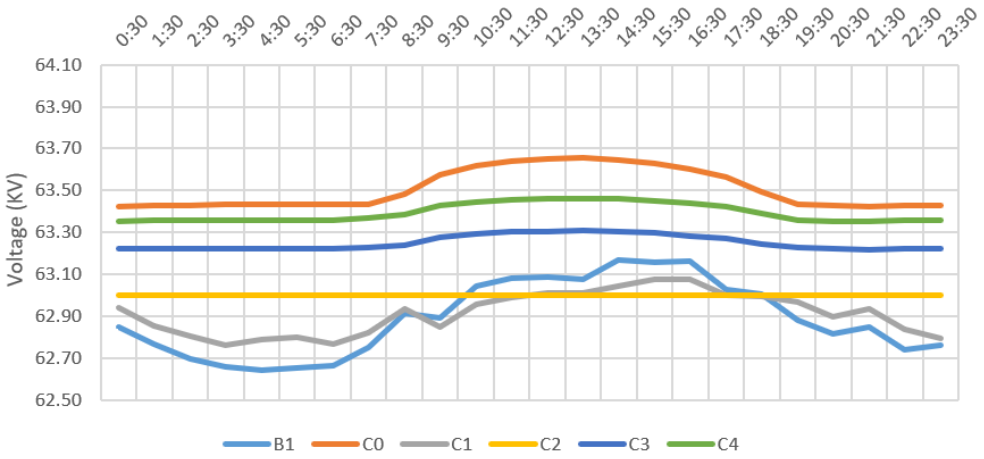

Figure 6-3: Voltage Profile of Tavira substation on The Malhanito and Baixo Alentejo wind power plants- GC & GD (63 KV)

6.1.4 Analysis of The Voltage Profiles of Tavira Substation

From figures 6-1 to 6-3 it can be seen that the voltage level in "C0" case scenario is much higher than declared voltages. The voltage level in "B1" scenario is similar to "C1" scenario for many hours specially for GC and GD, due to the power plants on the chosen day were working close to tangent ϕ equal to -0.2. In "C2" scenario the generators maintain the declared voltage on the Tavira substation bus-bars in all hours. Although the voltage profiles of "C3" and "C4" are not same but they maintain kind of the same variation in each hour. For "C3" and "C4" scenarios the voltage profile on 63 kV bus-bar is closer to declared voltage than in Base scenario "B1", but higher on 400 kV and 150 KV bus-bars in some hours of day time because

of voltage droop control curve.

6.2 Reactive Power Profile on Tavira Substation

In this section the reactive power profile of the generators of Tavira Substation is shown. Just like the voltage profiles the reactive power profiles are shown in 24 hours basis.

6.2.1 Reactive Power Profile of Tavira substation on The Alcoutim PV plant-GA (400 KV)

The reactive power profile of Alcoutim PV plant-GA (400 KV) is shown below in figure 6-4.

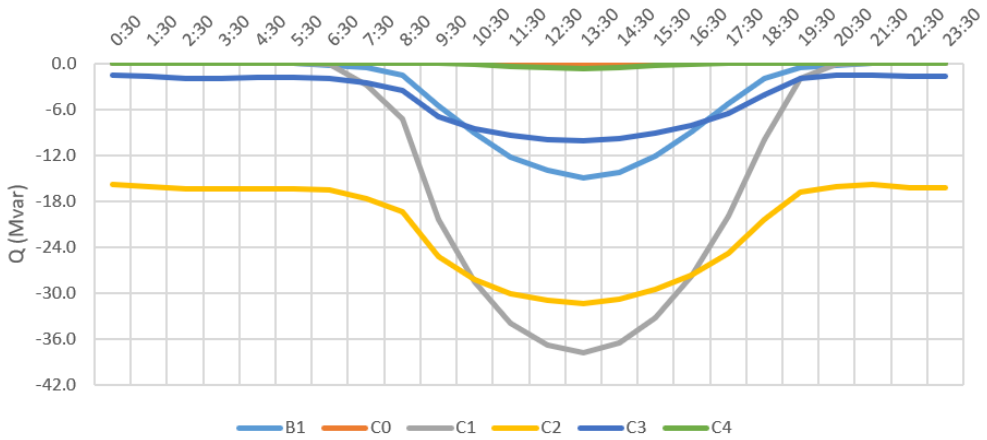

Figure 6-4: Reactive Power Profile of Tavira substation on The Alcoutim PV plant-GA (400 KV)

6.2.2 Reactive Power Profile of Tavira substation on The São Marcos PV plant-GB (150 KV)

From figure 6-5 the reactive power profile of São Marcos PV plant (150 KV) can be seen.

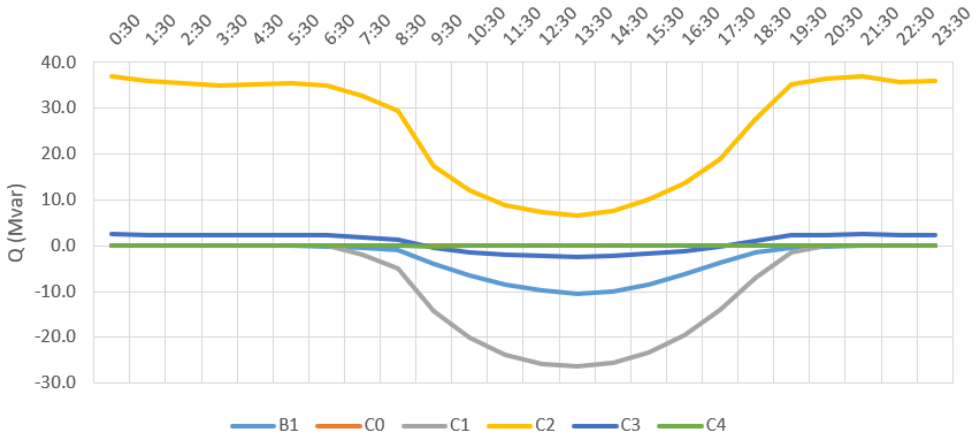

Figure 6-5: Reactive Power Profile of Tavira substation on The São Marcos PV plant- GB (150 KV)

6.2.3 Reactive Power Profile of Tavira substation on The Baixo Alentejo & Malhanito Wind Power Plant- GC & GD (63 KV)

Although the Baixo Alentejo wind power plant and the Malhanito wind power plant both are connected at the 63 KV bus, but their reactive power profiles were different. Figure 6-6 and 6-7 shows the reactive power profiles of the Baixo Alentejo and Malhanito wind power plants.

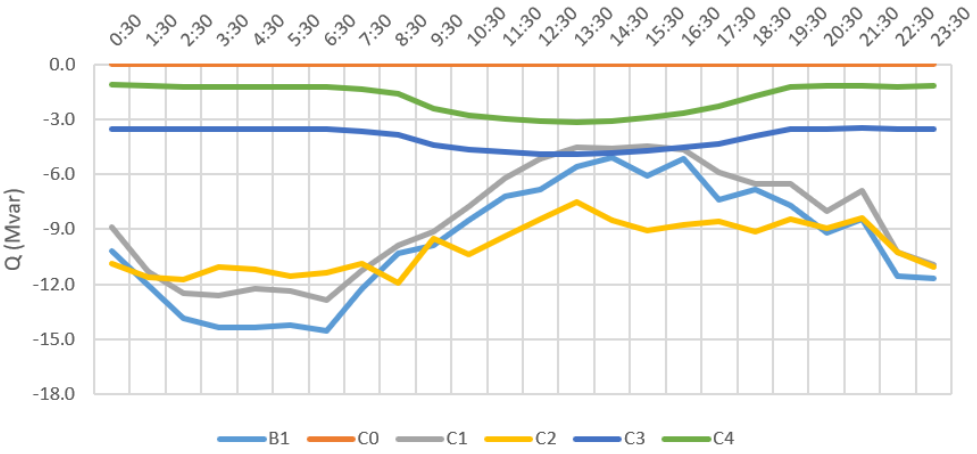

Figure 6-6: Reactive Power Profile of Tavira substation on The Malhanito Wind Power Plant- GC (63 KV)

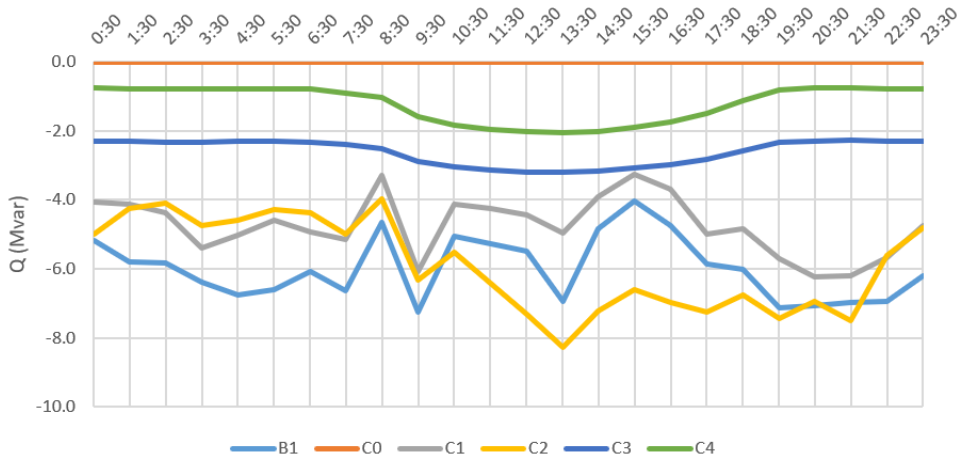

Figure 6-7: Reactive Power Profile of Tavira substation on The Baixo Alentejo Wind Power Plant- GD (63 KV)

6.2.4 Analysis of The Reactive Power Profiles of Tavira Substation

Looking into the figures it can be seen that the Alcoutim PV plant (400 KV), Baixo Alentejo (63 KV) and Malhanito Wind Power Plant (63 KV) are all absorbing reactive powers. The São Marcos PV plant (150 KV) is not absorbing reactive power all the time and with "C2" scenario it is not absorbing reactive power at all. The reactive power profile for the Alcoutim PV plant (400 KV) and the São Marcos PV plant (150 KV) is quite smooth for all the cases but for the Baixo Alentejo (63 KV) and Malhanito wind Power Plant (63 KV) there are a lot of fluctuations with the cases "B1", "C1", and "C2" but for "C3" and "C4" cases with the VDC curve the reactive power profiles are quite smooth. Because of the VDC curve with cubic spline the "C4" case tries to follow the reactive power profiles of "C0" in the the Alcoutim PV plant (400 KV) and the São Marcos PV plant (150 KV). For all the generators it can be observed that "C0" is always maintaining zero reactive power and in the day time except "C2" in São Marcos PV plant (150 KV) the reactive power absorption for all the generators with all the cases are very low compared to other hours. Although the declared voltage is not maintained in case "C3" and "C4" on the Tavira substation busbars, but the distribution of reactive power between power plants is more optimal and it reduce losses in the network.

6.3 Validating the Voltage Droop Control Curves

To validate the voltage droop curves of cases "C3" and "C4", the voltages and reactive powers from final iterations of "C3" and "C4" were inserted accordingly in the corresponding VDC curves.

6.3.1 Validation of the VDC curve without Dead-band : Case "C3"

The correspondence of the "C3" case of the generators of Tavira substation are shown in the figures 6-8 to 6-11

By looking into the curves it can be said that, as all the reactive powers from case "C3" intersects in their corresponding VDC curves (without dead-band) so the VDC curves are validated and it is working properly.

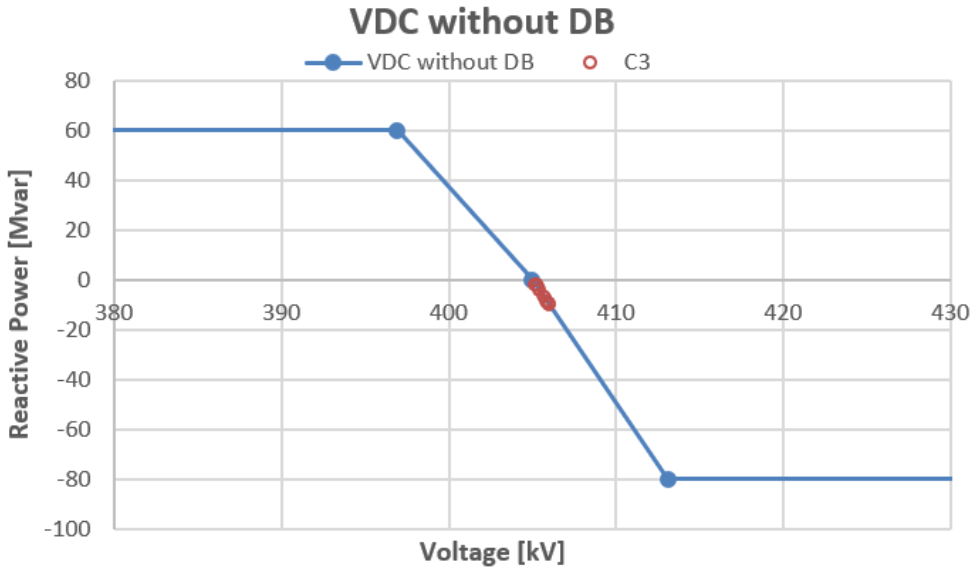

Figure 6-8: Validation of The Case "C3" for The Alcoutim PV plant-GA (400 KV)

The Alcoutim PV plant, Malhanito and Baixo Alentejo wind Power Plants are always absorbing reactive powers. Between 9.30 h to 17.30 h The São Marcos PV plant is absorbing reactive power. Here the relation between the voltages and the reactive powers are always linear, so it is not ideal. These linear characteristics create numerical complexities in the system hence the power flow solutions are not exact.

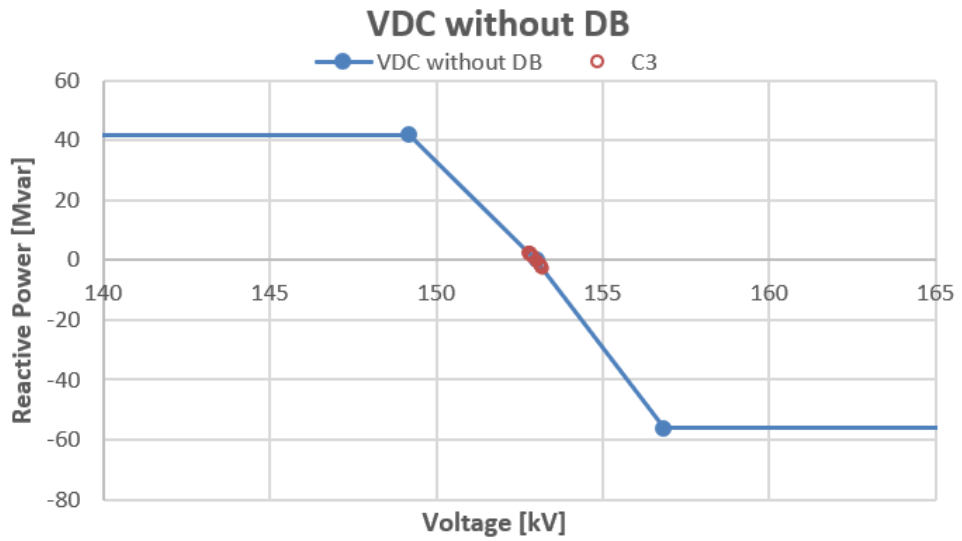

Figure 6-9: Validation of The Case "C3" for The São Marcos PV plant-GB (150 KV)

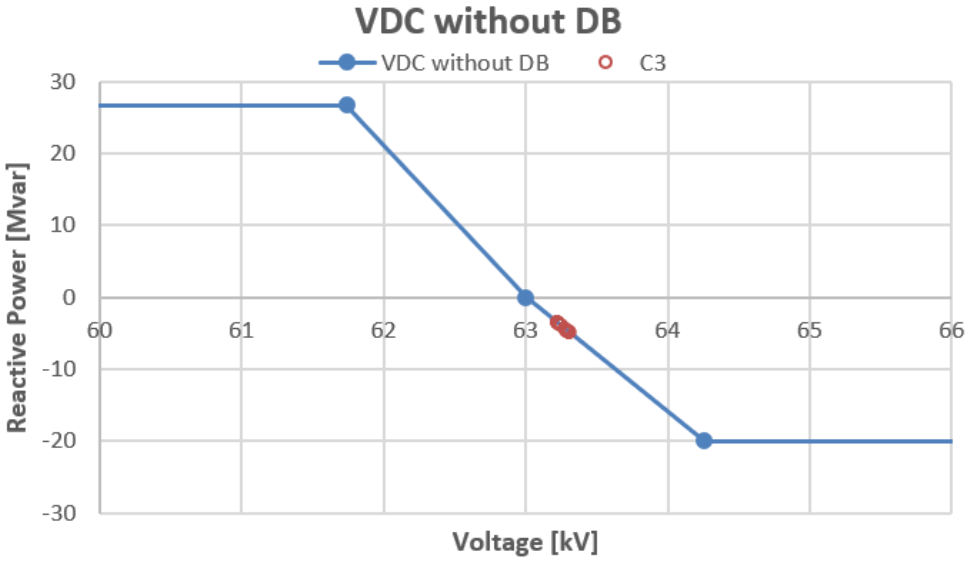

Figure 6-10: Validation of The Case "C3" for The Malhanito Wind Power Plant- GC (63 KV

The voltages and reactive powers are stacked closely to together in here because of the absence of dead-band zone.

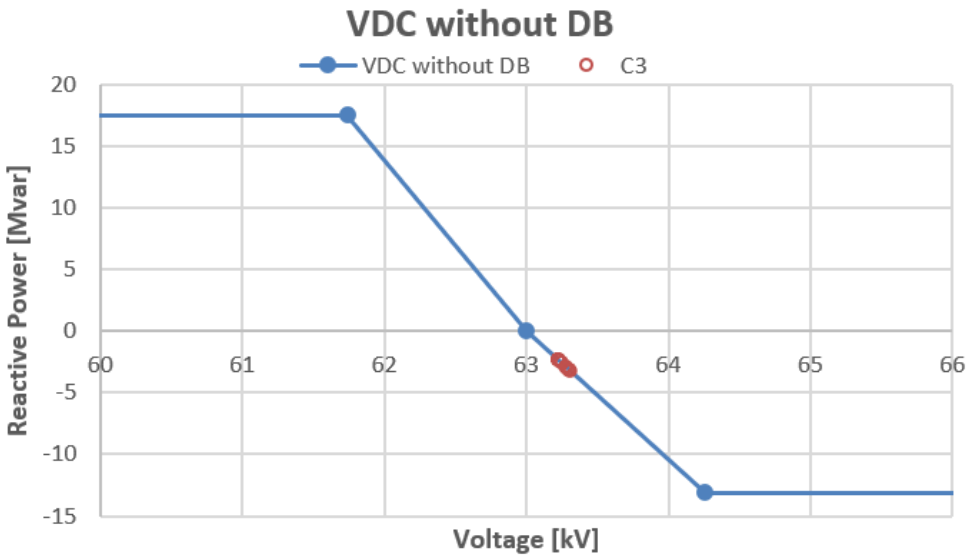

Figure 6-11: Validation of The Case "C3" for The Baixo Alentejo Wind Power Plant-GD (63 KV)

6.3.2 Validation of the VDC curve with cubic Spline : Case "C4"

The correspondence of the "C4" case in the Alcoutim PV plant (400 KV), São Marcos PV plant (150 KV), Baixo Alentejo (63 KV) and Malhanito Wind Power Plant (63 KV) are shown in the figures 6-12 to 6-15.

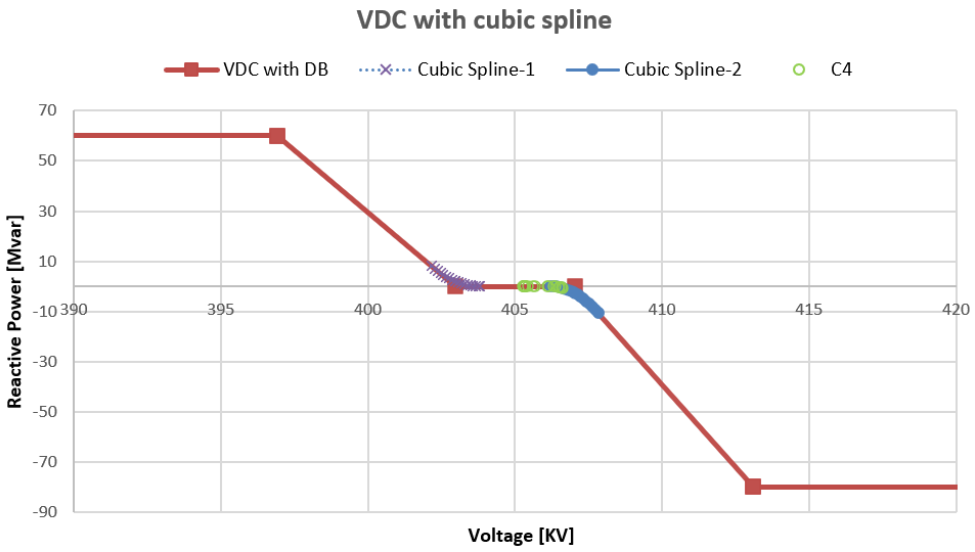

Figure 6-12: Validation of The Case "C4" for The Alcoutim PV plant-GA (400 KV)

The cubic spline based VDC curve with dead-band is the efficient operation because it solves the numerical complexities. With these the optimum voltages and reactive powers of all the generators of the Tavira substation can be achieved.

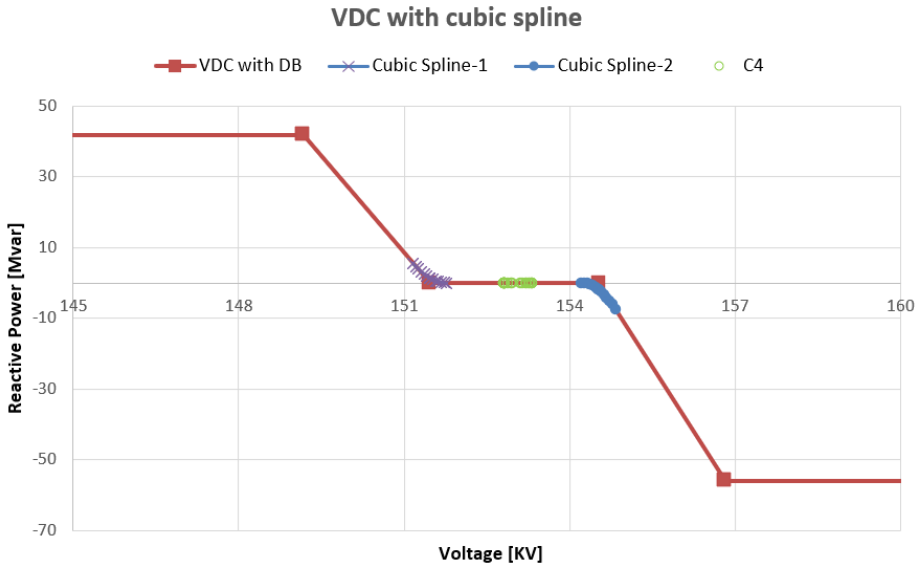

Figure 6-13: Validation of The Case "C4" for The São Marcos PV plant-GB (150 KV)

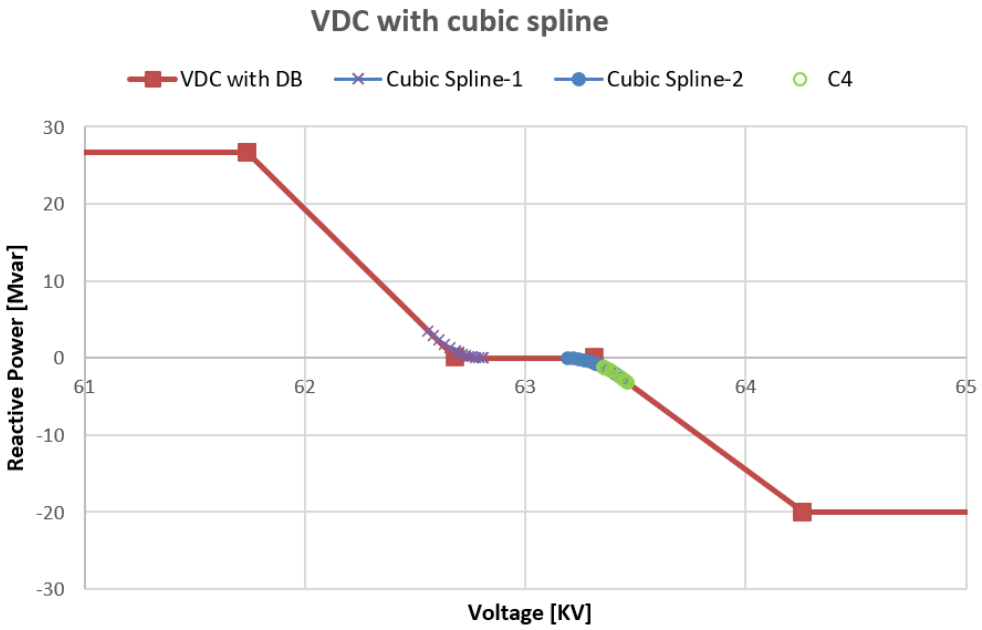

Figure 6-14: Validation of The Case "C4" for The Malhanito Wind Power Plant- GC (63 KV

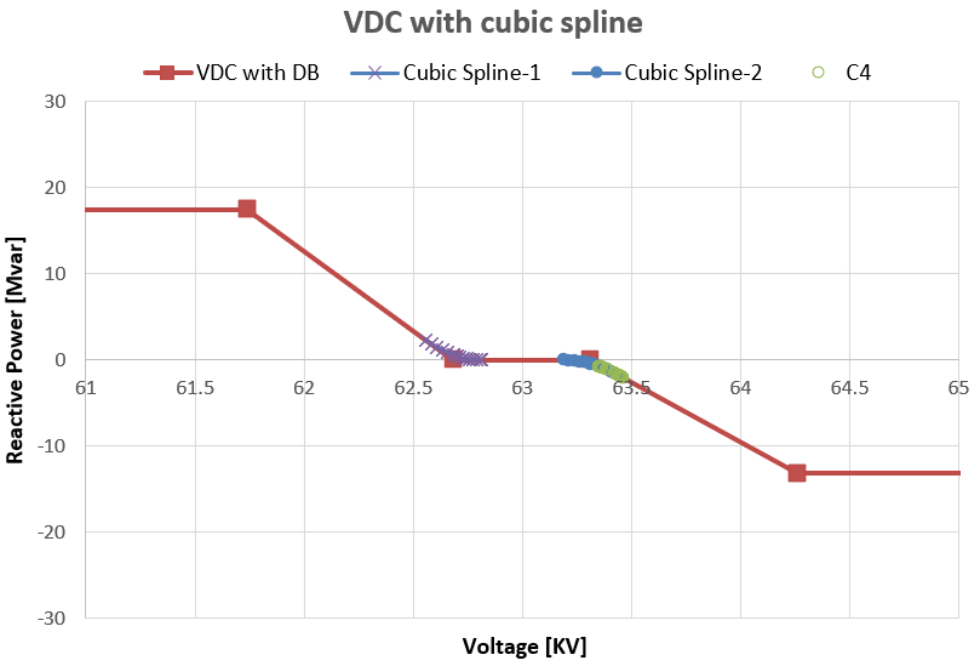

Figure 6-15: Validation of The Case "C4" for The Baixo Alentejo Wind Power Plant-GD (63 KV)

From the figures it can be seen that the reactive powers from case "C4" are aligned in the VDC curves with cubic splines. The relationship between the voltages and reactive powers are non linear and in most cases they are aligning with the cubic spline-2.

In this case scenario, the Malhanito and Baixo Alentejo Wind Power Plant are always absorbing reactive power. The São Marcos PV plant neither absorbing nor generating any reactive powers. Same goes with the Alcoutim PV plant but for some specific hours it is absorbing very low amount of reactive powers.

6.4 Absorption of Reactive Power in Tavira Substation

The Alcoutim PV plant, Malhanito and Baixo Alentejo wind Power Plants are always absorbing reactive powers in Tavira Substation in all case scenarios except "C0". From the below figures the relationship between the voltages and the reactive powers

can be observed.

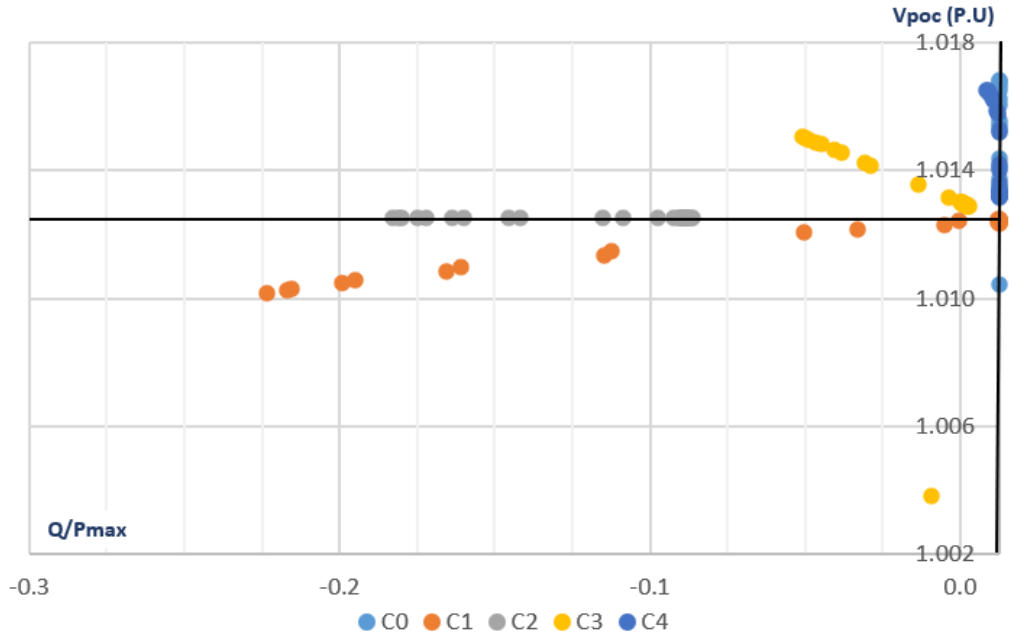

Figure 6-16: Reactive Power Absorption for The Alcoutim PV plant-GA (400 KV)

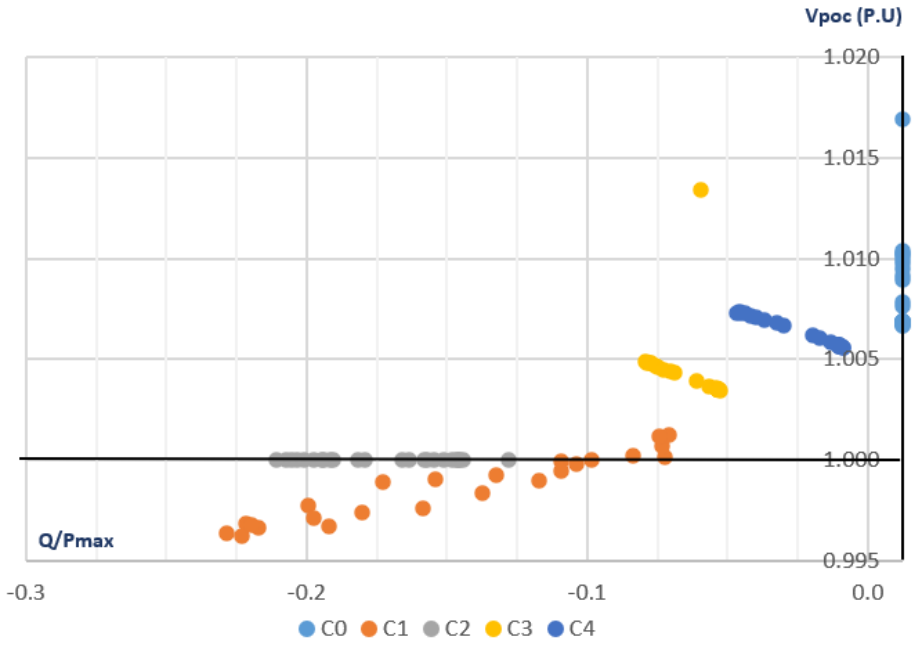

Figure 6-17: Reactive Power Absorption for The Malhanito Wind Power Plant- GC (63 KV)

It can be seen that whenever these generators are operating under the set point

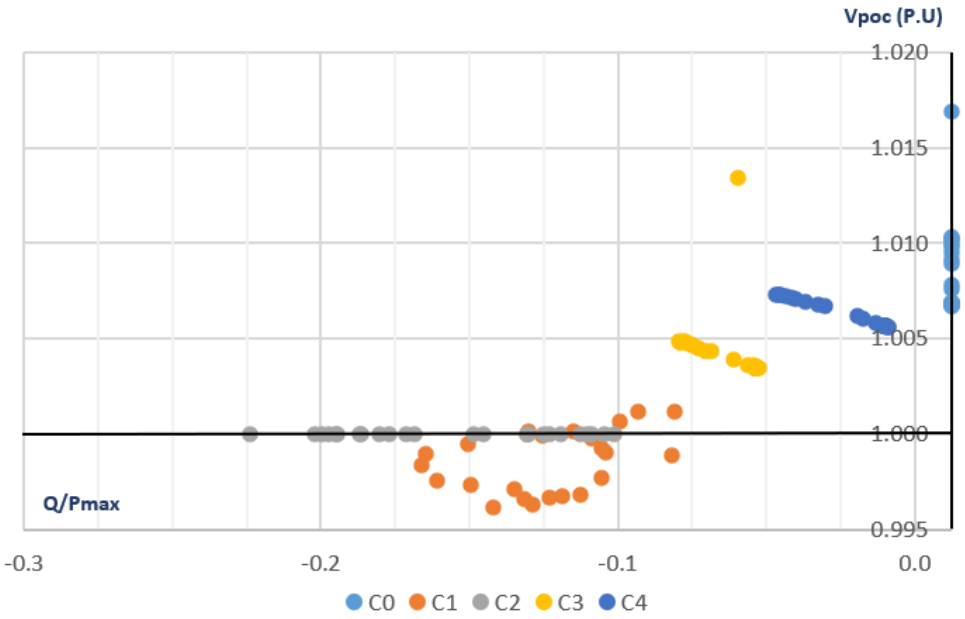

Figure 6-18: Reactive Power Absorption for The Baixo Alentejo Wind Power Plant-GD (63 KV)

voltage limits the reactive power absorption is more. Mainly with the "C1" case the generators mostly operate under the voltage limit which is "below-left" quadrant, quadrant (III). In this quadrant (III) it decrease the voltage more and degrade the voltage stability of the system. The "C3" and "C4" cases maintain a good adjustment of the reactive powers and voltages as they are operating by means of the voltage droop controls.

6.5 Reactive Power Circulation in Tavira Substation

After all the simulations are done with the "C2", "C3", and "C4" cases where the voltage and reactive power regulations are performed, we can draw the reactive power circulation curve for the Tavira substation for these cases. Figure 6-19 shows the reactive power circulation curve for the cases "C2", "C3", and "C4" on the selected day.

This circulation appears if the power plants of the substation operates in different

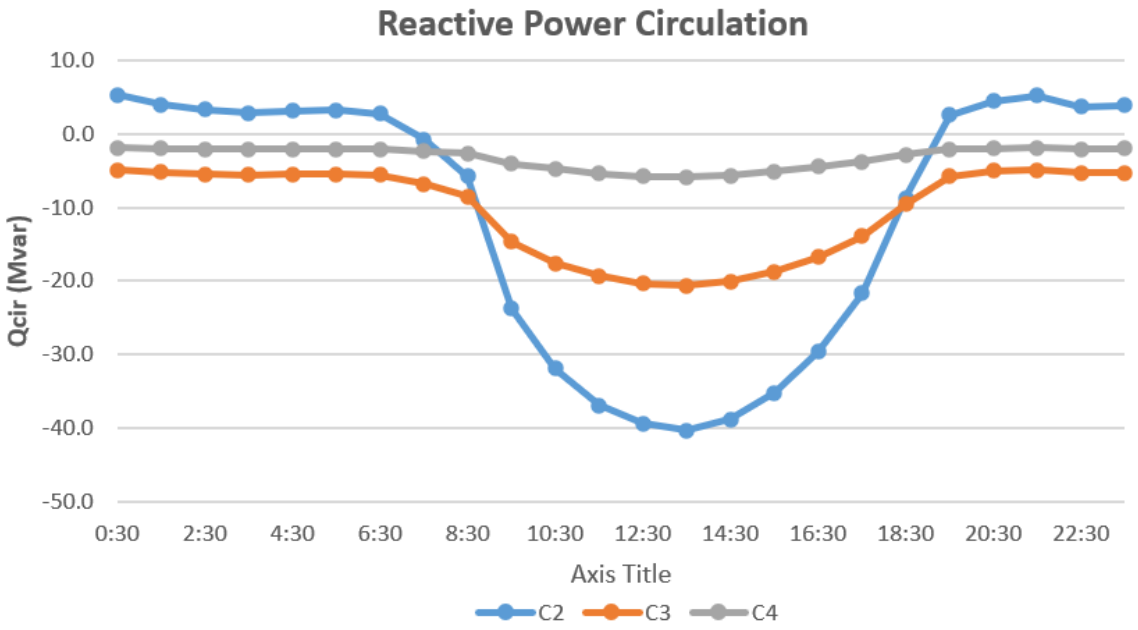

Figure 6-19: Reactive Power Circulation Curve for The Tavira Substation

conditions meaning some of them absorb and some of them generating reactive powers and equals the minimum value. As it appears from the curve with the "C2" case the reactive power circulation reaches the maximum and minimum values. The maximum value of reactive power circulation for "C2" case is 5.4 Mvar and the minimum value is -40.4 Mvar. With "C3" and "C4" cases there is no generation of reactive power and the minimum values which were found are -20.7 Mvar and - 5.9 Mvar respectively. Among these three cases the reactive power circulation with "C4" case is more convenient as in all time it is near zero than other cases.

Chapter 7

Conclusion

This chapter presents the main conclusions reached out in this thesis. The comparison of all the case scenarios performed in this thesis are presented and the efficiency and accuracy of the proposed drrop control is discussed. An outlook of the future works along with the works which could have been done in this thesis are also discussed.

7.1 Results from the simulation

The first case scenario that was performed was the base case where the voltage and reactive power doesn't have any dependency because there were no control scheme performed. Also with case "C1" the reactive power that were imposed onto the generators was based on the tangent ϕ rule which also doesn't have the voltage and reactive power dependency. For the "C0" there are fix voltage levels in all the hours and although there is no dependency but the reactive power is zero all the time.

To compare the different case scenarios let's look into the below figure 7-1 where the dependence of reactive power on voltage in the point of interconnection bus is shown.

As we can see from the figure with "C0" case there is no reactive power contribution from the wind and solar. Here the passive mode is not considered where the generation from wind plants are above the load. Same thing is considered with the solar pv plants, although it is predicted that in future the generation from solar

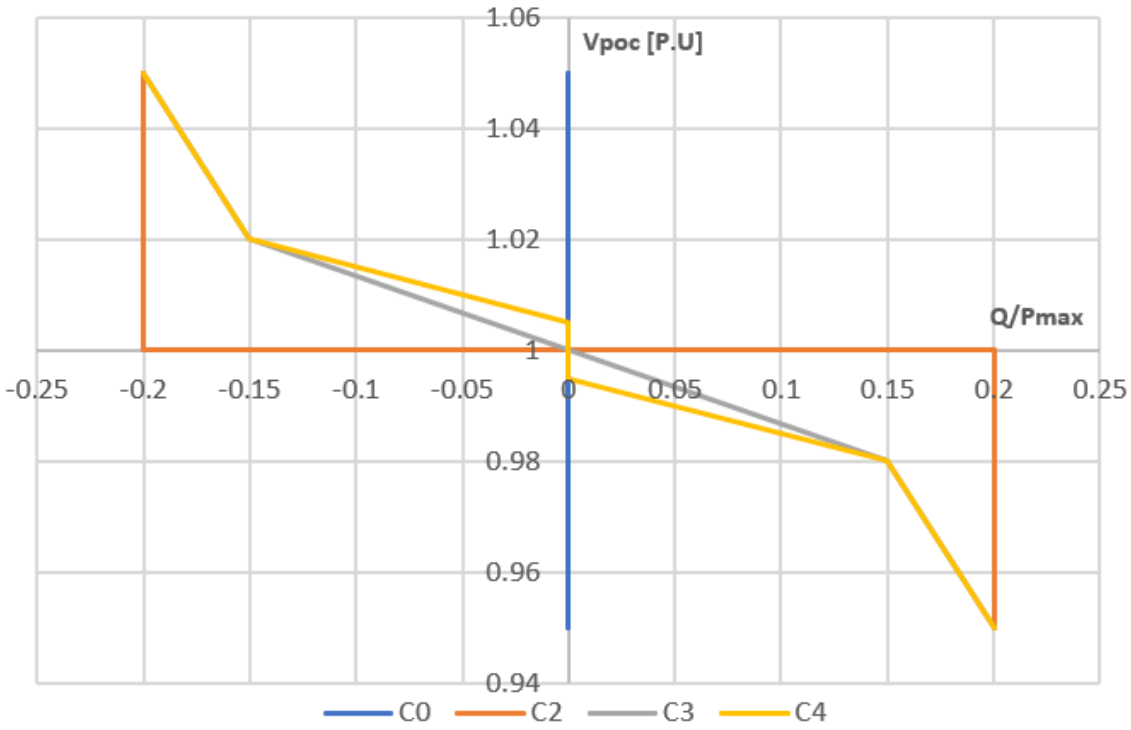

Figure 7-1: Reactive Power Dependence on Voltage

plants will also increase. A good thing about the "C0" case is that in case there is a loss of wind or solar energy the operator just need to consider the instability of loosing the active power from the plants. Although it can be done but often losing the active and reactive powers from wind and solar may cause high voltage excursion in the grid with lower short-circuit power. This is a situation that often occurs in the distribution grids. As all the generators from the Tavira substation contains very high voltages, even without the contribution from wind and solar power plants the voltages were outside the agreed limits as seen from figures 6-1 to 6-3.

The "C1" case, corresponds the tangent ϕ equal -0.2 rule. From figure 6-16 to 6-18 we can see that the reactive power absorption from the Alcoutim PV plant, Malhanito and Baixo Alentejo wind power plants with this type of control are in the quadrant (III) where they are not contributing to the voltage profile as they are absorbing reactive power when the voltage is already low. Here the adequate operational zone is quadrant III and IV. This case scenario makes the use of power factor mode which is suitable for reactive tariff mechanism in the distribution system. Power factor means

the reactive power will be proportional to the active power. For wind power it is proportional to wind speed and for solar power it is proportional to solar radiation. The voltage control mechanism has nothing to do with power factor.

The "C2" case with voltage control improves the voltage control capability of the power plant by providing a higher reactive power contribution. But, with this the losses inside the power plants also increases and as seen from figure 6-19 it may also cause reactive power circulation that would increase the losses on the whole network.

The "C3" and "C4" cases are based on a voltage droop control, which are not so demanding as "C2", but they ensure that the voltage is near the declared target voltage (Udec). In both "C3" and "C4" cases where the Malhanito and Baixo Alentejo wind power plants are controlling the bus no. 40, to ensure the declared target voltage they will provide the same relative reactive power output (% of Q/Pmax will be same for both) independent of their size. Which means that they will contribute to the voltage control together in the same proportion depending on their actual capacity.

The "C3" case is providing voltage droop control without the dead-band. Although it provides sufficient voltage management for all the generators of Tavira substation but here without the dead-band the optimization of the reactive power is not solved properly and for this reason the reactive power circulation is a big issue.

The "C4" case is the cubic spline based voltage droop control scenario with the dead-band where both the voltage and reactive power management has been achived together. The cubic splines solves the numerical complexities of the power flow, providing the accurate reactive power output for the efficient operation of the network. As seen from figure 6-19 this case leads to lower reactive power circulation thus providing lower losses at the power plant and in the grid.

In conclusion, The thesis identified that the "C4" case with the cubic spline based voltage droop control with the dead-band is the most appropriate voltage control scheme for the solar and wind power plants. For the operational cases with no thermal power plant in the grid, and for the future energy generation where there will be more renewable plants, the TSO must rely on stable voltage control from renewable energy generation. This solution can be an ideal one in this aspect.

7.2 Future Works and Areas Left Unexplored

The primary idea of the thesis was to perform the simulation for 1 or 2 weeks of data. For that the interaction of python with PSS®E Xplore 34 in which the simulations are done was required. The problem was, PSS®E Xplore 34 has some downside as it is a student version and only works with 50 bus system. To interact it with python, some library functions were required but with this version those functions didn't work. Although we designed the Tavira substation perfectly but with the limitations of 50 bus system the whole design of Portuguese national transmission system operator was hard to design. In future there is a plan to perform the simulation for 1 or 2 weeks of data.

In this thesis the design of the voltage droop control was done based on the voltage reactive power (volt-var) method. Being the most used and efficient voltage droop control method this method was chosen. The droop control with active power-reactive power mode (watt-var) and the new addition voltage-active power mode (volt-watt) are proving to be also efficient and there are a lot of research going on in these fields. These unexplored areas are also potential future works.

At the end it was realized that the voltage droop control that has been developed here in this thesis is quite unique especially for the control of voltage and reactive power of a substation. The cubic spline function makes it a potential solution in the contingency scenario of power system and in the future there is a plan to publish the work as a journal or a conference paper.

Bibliography

[1] Redes Energéticas Nacionais, "Technical Data," 2019.

[2] A. N. Nunes, "Energy changes in portugal. an overview of the last century," *Méditerranée. Revue géographique des pays méditerranéens/Journal of Mediterranean geography*, no. 130, 2018.

[3] C. A. Gross, "Power system analysis," 1986.

[4] D. G. Photovoltaics and E. Storage, "IEEE standard for interconnection and interoperability of distributed energy resources with associated electric power systems interfaces," *IEEE Std*, pp. 1547–2018, 2018.

[5] PowerWorld Corporation, "Voltage droop control in power flow solutions," November 2018.

[6] PowerWorld Corporation, "Power Flow Solution Algorithms and Methodology," Novebmer 2018.

[7] David Aldrich and Bob McFetridge, "Distributed generation voltage control issues and solutions," in *2014 IEEE Rural Electric Power Conference (REPC)*, IEEE, May 2014.

[8] J. P. Lopes, N. Hatziargyriou, J. Mutale, P. Djapic, and N. Jenkins, "Integrating distributed generation into electric power systems: A review of drivers, challenges and opportunities," *Electric power systems research*, vol. 77, no. 9, pp. 1189–1203, 2007.

[9] M. H. Bollen and F. Hassan, *Integration of distributed generation in the power system*, vol. 80. John wiley & sons, 2011.

[10] P. Wlodarczyk, A. Sumper, and M. Cruz, "Voltage control of distribution grids with multi-microgrids using reactive power management," *Advances in Electrical and Computer Engineering*, vol. 15, no. 1, pp. 83–88, 2015.

[11] F. Viawan and A. Sannino, "Analysis of voltage profile on lv distribution feeders with dg and maximization of dg integration limit," in *2005 CIGRE Symposium on power systems with dispersed generation*, vol. 2, 2005.

[12] F. Viawan and A. Sannino, "Voltage control with distributed generation and its impact on losses in lv distribution systems," in *2005 IEEE Russia Power Tech*, pp. 1–7, IEEE, 2005.

[13] J. Aibangbee, "Voltages and reactive power controls in power system network using automatic voltage regulator (AVR) and static var compensator methods,"

[14] Redes Energéticas Nacionais, "Portuguese transmission system operator."

[15] Henrique Carvalho Alves de Amorim, *Equity Research-REN-Redes Energéticas Nacionais, SGPS, SA*. PhD thesis, Higher Institute of Economics and Management, 2016.

[16] T. M. Dralle, *Ownership Unbundling and Related Measures in the EU Energy Sector: Foundations, the Impact of WTO Law and Investment Protection*, vol. 5. Springer, 2018.

[17] J. F. L. Ferreira, "Long-term energy planning applied to the national scenario with high penetration of renewable energies," 2016.

[18] Ziegler and Friedrich, "Consumer protection law in the ongoing european internal energy market by the example of the electricity directive 2009/72/EC - CU Digital Repository," 2014.

[19] IEA-ETSAP and IRENA© Technology Brief E15-April 2015, "Renewable energy integration in power grids," April 2015.

[20] French Energy Regulatory Commission (CRE), "Deliberation of the french energy regulatory commission of 12 december 2013 concerning decision on the tariffs for the use of a public electricity grid in the HVA or LV voltage range," 2013.

[21] C. Hoong, S. Taib, K. Rao, and I. Daut, "Development of automatic voltage regulator for synchronous generator," in *PECon 2004. Proceedings. National Power and Energy Conference, 2004.*, IEEE.

[22] CRC Press, "Future communication technology and engineering: Proceedings of the 2014," Published in-2015.

[23] W. Moondee and W. Srirattanawichaikul, "Study of coordinated reactive power control for distribution grid voltage regulation with photovoltaic systems," in *2019 IEEE PES GTD Grand International Conference and Exposition Asia (GTD Asia)*, IEEE, Mar. 2019.

[24] M. Siira, "Introduction to IEEE std 1547-2018," Published in 2019.

[25] A. Samadi, M. Ghandhari, and L. Söder, "Reactive power dynamic assessment of a pv system in a distribution grid," *Energy Procedia*, vol. 20, pp. 98–107, 2012.

[26] B. I. Craciun, D. Sera, E. A. Man, T. Kerekes, V. A. Muresan, and R. Teodorescu, "Improved voltage regulation strategies by PV inverters in LV rural networks," in *2012 3rd IEEE International Symposium on Power Electronics for Distributed Generation Systems (PEDG)*, pp. 775–781, IEEE, 2012.

[27] A. Samadi, R. Eriksson, L. Söder, B. G. Rawn, and J. C. Boemer, "Coordinated active power-dependent voltage regulation in distribution grids with pv systems," *IEEE Transactions on power delivery*, vol. 29, no. 3, pp. 1454–1464, 2014.

[28] R. O'Connell, C. Volkmann, and P. Brucke, "Regulating Voltage: Recommendations For Smart Inverters," 2019.

[29] B. Allison, D. Wallison, T. Overbye, and J. Weber, "Voltage droop controls in power flow simulation," in *2019 IEEE Texas Power and Energy Conference (TPEC)*, pp. 1–6, IEEE, 2019.

[30] R. E. Torres-Olguin, A. R. Årdal, H. Støylen, A. G. Endegnanew, K. Ljøkelsøy, and J. O. Tande, "Experimental verification of a voltage droop control for grid integration of offshore wind farms using multi-terminal hvdc," *Energy Procedia*, vol. 53, pp. 104–113, 2014.

[31] T. K. Vrana, L. Zeni, and O. Fosso, "Dynamic active power control with improved undead-band droop for hvdc grids," 2012.

[32] C. B.-. W. Group *et al.*, "HVDC grid feasibility study," *Melbourne: International Council on Large Electric Systems*, 2011.

[33] T. Athay, R. Podmore, and S. Virmani, "A practical method for the direct analysis of transient stability," *IEEE Transactions on Power Apparatus and Systems*, no. 2, pp. 573–584, 1979.

[34] P. Gopi, I. P. Reddy, and P. S. Hari, "Shunt facts devices for first-swing stability enhancement in inter-area power system," 2012.

[35] "Commission regulation (*EU*) 2016/631 of 14 april 2016- *E*stablishing a network code on requirements for grid connection of generators," May 2017.

[36] Diário da República Eletrônico (DRE), "Diário da República no. 53/2020, series I of 2020-03-16," March 2020.